Universidad
Rey Juan Carlos

TESIS DOCTORAL

New Developments in the Partial Control of Chaotic Systems

Autor:

Rubén Capeáns Rivas

Directores:

Miguel Ángel Fernández Sanjuán

Juan Sabuco

Programa de Doctorado en Ciencias
Escuela Internacional de Doctorado

2018

A meus pais e irmáns.

Agradecimientos

Esta tesis es el resultado de años de investigación y continuo aprendizaje. Un camino que sin duda ha estado influenciado por muchas personas que con su experiencia, consejos y ayuda han hecho posible este trabajo. En primer lugar quiero expresar mi agradecimiento a mi director de tesis Miguel Ángel Fernández Sanjuán, catedrático de Física de la Universidad Rey Juan Carlos, por ofrecerme esta primera oportunidad y depositar en mí la confianza para acometer este proyecto investigador en un campo tan apasionante. He de agradecerle además su continuo apoyo, así como el tiempo dedicado a la supervisión y mejora de todos los trabajos que dieron lugar a esta tesis.

A mi codirector Juan Sabuco Larrosa, cuya ayuda y guía en esta tesis ha sido fundamental. Este trabajo es en cierto modo, una continuación de su trabajo doctoral acerca del método de control parcial de sistemas caóticos. Han sido muchas y muy enriquecedoras las discusiones, ideas, y revisiones que Juan ha aportado a este trabajo.

A mis profesores de la Universidad de Santiago de Compostela, que me enseñaron muchas de las herramientas usadas durante esta tesis. Especial importancia para mí tienen algunas de las asignaturas cursadas en el último curso de licenciatura donde descubrí el mundo de la física no lineal y de la complejidad. Enseguida encontré fascinante esta rama de la Física y sin duda me marcó conceptualmente hasta el punto de querer continuar aprendiendo e iniciarme en la investigación.

A Jesús Seoane por su disponibilidad para solucionar cualquier duda o problema, así como su eterno sentido del humor y por supuesto, a mis compañeros del grupo de Dinámica No lineal de la URJC, por ser magníficos amigos y crear entre todos un ambiente de trabajo acogedor a la vez que estimulante.

Durante esta tesis se ha realizado una estancia en el extranjero. Quiero agradecer al Prof. Balakumar Balachandran del Departamento de Ingeniería Mecánica de la Universidad de Maryland por acogerme y poner a mi disposición el material de su Laboratorio. Gracias también a Vipin y Celeste por su acogida y ayuda durante esta estancia. En este mismo periodo, he podido conversar con el profesor James A. Yorke al cual agradezco su tiempo y buenos consejos, así como sus contribuciones a algunos de los trabajos que figuran en esta tesis.

Quiero agradecer también a mi familia, que aunque no entiendan muy bien lo que hago, siempre han mostrado su interés y apoyo. A mis padres José y Maricarmen, por su confianza y paciencia, y por hacer posible que haya llegado hasta aquí. A mis hermanos Pablo y Lucía por ser parte de esta aventura y a la vez permitirme

ser parte de la suya.

Por último, el trabajo de investigación que ha dado lugar a esta tesis doctoral se ha beneficiado de los proyectos de investigación FIS2009-098981 del Ministerio de Ciencia e Innovación y FIS2013-40653-P del Ministerio de Economía y Competitividad. También se ha beneficiado del proyecto de investigación FIS2016-76883-P de la Agencia Española de Investigación (AEI) y el Fondo Europeo de Desarrollo Regional (FEDER). Igualmente se ha beneficiado por parte de la Universidad Rey Juan Carlos de una beca de ayuda a la movilidad para la realización de estancias predoctorales en Universidades y Centros de Investigación extranjeros, dentro del Programa Propio de Investigación, que tuvo lugar durante el año 2016 en la Universidad de Maryland.

Septiembre, 2018
Rubén Capeáns Rivas

Preface

This thesis has been developed during the past years in the Research Group on Nonlinear Dynamics, Chaos and Complex Systems of the URJC. All this work is devoted to new developments of the partial control method. The main goal of this technique is to control chaotic dynamics with escapes and affected by external disturbances. This thesis is organized as follows.

Chapter 1. Introduction

This chapter is a brief introduction to the main topics of our work. We describe the first steps of chaos theory and how the need of control arose in that field. Then we analize the main features of transient chaotic behaviour and the first attempts to control it. Finally, we show the evolution of the partial control method from the first ideas until the point this thesis was started.

Chapter 2. Description of the partial control method

The partial control method is used under different approaches along this thesis. In this chapter a general introduction to this method is given. The motivation to apply this method and the main dynamical conditions to apply it are presented. An algorithm to compute safe sets and how this set is used to control the system, is briefly described.

Chapter 3. Partial control to avoid a species extinction

In this chapter we present the first application of the partial control method in this thesis. Here, we have worked with an ecological model that describes the interaction between 3-species: resources, consumers and predators. The interest of this model lies in the fact that, for a choice of parameters, transient chaos involves the extinction of one of the species. Taking into account that the system is affected by external disturbances, we implement the partial control with the goal of avoiding the extinction.

Chapter 4. Controlling chaos in the Lorenz system

The Lorenz system is one of the most well-known systems in Nonlinear Dynamics. This makes it an excellent candidate to show how the partial control method can be applied in different ways depending on our requirements. For a certain choice

of parameters, trajectories of this system eventually converge to two fixed points attractors via transient chaos. In order to avoid this escape, we describe three different ways based on building maps of one, two and three dimensions, respectively. Pros and cons of each one are analized, and for the first time a three-dimensional safe set is shown.

Chapter 5. A different application of partial control

In all the previous works, the computed safe set were used to keep the trajectories in the region of interest. Here we consider a new application of the safe set. Without any extra computation, we show in this chapter how this set can be also used to accelerate the escape of the trajectories if necessary. This fact, allows the controller a great flexibility to avoid or force the escape when it is required.

Chapter 6. When disturbance affects a parameter

Random maps are discrete dynamical systems where one or several of their parameters vary randomly at every iteration. It is possible to find in these maps a transient chaotic behaviour, however few methodologies have been proposed to control them. Here, we propose an extension of the partial control method, that we call parametric partial control. To do that, we consider the scenario where the disturbances and the control terms are affecting directly some parameter of the system. To illustrate how the method works, we have applied it to three paradigmatic models in Nonlinear Dynamics, the logistic map, the Hénon map and the Duffing oscillator.

Chapter 7. Controlling time-delay coordinate maps

Delay-coordinate maps are a family of discrete maps where the dynamics have certain dependence on past states of the system. We consider these maps specially relevant because they can appear in the delay reconstruction technique of time series from experimental data. The main obstacle of these maps is that only the present state of the system can be modified. In this chapter, we study the convenience of the application of partial control under this constraint. To do that, a modified version of the partial control method is presented and some examples are illustrated. For the first time, it is treated a system that exhibits Hamiltonian chaos, and also a system that presents hyperchaos.

Chapter 8. A new approach: the safety functions

With the aim of dealing with more general systems and new circumstances where the control is needed, a new approach of partial control is proposed. Instead of using the information given by the safe sets, we have developed a new tool called the *safety function*. This tool allows us to know how safe is each point and also enable us to deal with more general situations where the system is affected by disturbances in different ways. In this chapter, we have designed an algorithm to compute these functions. Furthermore, we also show how safe sets and the safety functions are closely connected. To illustrate this new approach some examples are treated with

special emphasis in the time series example. We believe that this work will open a door to new and stimulating applications in the field of control of chaotic systems.

Chapter 9. Discussion

A brief overview of the main results of this thesis and the possible research lines for a future work, is given in this chapter.

Chapter 10. Conclusions

In this chapter we summarize the main conclusions of the research work done during this thesis.

Contents

Chapter 1
Introduction

1.1 A brief history of chaos

In the middle of the 17th century a great revolution in mathematics came up with the development of Calculus due to Isaac Newton and Gottfried Leibniz. One of the first and more significant applications was the development of Celestial Mechanics. With the knowledge of the gravitational interaction between the masses of celestial objects and its current position, it was possible to predict the future positions of the bodies, simply by using a set of differential equations.

Soon, this method was successfully applied to many other physical systems, creating a certain "euphoria" that is well summarized in the mathematician Pierre-Simon Laplace thought, who believes that given the initial state and the physical laws governing a system, its evolution can be perfectly predicted.

In the middle of the 19th century, it became clear that the motion of gases was far more complex to calculate than that of planets. The amount of calculations required for these systems made useless the mechanical approaches, thereby leading James Clerk Maxwell and Ludwig Boltzmann to create statistical physics. This was one of the first warnings about the limitation of predictability in physics, but still persisted the idea that, with the sufficient knowledge and calculus power, even those systems could be perfectly predicted.

In 20th century, one of the biggest revolutions appears in physics, Quantum Mechanics. The uncertainty principle stated by Werner Heisenberg, was the first big conceptual obstacle against the predictability principle. The position and velocity of an object cannot be, even in theory, exactly measured. This physical limitation involves that the Laplace presumption is not physically realizable. However the effects of the uncertainty principle are so small in ordinary size objects, that the Laplace statement remains still applicable in the sense that approximate causes follow approximate effects.

Few decades ago, at the end of 19th century, the French mathematician Henri Poincaré, studying the stability of the solar system, showed mathematically that even low-dimensional systems like the famous 3-body problem, can exhibit a highly complex dynamical behaviour. He realized that in some nonlinear systems, even

small deviations in the initial conditions could produce enormous differences in the final state of the system. Long term predictions become impossible, burying forever the Laplace dream. Later, in 1892, Poincaré published his major work *Les Méthodes nouvelles de la Mécanique Céleste* where new fundamental tools in Nonlinear Dynamics were introduced. He is considered one of the founding fathers of chaos theory.

The enthusiasm generated by the discovery of Quantum Mechanics and Special Relativity in physics, provoked that the studies of Poincaré and others like George D. Birkhoff, Eberhard Hopf, or Andrey Kolmogorov did not receive much attention in the physics community. The complexity that often comes out from the study of nonlinear systems made it very difficult to achieve substantial results in this field. It was only with the advent of computers, and the access to a huge amount of calculations, when serious studies of nonlinear systems were possible. In this sense, one of the first works was made by the American meteorologist Edward Lorenz in 1963. He recognized the unpredictability of the dynamical behaviour in connection with the numerical solution of the model named after him. He also observed that his simple model of three ordinary differential equations presented non-periodic solutions, and for some value parameters, the trajectories are attracted to an strange topological object, not a surface, neither a volume, that was found to be fractal (Mandelbrot, 1982). This kind of new motion was first named chaos by the American mathematician James Yorke in 1975.

1.2 Chaos and control

The word chaos itself may seem confusing if one interprets it with the colloquial meaning of "lack of order". However deterministic chaotic systems are quite ordered and even predictable on short-time scales. The goal of modern dynamicists is to find the hidden order in the apparent chaos. In this sense important contributions have been made by J. A. Yorke, J. P. Eckmann, P. Grassberger, C. Grebogi, M. Hénon, P. Holmes, E. Ott, O. Rössler, D. Ruelle, Y. Sinai, and S. Smale among others. They have shown, roughly speaking, that chaos is the consequence of infinite local instabilities (over short times nearby states that move away from each other), but with stable behavior over long times.

Nowadays, chaos still admits several technical definitions, however the common underlying ideas (see Ref. [1]) can be described in a few variables. Without going into details the main features and associated measures to describe chaotic motion are:

- Irregular in time, aperiodicity $\rightarrow$ positive topological entropy.
- Sensitivity to initial conditions (unpredictable in the long term) $\rightarrow$ positive average Lyapunov exponent.
- Complex but ordered in phase space (fractal structures) $\rightarrow$ Fractal dimension smaller than the dimension of the phase space.

Any of these properties may help in deciding whether a system is chaotic or not.

With the introduction of computers, chaotic dynamics was found in many different fields like meteorology, geophysics, plasmas and lasers, electronic circuits, acoustics among others. The high irregular and unpredictable motion associated with chaos, can make desirable in some situations to suppress the chaotic behaviour and make the system to behave in a regular and predictable manner. At the beginning, some physicists thought that this control task was impossible to achieve. Considering that for a chaotic system any small variation in the system's state is followed by an exponentially growing variation of the motion, it was thought that any attempt to guide a chaotic system by using small perturbations would just lead it to other chaotic and uncontrolled motions.

However, this was the wrong point of view. If we have a system that presents sensitive dependence to initial conditions, a small but accurately chosen perturbation might induce a huge change in its dynamics. Thus, the exponential divergence of the initial conditions induced by chaos can be considered an advantage. In 1990 Edward Ott, Celso Grebogi and James A. Yorke addressed this question. In a seminal paper they proposed the stabilization of some of the infinite unstable periodic orbits embedded in the chaotic attractor by applying small temporal perturbations to an accessible parameter of the system (OGY method, [2]).

The OGY approach requires quite a lot of knowledge about the orbit, including its position and stability properties that are not always straightforward to find in a real-life situation. A different approach that lacks the above shortcomings but pursue the same goal was proposed by the Lithuanian physicist Kestutis Pyragas [3]. He proposed a delayed feedback control in the form of a signal that is proportional to the difference between the current system state and its state a period T ago. This approach is especially appealing for experimentalists, since one does not need to know anything about the target orbit beyond its period T.

1.3 Transient chaos and control

Under certain circumstances chaotic behaviour is only of finite duration, i.e. the complexity and unpredictability of the motion can be observed over a finite time interval. This type of chaos is called transient chaos.

Chaotic transients emerge when, due to the change of some parameter of the system, trajectories can escape from the chaotic region. When the parameter reaches this critical value, it is referred to as a crisis. To explain the main mechanism of a crisis it is necessary to introduce the concept of basin of attraction. The set of initial conditions leading to some asymptotic final state is called basin of attraction, and its geometry is specially related with the kind of motion present in the system. When more than one attractor is present, there is a boundary between the basins, and this can be a smooth curve or even a fractal curve. The main mechanisms [1] that lead to a chaotic crisis are:

- Boundary crisis → The chaotic attractor collides with its own boundary basin.

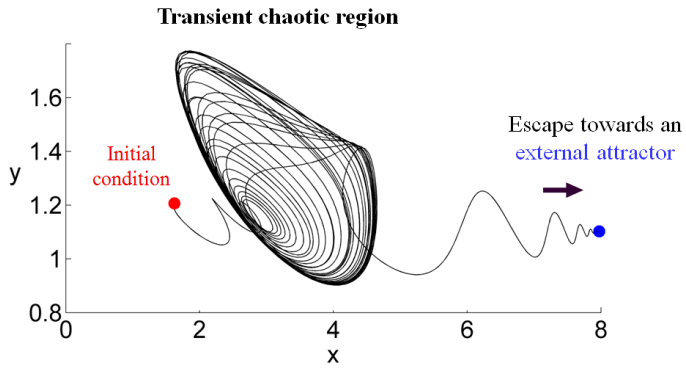

Figure 1.1. Transient chaos. The figure illustrates the chaotic transient behavior of a trajectory. Starting in the red point, the trajectory falls in the chaotic region where it remains for a while. After a finite amount of time, the trajectory escapes from the chaotic region towards an external attractor (blue fixed point). The transient chaotic behavior is due to the presence of a chaotic saddle in phase space. This invariant set is a non-attractive chaotic set and this is the reason why the trajectory eventually escapes. The goal of applying control is to sustain the chaotic behavior forever, avoiding the escape of the trajectories.

The chaotic attractor ceases to exist and it is converted into a chaotic saddle, which is an invariant fractal set in the phase space.

- Internal crisis → the chaotic attractor suddenly enlarges and a saddle is merged with a small size attractor.

- Basin boundary metamorphosis → the basin boundary changes its fractal character: a hyperbolic point on the boundary becomes part of the chaotic saddle.

In comparison with permanent chaos, the basic new feature here is the finite lifetime of chaos. Almost all initial conditions in the chaotic region, escape after a chaotic transient. There is an exception, a few set of points (a Cantor-like set that is known as the chaotic saddle) that never escapes, but any minimal deviation from this set lead the trajectory to the external attractor. If individual lifetimes for different initial conditions are computed, the ensemble is fractal. This feature together with the fractal basins of attraction represents the main fingerprints to identify transient chaos.

From the point of view of control, if the goal is to suppress the chaotic behaviour, only is needed to wait until the chaotic motion eventually ceases. However, it has been stressed recently the importance of the chaotic motion in some practical systems. In mechanics for example, chaos helps to prevent undesirable resonances ([4]). In engineering, the thermal pulse combustor is more efficient in the chaotic regime [5]. In living organisms, chaotic dynamics in vital functions can make the difference between health and disease [6]. In biology, it has been suggested that the disap-

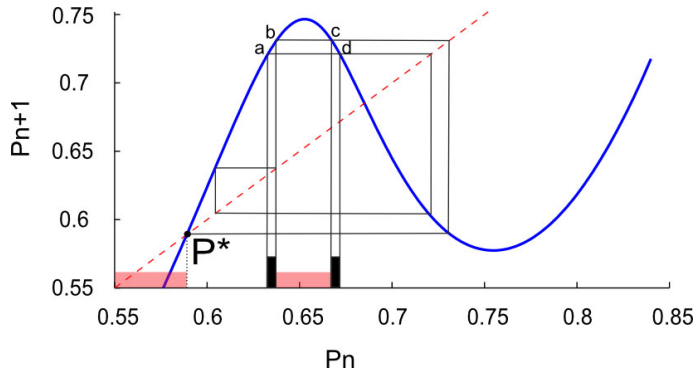

Figure 1.2. Loss regions in the Dhamala and Lai control method. The figure represents a one-dimensional map that presents transient chaos. Orbits behave chaotic in the interval $[0.58, 0.73]$. When the orbit passes through the segment $b - c$, escapes from that interval. The central red set represents the original escape regions. However, when noise is present orbits can also escape through the right escape region (also in red). The black sets represent the two target regions (or loss regions) used to control the trajectories with the aim of avoiding the escape. We colored the regions with different thickness just to help the visualization.

pearance of chaos may be the signal of pathological behavior [7]. In all these cases, chaos is a desirable property that is worth preserving.

With the aim of sustaining the chaotic behaviour in the case of transient chaos, different control methods were proposed. The most important are the methods proposed by Yang et al. ([7], 1995), Schwartz and Triandaf ([8], 1996) and Dhamala and Lai ([9], 1999). Although the control scheme is different in each case, all of them are based on identifying some"loss regions" of the dynamics. Chaotic trajectories sooner or later pass trough these regions to then escape to an external attractor. The idea of these methods is to use the "loss regions" or pre-images of them as a control regions. Every time a trajectory pass through these regions, a suitable control is applied to re-inject the trajectory to the nearest chaotic region. (see Fig 1.2).

These methods work well in ideal conditions, however practical experimentation always involve approximations and external factors interfering with the system. Even if the deviations from the experiment and the theoretical model are very small, the action of the unstable chaotic dynamics makes that these deviations grow exponentially. For example, in the control methods cited before, if the choice of "loss regions" is not made carefully one might kick the dynamics into faster escaping regions, having as a consequence the increase of the frequency of perturbations required to maintain chaos.

The other important problem is the unavoidable presence of some amount of noise in all real experiments. Even if this amount of noise is small, it should be taken into account since the chaotic motion is an error amplifier, and small deviations at the beginning can ruin even the best control strategies.

The presence of noise modifies the trajectories and can allow them to explore

new paths. For example, in the case of control by means of the loss regions, the presence of noise makes it possible that some trajectories leave the chaotic region without going trough the loss region, and making the control strategy to fail (see Fig. 1.2). However, there are other sources of deviations that should be taken into account. For example, mismatches in the mathematical modelling of the system or imprecision in the application of control must also be considered when a robust control strategy is designed. For all these reasons the partial control approach was conceived.

1.4 Evolution of partial control

The partial control method was proposed with the aim of sustaining the transient chaotic behaviour indefinitely in certain region Q of phase space, avoiding the undesirable escape of the trajectories. With a similar goal, different control methods have been proposed in the literature ([8, 9, 10, 11]). However, these methods differ from the partial control method in that they have been mainly designed to be applied in deterministic systems, while partial control is a robust method able to deal with random disturbances affecting the systems. **The more remarkable feature of the partial control is the ability to keep a control smaller than the disturbances**. This counterintuitive and surprising result is possible due to the presence of the chaotic saddle in the phase space which is responsible of the transient chaos. The partial control method benefits from the fractal structure of the chaotic saddle, to reduce the impact of the disturbances and at the same time, to enhance the effect of the control applied.

The development of the partial control method begins with the Yorke's game of survival ([12], 2004). This game was based on the tent map dynamics for a parameter value where transient chaos exists. In the game some external disturbance is present and the goal was to design a control strategy to remain in the chaotic region. The work revealed that some pre-images of the middle point of the map can be used as safe points. Trajectories forced to pass through these points can counteract the effect of disturbances with a smaller control effort.

This strategy was later extended to two-dimensional maps by Zambrano et al. ([13, 14]) in 2008 and 2009. They made use of the fact that typically chaotic saddles arise due to the existence of a horseshoe map in phase space. The particular geometrical action of this map may involve the existence of transient chaos on the system considered. However, they showed that precisely this geometrical action also implied the existence of certain sets, the safe sets, that can be used to keep the trajectories close to the chaotic saddle (see Fig 1.3). Also in these works they proposed a generic procedure to obtain these safe sets in every system with a horseshoe map.

The next development in partial control was carried out by Sabuco et al. [15] in 2010, introducing a generalization of the safe sets, the extended safe sets. They showed that these sets can be related with another important family of sets, the escape time sets inside Q, that correspond to points in the square that escape from it under different numbers of iterations. By discarding some points from the escape

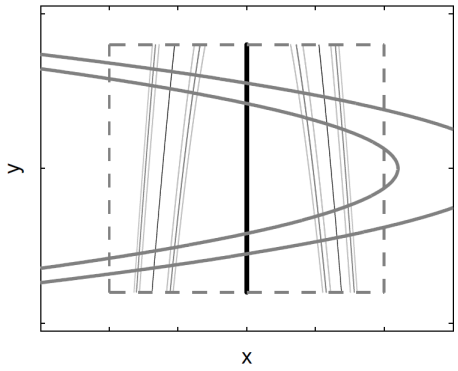

Figure 1.3. Sets in the Hénon map. This figure corresponds to the Hénon map where the central square (dotted line) maps in the horseshoe region. Note that some points map outside the initial square and therefore escape from it. Taking the central line (thick black line) it is possible to compute the preimages S_1 (black), S_2 (grey) and S_3 (silver) consisting on 1, 2, 4 and 8 vertical curves, respectively. These lines can be used to control the orbits and avoid their escape from the initial square.

sets it has been proven that trajectories can be kept in Q, even with a control smaller than the external disturbances. (See Fig. 1.4)

The next step was to generalize this to an arbitrary set. In 2012 Sabuco et al. ([16, 17]) proposed a new approach to generalize the search of safe sets in systems of arbitrary dimension that exhibit transient chaos. The algorithm that was proposed was able to compute the safe sets for a specified region in phase space, given the map, the maximum disturbance value, and the maximum allowed control. They called it the Sculpting Algorithm, because literally the algorithm sculpts the safe sets, discarding the points of the initial region that can not be controlled. An example of the application in the Duffing oscillator is shown in Fig 1.5.

This thesis started from this point showing how the partial control technique can be applied to different models. In Chapter 3, an experimental ecological model is treated. For certain parameters one of the species of the model gets extinct after a chaotic transient. We will show how the application of partial control is able to avoid the extinction. In Chapter 4, the method is applied to the well-known Lorenz system. Among other results we compute for the first time, 3-dimensional safe sets.

A new application of the safe sets is studied in Chapter 5. Instead of using the safe sets only to sustain the trajectories in some region, we use them also to accelerate the escapes of the trajectories. This dual application of the safe sets, give the controller a great flexibility since the trajectories can be kept chaotic or force them to escape when it is needed.

In order to extend the application of the partial control method to other scenarios, we explore in Chapter 6 the possibility of controlling parameters of the system affected by disturbances, to avoid escapes in the trajectories of some chaotic systems. Chapter 7 is devoted to analyse a very important type of maps, the delay-coordinate maps, where the dynamics includes some memory term (a dependence with the state

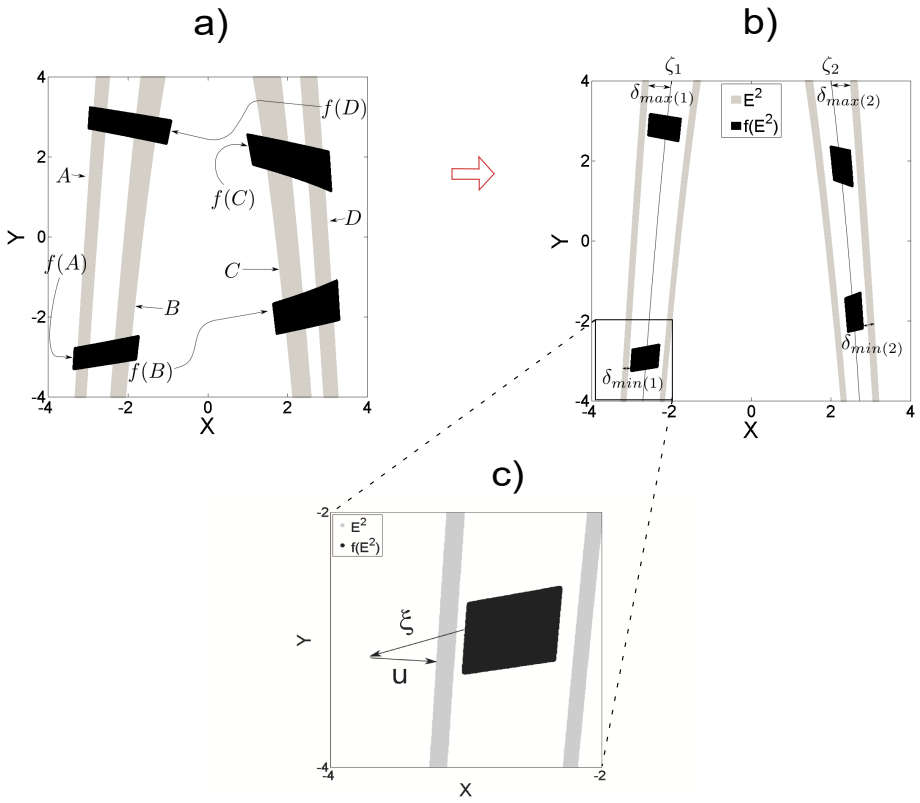

Figure 1.4. Safe sets from escape times sets in the Hénon map. (a)The escape time set, i.e., the set of points that escape from Q after 3 or more iterations. It consists of four pairs of strips. We have also plotted in black the images of those points under one iteration. Due to the fact that the images of the strips do not lay between the pairs of strips, it is impossible to use these images to keep trajectories inside Q with a control smaller than the disturbances . (b) Safe set after sculpting the escape sets. Now the images fall inside the bands. (c) A zoom of escape sets. Independently from the disturbance deviation ξ a smaller control u can put the trajectory back on the safe set.

of the system a delta time ago).

Finally, in Chapter 8, a new and more general approach of partial control is presented. Instead of working with safe sets, we introduce a new tool, the safety functions U_∞. This function is defined in the region Q, and represents the minimum bound of control necessary to sustain a trajectory in Q forever. The function takes different values depending on the initial condition point $q \in Q$. An algorithm to compute the safety function has been developed. It is also shown how the safe sets can be obtained from the safety functions, and how more general maps affected by disturbances can be treated with this approach.

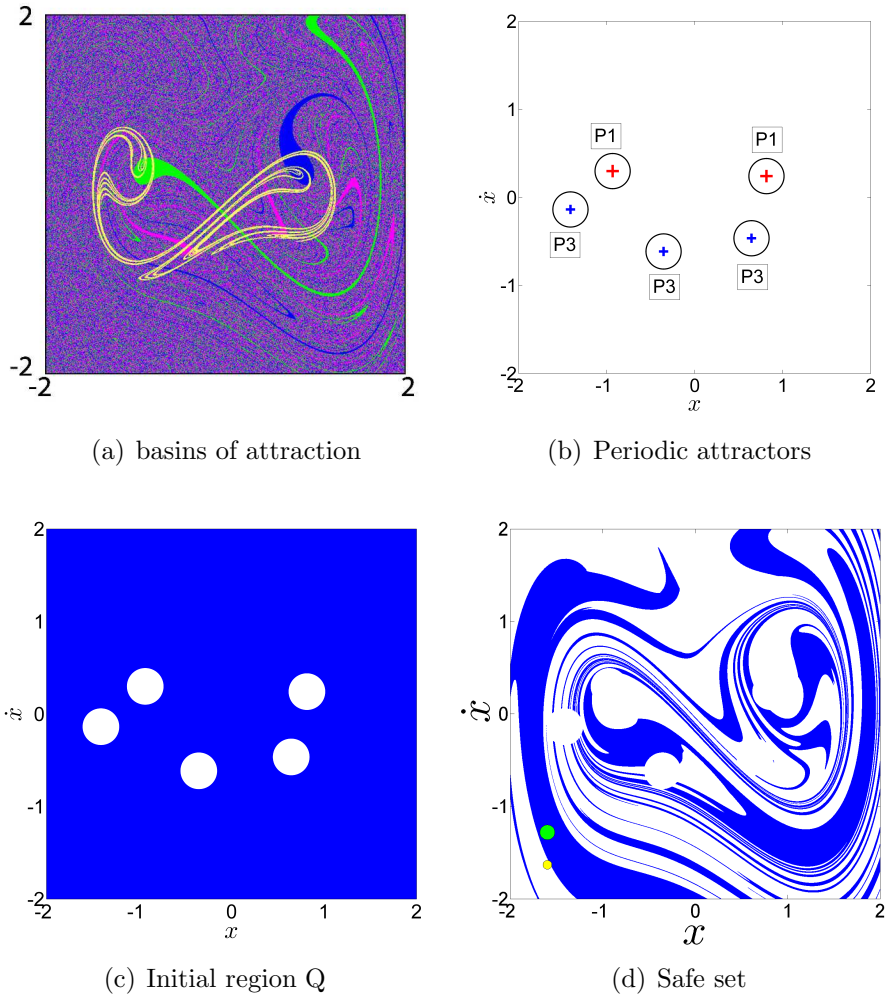

(a) basins of attraction (b) Periodic attractors

(c) Initial region Q (d) Safe set

Figure 1.5. Periodic attractors of the Duffing oscillator. (a) In this figure it is drawn the complex structure of the phase space for the Duffing oscillator $\ddot{x}+0.15\dot{x}-x+x^3 = 0.245\sin t$. Three different basins of attraction (magenta, blue and green) are presented in this system. The invariant unstable manifold associated to the chaotic saddle appears in yellow. (b) This figure shows the periodic attractors: two period-1 attractors and one period-3 attractor. We also show with circles of radius 0.2 the region of the phase space that we want to avoid, whatever the disturbances. (c) We use a grid of 6000×6000 points in the square $[-2,2] \times [-2,2]$ as our initial set, but removing the zones that we want to avoid, that is the circles. Applying the Sculpting Algorithm over several iterations, we will obtain the desired safe set. We let $\xi_0 = 0.08$ be the maximum size of the vector perturbation. (d)In this figure we can see the result of applying the Sculpting Algorithm to the Duffing oscillator. The safe set appears in blue. The minimum control allowed, so that it exits a safe set is $u_0 = 0.0475$ (yellow circle), with a maximum disturbance of $\xi_0 = 0.08$ (green circle). This is equal to a safe ratio $\rho \approx 0.59$.

Chapter 2
Description of the partial control method

2.1 Introduction

The transient chaotic behavior is caused by the presence of a chaotic saddle in phase space. The main mechanism to create a chaotic saddle is when a chaotic attractor collides with the boundary of its own basin of attraction, causing a **boundary crisis**. In contrast to a chaotic attractor that possesses a fractal structure only in the stable direction, the chaotic saddle is a nonattractive invariant set that is fractal in both, the stable and unstable directions. Due to the fractal structure in the unstable direction, infinite holes arise along the unstable manifold of the chaotic saddle. A trajectory that is initially attracted along the stable direction for some finite amount of time, eventually escapes through one of the gaps present in the unstable direction. These escapes allow the trajectories to reach other regions of the phase space, involving catastrophic consequences for the system in some cases. For example in a thermal combustor model [5], the crisis leads to the flame-out making the device useless. Also, in the McCann-Yodzis ecological model [18] the crisis conducts irreversibly to the extinction of one of the species.

With the aim of avoiding these undesirable escapes, even when an external disturbance is affecting the chaotic dynamics, the partial control method was proposed. This control method, and some variations of it, are used along this thesis. In this chapter a general introduction of the partial control method is given.

2.2 The partial control method

The partial control method is a recently developed control strategy ([16, 17]) for preventing escapes associated with a transient chaotic behaviour. It is particularly appropriate when it is desirable to keep the magnitude of the control small in a system affected by external disturbances [19, 20]. Since in many experimental systems, the presence of disturbances may be unavoidable, a robust control strategy must

take it into account, especially when it is necessary to keep the control as small as possible.

Methods that perform well in systems in absence of disturbances can fail dramatically when disturbances appear. For this reason, it is necessary to consider a term, that we call **disturbance**, that encloses all the uncertainty affecting the dynamics of the system, like modelling mismatches, finite precision in the measure of initial conditions or even systematic or random external disturbances. In most cases the amplitude of these disturbances can be limited, so we consider in the method bounded disturbances. On the other hand, the control available is usually limited by the experimental conditions. For this reason, we also consider in this scheme that the control available in the most real scenarios, is bounded.

The intrinsic instability of the chaotic saddle together with the action of disturbance creates a difficult scenario where keeping the control small might seem not realistic. However it is possible to keep the trajectories close to the chaotic saddle taking advantage of the horseshoe map present in the phase space that produces the chaotic saddle. This geometrical action implies the existence of certain sets called safe sets that lie in the vicinity of the chaotic saddle. These sets are used to keep the trajectories controlled (close to the chaotic saddle).

To find these sets, we consider that in the region Q of the phase space where the transient chaos is located, the dynamics can be described with the map:

$$q_{n+1} = f(q_n) + \xi_n + u_n, \qquad \text{with} \quad |\xi_n| \leq \xi_0, \quad |u_n| \leq u_0.$$

Here $q_n \in \mathbb{R}^n$ represents certain phase state of the system, and we assume that the map f acts on a region Q like a horseshoe map ([17]). The disturbance ξ affecting the map is considered to be bounded so that $|\xi_n| \leq \xi_0$. The control term u is also limited so that $|u_n| \leq u_0$.

Without the action of a disturbance and a control, nearly all trajectories inside Q (except a zero measure set) escape from it after some iterations. However if disturbances are present, all trajectories eventually escape.

Under this control scheme, the safe set (represented by Q_∞) is a subset of Q, such that for all $q \in Q_\infty$, the trajectory $q_{n+1} = f(q_n) + \xi_n + u_n$ stay in Q_∞ forever (see Fig. 2.1). The control u_n is chosen at each iteration, with the knowledge of $f(q_n) + \xi_n$, and applied to place the trajectory again in the set Q_∞. We say that trajectories found under these conditions are **admissible trajectories**.

The set Q_∞ can be directly computed following an iterative process. Starting with the set Q represented by a grid stored in the computer, the algorithm takes initially the set $Q_0 = Q$. Then, given the grid point $q \in Q_0$ and the disturbed image $f(q) + \xi$, the algorithm checks whether exist a suitable control $|u| \leq u_0$ such that $f(q) + \xi + u$ falls again in Q_0. If all possible disturbed images $f(q) + \xi$ corresponding to q are controllable, then the point q is conserved. If not, it is removed. Proceeding similarly with all points of Q_0 a new set $Q_1 \subset Q_0$ is obtained.

However we do not know yet if Q_1 is a safe set. To do that, it is necessary to repeat the process described above, but now with the set Q_1 instead of Q_0. As

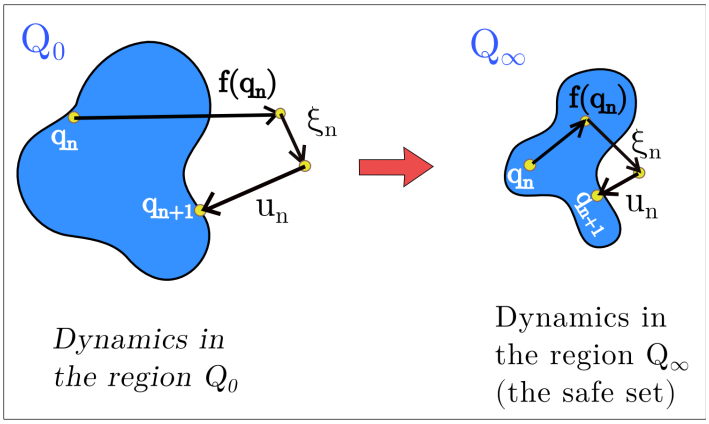

Figure 2.1. Dynamics in Q_0 and Q_∞. The left side shows an example of a region Q_0 (in blue) in which we want to keep the dynamics described by $q_{n+1} = f(q_n) + \xi_n + u_n$. We say that $|\xi_n| \leq \xi_0$ is a bounded disturbance affecting the map, and u_n is the control chosen so that q_{n+1} is again in Q_0. To apply the control, the controller only needs to measure the state of the disturbed system, that is $[f(q_n) + \xi_n]$. The knowledge of $f(q_n)$ or ξ_n individually is not required. The right side of the figure, shows the region $Q_\infty \subset Q_0$ (in blue), called the *safe set*, where each $x_n \in Q_\infty$ has $x_{n+1} \in Q_\infty$ for some control $|u_n| \leq u_0$, which is chosen depending on ξ_n. Notice that the removed region does not satisfy $|u_n| \leq u_0$.

a result, a smaller set $Q_2 \subset Q_1 \subset Q_0$ is obtained. This process is repeated until it converges, in which case Q_∞ is found. This set is known as the **safe set**. All the disturbed images $f(q) + \xi$ corresponding to the safe set, can be put them back (with control $|u| \leq u_0$) again in the safe set. Due to this, the safe set is a positively invariant set [21, 22, 23, 24, 25]. The surprising result, and the main fingerprint of this method is the existence of safe sets with control values $0 > u_0 > \xi_0$. This means that the action of a disturbance to distort the dynamics can be counteracted with a smaller effort of control.

Based on the process presented above, it has been developed an algorithm called the **Sculpting Algorithm** [16], to automatically compute the successive regions Q_n until the safe set is finally found. We illustrate the procedure of finding the safe set in Fig. 2.2. We fix the bound u_0 and ξ_0 and the region $Q_0 = Q$. The *ith* step can be summarized as follows:

1. Morphological dilation of the set Q_i by u_0, obtaining the set denoted by $Q_i + u_0$.
2. Morphological erosion of set $Q_i + u_0$ by ξ_0, obtaining the set denoted by $Q_i + u_0 - \xi_0$.
3. Let Q_{i+1} be the points q of Q_i, for which $f(q)$ is inside the set denoted $Q_i + u_0 - \xi_0$.
4. Return to step 1, unless $Q_{i+1} = Q_i$, in which case we set $Q_\infty = Q_i$. We call

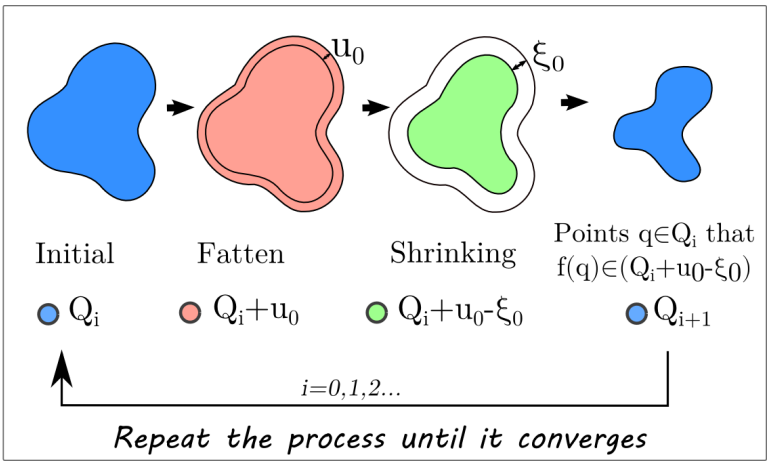

Figure 2.2. Graphical process used by the Sculpting Algorithm to obtain the safe set. The denoted set Q_i is fattened by the thickness u_0. The fattened set is displayed in red. Then, the new set is shrunk or contracted by a distance ξ_0, obtaining the set denoted $Q_i + u_0 - \xi_0$ (in green). Finally we remove the grid points $q \in Q_i$ whose image $f(q)$ falls outside $Q_i + u_0 - \xi_0$. Notice that $Q_{i+1} \subset Q_i$.

this final region, the *safe set*. Note that if the chosen u_0 is too small, then Q_∞ may be the empty set, so that a bigger value of u_0 is required to control the trajectories.

The computation of the safe set Q_∞ requires to take a finite grid covering Q_0, since it is not possible to compute the infinite number of points in Q_0. We will call the grid resolution as the distance between two adjacent points q. Higher resolutions give a more accurate safe set, and beyond a critical resolution of the grid covering Q and ξ, the safe set remains practically unchanged. Due to the complex shape of the chaotic saddle underlying the chaotic dynamics, the derivation of a rigorous proof of the convergence of the algorithm would be extremely difficult. However, from a computational view, it is easy to show that the algorithm converges in a finite number of steps, since the grid used is composed of a finite amount of points. From a practical point of view, we recommend to compute the safe set with the algorithm proposed with increasing resolutions until finding the critical value for which the shape of the safe set found remains unchanged. That one will be a very good approximation of the real safe set. We also should take into account that the finite resolution of the computation is by itself a source of disturbance, so the magnitude of the disturbance can never be zero.

In Fig. 2.3 it is shown an example of a safe set that was computed for the Lorenz system for a choice of parameters where transient chaos is present. Without control, trajectories eventually escape toward two external fixed points. The points belonging to the safe set, can be controlled and kept in the chaotic region forever. In Chapter 4, this system is studied in detail.

The procedure explained here is applicable when the disturbance and the control

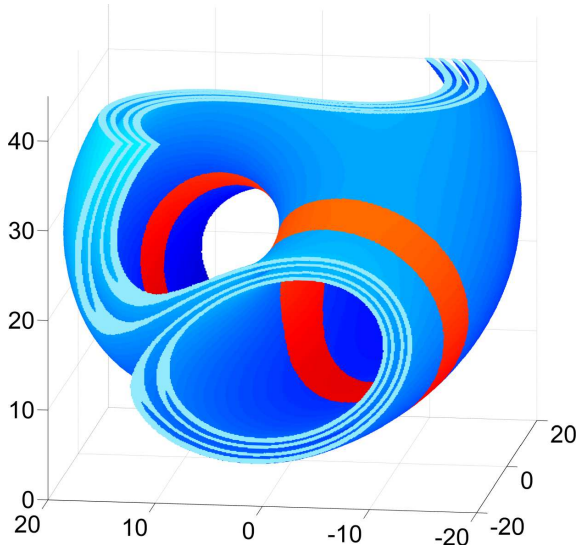

Figure 2.3. Example of the set needed to partially control the Lorenz system. The figure shows an example of a 3D safe set in the phase space computed for the partially controlled Lorenz system in the transient chaotic regime. The blue set represents the points of the phase space that satisfy the control condition defined by the partial control method. The red set is a subset of the blue set, and represents the asymptotic region where the controlled dynamics converges.

affect the variables of the system. A simple code in Matlab is available in [26]. In Chapters 5 however, we will show a similar procedure (after minor modifications) where the disturbance and control is applied on some parameter of the system. In Chapter 6 other variation of the partial control scheme is shown to deal with delay-coordinates maps. Nonetheless, in Chapter 8 a completely new way to compute safe sets is presented.

Chapter 3
Partial control to avoid a species extinction

Extinction of species is one of the most dramatic processes in ecology. In case where extinction depends on the population dynamics of other species, to avoid the extinction might is a big challenge from an ecological point of view. The nonlinear interactions among species together with the presence of noise, often result in a complex global dynamics, making difficult to predict external actions over the system.

Here we use an extended version of the McCann-Yodzis [18] three-species food chain model proposed by Duarte et al. [27], where a cooperative hunting term was added to the original McCann-Yodzis model and where the three species coexist: resources, consumers and predators. We consider a situation for which a chaotic transient is present in the dynamics implying the predators extinction. Taking into account that the system is affected by external disturbances, we implement the partial control with the goal of avoiding the extinction. We have also shown that the partial control method implies smaller controls.

3.1 Partial control to avoid a species extinction

In this application of the partial control method, we have worked with an ecological model that describes the interaction between three species: resources, consumers and predators. The interest of this model lies in the fact that, for some choices of parameters, transient chaos appears involving the extinction of one of the species, the predators. Without no control, the system evolves from a situation where the three species coexist towards a limit cycle where just resources and consumers survive.

The model that we have used is an extension of the McCann-Yodzis model [18] proposed by Duarte et al. [27], which describes the dynamics of the population density of a resource species R, a consumer C and a predator P. The resulting model is given by the following set of nonlinear differential equations:

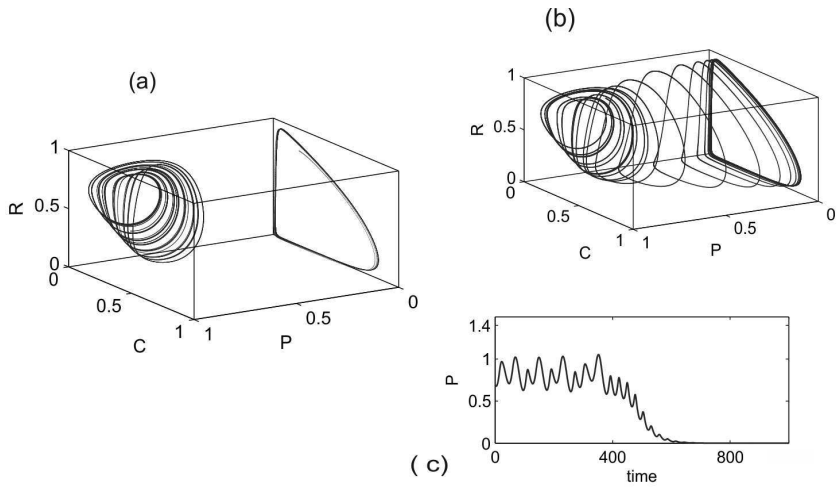

Figure 3.1. Dynamics of the extended McCann-Yodzis model proposed by Duarte et al. from Eqs. (3.1). Depending on the values of the parameters (K, σ) different dynamics are possible. Fixing $K = 0.99$, the boundary crisis appears at $\sigma_c = 0.04166$. (a) Before the boundary crisis ($K = 0.99$, $\sigma = 0$), there are two possible attractors depending on the initial conditions: one chaotic attractor where the three species coexist, and one limit cycle where only the resources and consumers coexist. (b) After the boundary crisis ($K = 0.99$, $\sigma = 0.07$), the limit cycle is the only asymptotic attractor. (c) Time series of the predators population corresponding to the case (b), where the chaotic transient before the extinction is shown.

$$\begin{aligned}
\frac{dR}{dt} &= R\left(1 - \frac{R}{K}\right) - \frac{x_c y_c C R}{R + R_0} \\
\frac{dC}{dt} &= x_c C\left(\frac{y_c R}{R + R_0} - 1\right) - \psi(P)\frac{y_p C}{C + C_0} \\
\frac{dP}{dt} &= \psi(P)\frac{y_p C}{C + C_0} - x_p P.
\end{aligned} \tag{3.1}$$

Note that R, C and P are non-dimensional variables. Following [18] and [27], we have fixed the ecological parameters: $x_c = 0.4$, $y_c = 2.009$, $x_p = 0.08$, $y_p = 2.876$, $R_0 = 0.16129$, $C_0 = 0.5$, $K = 0.99$ and $\sigma = 0.07$. For these values transient chaos behaviour appears, and the predators eventually get extinct (see Fig 3.1).

With the aim of avoiding the extinction, we have applied the partial control method [16]. Since this model is a flow, we need first to discretize the dynamics to built a map. Different choices are possible. In this case we have chosen to build the map by using the successive local minima (P_n, P_{n+1}), where P_n denotes the nth local minimum of the P variable time series. This set of points generates an approximately one-dimensional curve in the phase space as shown in Fig. 3.2. The corresponding return map of the form $P_{n+1} = f(P_n)$ is shown in Fig. 3.3. Notice that, the iterates of any initial point for which $P_n > P^*$, have a chaotic behaviour until they finally asymptotes to zero when it crosses a critical value $P_n < P^*$, which actually implies

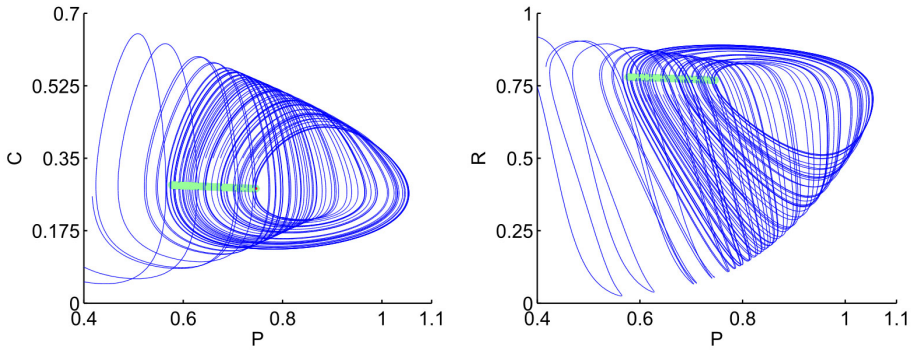

Figure 3.2. Set of local minima in phase space. Blue line: trajectories in phase plane (P, C) and (P, R). Green line: set of local minima of $P(t)$ used to build the one-dimensional map. As shown, the set of local minima is approximately parallel to the P axis.

the extinction of the predators population. We assume that the map constructed in this way is just an approximation, so we also introduce a disturbance term ξ_n into the map, in order to model potential mismatches.

After introducing the disturbance term ξ_n and the control term u_n in the map, the partially controlled dynamics is given by:

$$P_{n+1} = f(P_n) + \xi_n + u_n. \tag{3.2}$$

In our case, we want to sustain the dynamics close to the chaotic attractor, avoiding the escape produced when $P_n < P^* = 0.589$, therefore we choose the initial Q region to be the interval $P_n \in [0.589, 0.84]$ indicated in Fig. 3.3. Then we use the Sculpting Algorithm to find the safe set.

The computation of the safe set depends on the chosen values of ξ_0 and u_0. To show an example, we have chosen for our simulations the values $\xi_0 = 0.0114$ and $u_0 = 0.0076$, where u_0 is very close to the minimum value for which the safe set exists. In Fig. 3.3 we represent the steps of the algorithm to build the safe set.

In Fig. 3.4, we represent the obtained final safe set that allows us to control the map constructed with the minima of the P variable. Notice that from the point of view of the real dynamics (continuous trajectories), the control is applied every time the trajectory crosses the set of minima. If the value $f(P_n) + \xi_n$ is inside a safe set, we do not apply control, and if it is outside, we relocate it inside the nearest safe point, resulting the new safe point $P_{n+1} = f(P_n) + \xi_n + u_n$. The criterion to control the point to the nearest safe set is only a choice, since in most cases there are other possible points belonging to the safe set which we can reach without exceeding the upper bound of control. From an ecological point of view, this flexibility allows us to choose the better option considering our specific needs. For example, depending on our ease to stocking or harvesting individuals we can make the choice which involves the smallest effort.

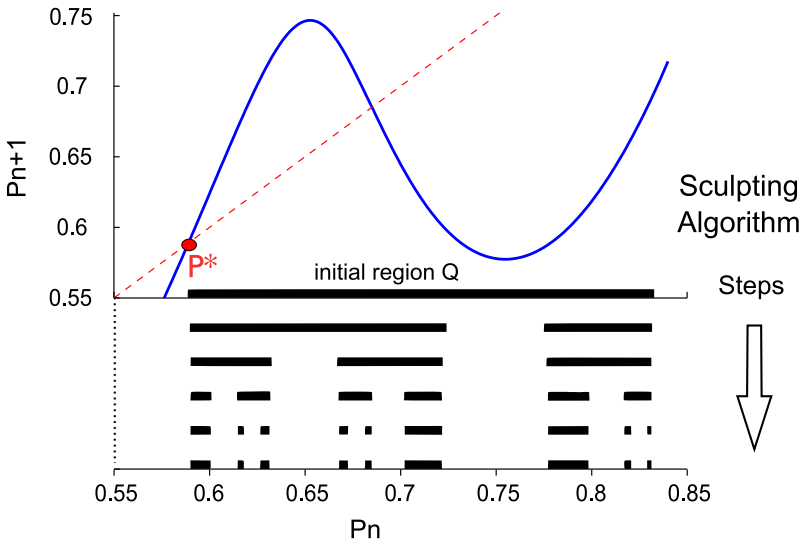

Figure 3.3. Return map $P_{n+1} = f(P_n)$ obtained by using the successive local minima of the time series $P(t)$. Notice that below $P^* = 0.589$ the trajectory asymptotes to zero. In order to keep the trajectory in the region Q indicated, we compute the safe set. In the lower part are shown the steps of the Sculpting Algorithm that converges to the final safe set. The horizontal *black bars* helps us to visualize the process and represent the points P_n that satisfy the condition to be a safe point at each step. In this case, the upper bound of disturbance and control used are $\xi_0 = 0.0114$ and $u_0 = 0.0076$, respectively.

In Fig. 3.4 it is also represented the *asymptotic safe set*. This subset of the safe set [17] appears typically when the system is dissipative, and represents the asymptotic region of the safe set where the controlled trajectories converge. Once the trajectories enter into the asymptotic safe set, they never abandon it.

Controlled trajectories in phase space are shown in Fig. 3.5, where we also indicate the safe set used with the projections on the set of the minima for a clear visualization. In Fig. 3.6, we represent the corresponding controlled time series of the predators population (blue line) in contrast to the uncontrolled trajectory (red line), involving the extinction. On the right of the figure we also represent a zoom of one minimum to highlight how the noise (that we call disturbance) appears and how the control is applied. Notice that the noise amplitude shown only represents the difference between the deterministic trajectory and the noisy one.

In order to see a further analysis, in Fig. 3.7 it is represented the strength of the noise and the strength of the control applied for 30.000 iterations corresponding to the time interval $[0, 1.2 \times 10^6]$ in the time series of $P(t)$. While the strength of the noise (absolute value) is distributed uniformly between the values 0 and $\xi_0 = 0.0114$, all values of the control (absolute value) are located under the maximum $u_0 = 0.0076$, showing that the partial control method works as it is designed. We also compare the mean of the noise and the control, obtaining an average control 0.0018 which is less than half the average noise 0.0057. As we will show later, the small average

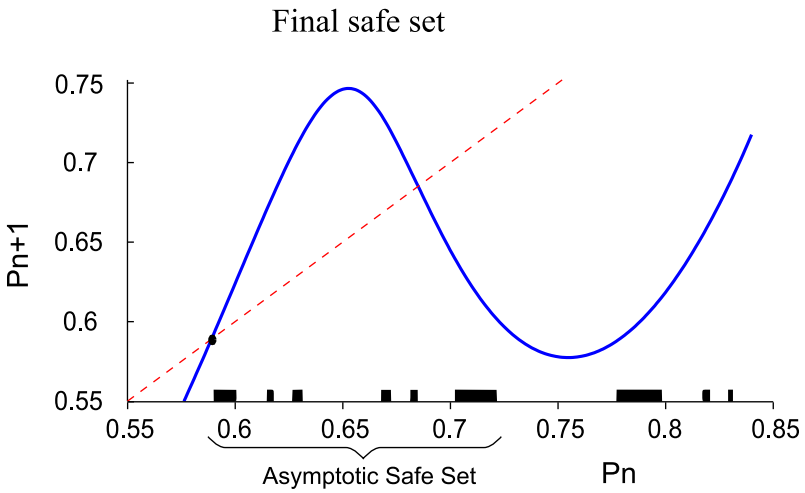

Figure 3.4. Final safe set. The safe set is composed of different subsets obtained with the Sculpting Algorithm using $\xi_0 = 0.0114$ and $u_0 = 0.0076$. We also indicate the group of subsets where the dynamics remains trapped, that is, the asymptotic safe set.

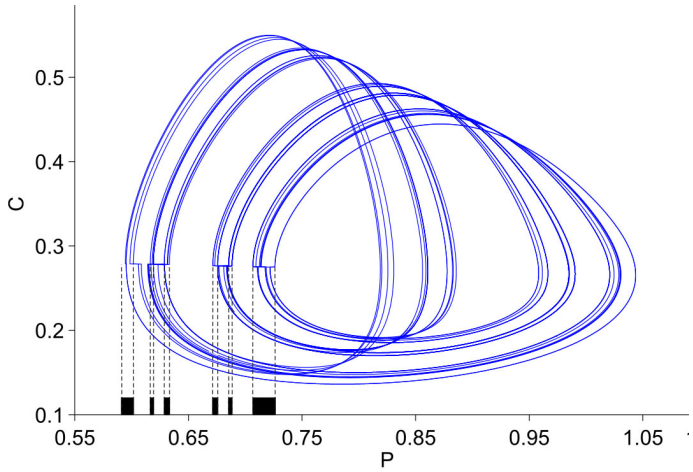

Figure 3.5. Controlled trajectory in the phase space. Controlled trajectory with $\xi_0 = 0.0114$, represented in the phase plane (P, C). We also show the asymptotic safe set computed with $\xi_0 = 0.0114$ and $u_0 = 0.0076$, and its projection in the set of minima (dashed line) where the control is applied.

control that we need to use, is another remarkable feature of this control method.

To show how the safe sets change depending on the upper bound value of noise ξ_0, we represent in Fig. 3.8 different safe sets with ξ_0 in the range $[0.001, 0.057]$, and the corresponding controlled trajectories in phase space. Note that the trajectories are sustained in the chaotic region with $|u_n| \leq u_0$ for all the iterations, and the average control used is less than twice the noise average. It is remarkable that the trajectories can be controlled without great modifications, keeping the chaotic behavior, as a permanent state.

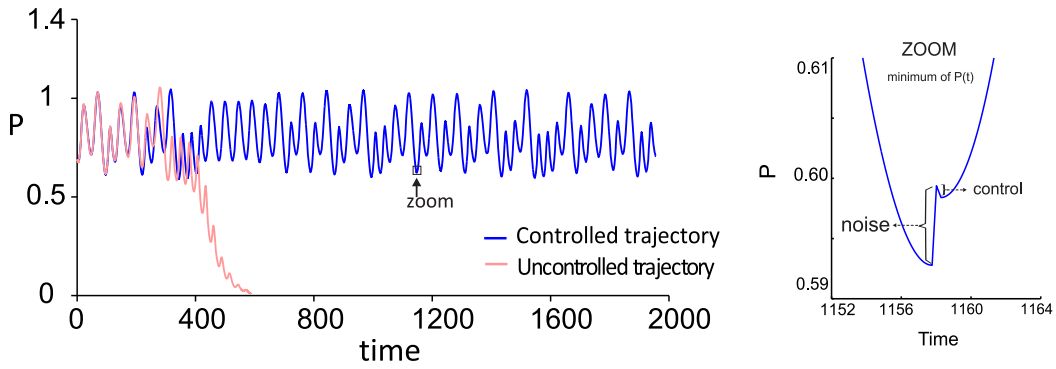

Figure 3.6. Controlled time series. Red line: Time series of the predators population without control exhibiting a escape towards zero, that implies the extinction of the predators. Blue line: Controlled time series of the predators population where the extinction is avoided. At every minimum, the value of P is evaluated and if necessary a small control is applied. This time series corresponds to 50 iterations in the return map $P_{n+1} = f(P_n)$. A zoom of one of the minima of the time series of $P(t)$ is also shown on the right in order to see how the noise is introduced and how the corresponding control is applied.

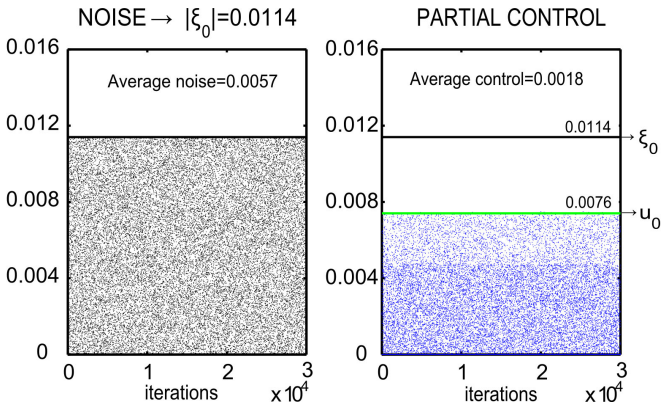

Figure 3.7. Strengths of noise and control applied for 30000 **iterations**. Noise and control amplitude are represented as points instead of bars for a clear visualization. On the left, the strength of the noise that affects the map. On the right, the respective strength of controls applied for the partial control method. We also indicate the upper bound of the noise $\xi_0 = 0.0114$ and upper bound of the control $u_0 = 0.0076$ used to compute the safe set.

3.2 The partial control method implies smaller controls

In the work [27], the authors apply a control method (Dhamala and Lai method) described in [9], in order to sustain the chaotic behavior after the crisis for the McCann-Yodzis ecological model [18] with cooperative hunting. This method is one of the main control methods applied in systems that exhibit transient chaos, however

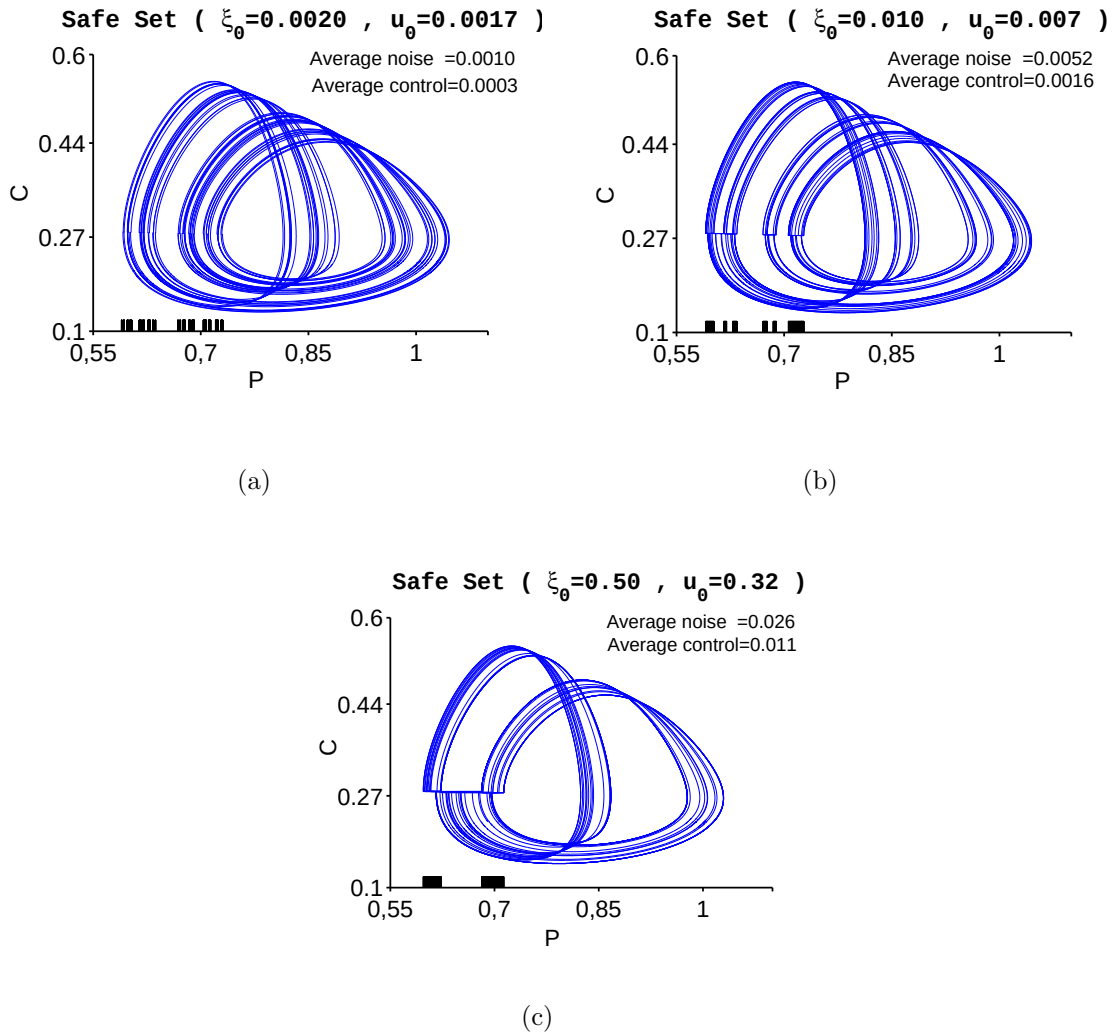

(a) (b)

(c)

Figure 3.8. Different disturbance magnitude. Controlled trajectories in the phase plane (P, C) and the respective asymptotic safe sets for different noise intensities in the range $\xi_0 = [0.002, 0.50]$.

it does not contemplate at all the presence of any external disturbance.

The main idea here is to consider the problem analyzed in [27], including an external disturbance, and compare both methods, the Dhamala and Lai strategy and the partial control.

The control method of Dhamala and Lai is based on the observation that a point $P < P^*$ in the return map, goes quickly to zero. In this sense, it is possible to identify one escaping zone and two target regions, by computing certain preimages of the fixed point P^* as shown in Fig. 3.9. The idea is that all points inside the escape region, fall above P^* in the next iteration, while the points of the target

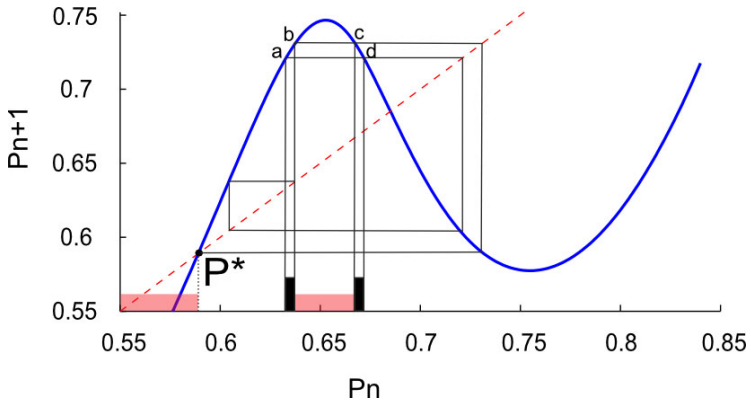

Figure 3.9. Dhamala and Lai method applied to the map. The *black sets* represent the two target regions used to control the trajectories. The *red sets* represent the escape regions. We colored the regions with different thicknesses to help us in the visualization.

region, survive a long time before escaping.

The control is defined as follows: we have two target regions (*black sets*) defined by the intervals $[a_1, b_1]$ and $[b_1, c_1]$. Now we define the escaping regions (*red sets*), composed by the points $P < P^*$ and the points between the target regions, see Fig. 3.9. When a given iteration falls into the escaping region, we apply a control to relocate P inside the nearest target point. Note that, in contrast with safe sets of the partial control that are different depending on the bounds of disturbance and control, the target sets of the Dhamala and Lai method are always the same.

In Fig 3.10, we represent the average control applied in both methods for different values of the strength of the disturbance in the range $\xi_0 = [10^{-3}, 10^{-1}]$. In view of the results, we can say that the Dhamala and Lai control strategy, implies larger controls than the partial control method in almost all situations.

One could think that this different performance is due to the presence of disturbance, and the fact that the Dhamala and Lai method was not designed to deal with disturbances, but in fact, the smaller the disturbance the better results achieves the partial control. In contrast, when the disturbance is too large, both methods achieve similar results. The reason is because large disturbances blur the chaotic saddle so much, that only a gross control is able to avoid the escape.

3.3 Conclusions

In this chapter, we have analyzed the problem of the species extinction using an extended McCann-Yodzis ecological model affected by external disturbances. This system, which is composed of three species, presents a boundary crisis involving the extinction of one of them. With the aim of avoiding the extinction, we have applied the partial control method. We show that the method is able to control the dynamics of the three-dimensional flow, applying control just on the predators population. Different strengths of noise have been studied, showing in all cases, that the partial control method, was able to sustain the transient chaotic dynamics,

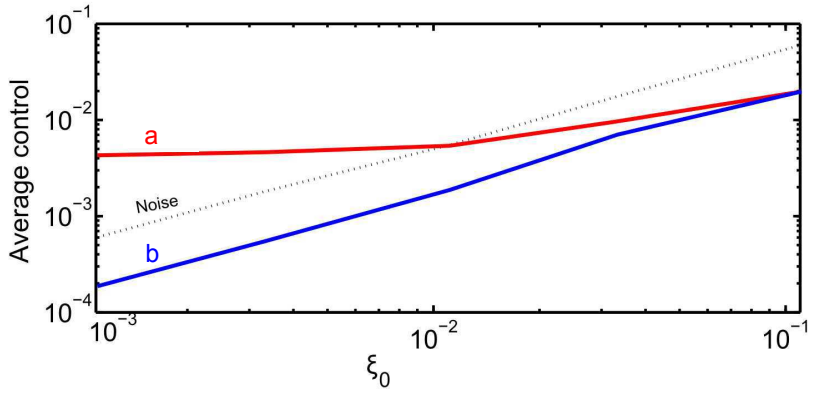

Figure 3.10. Dhamala and Lai method vs partial control method. Comparative of the average controls in a log-log scale. Dashed black line: Average strength of the noise in the range $\xi_0 = [10^{-3}, 10^{-1}]$. (a) Red line: Average strength of the control method used in [27]. (b) Blue line: Average strength of the partial control.

avoiding the extinction. In addition, a comparison with another well-known method was carried out. Taking different strengths of noise, it was shown that the amount of control needed by the partial control, is smaller than the control strategy proposed by Dhamala and Lai (1999), specially for small disturbances.

Chapter 4
Controlling chaos in the Lorenz system

The Lorenz system is a paradigmatic example in Nonlinear Dynamics that, exhibits transient chaos for a certain choice of parameters. In this regime trajectories eventually converge to two fixed points attractors. In this chapter, we analyze three quite different ways to implement the partial control method, in order to avoid escapes. First, we apply this method by building a 1D map using the successive maxima of one of the variables. Next, we implement it by building a 2D map by using a Poincaré section. Finally, we built a 3D map, which has the advantage of using a fixed time interval between the application of the control, which can be useful for practical applications.

4.1 Partial control to avoid the fixed point attractors in the Lorenz system

The Lorenz system [28] is a flow that describes a simplified model of atmospheric convection. The model consists of three ordinary differential equations,

$$\begin{aligned} \dot{x} &= -\sigma x + \sigma y \\ \dot{y} &= -xz + rx - y \\ \dot{z} &= xy - bz. \end{aligned} \tag{4.1}$$

Depending on the parameter values r, σ, and b, the system can exhibit different dynamical behaviors, either periodic solutions, chaotic attractors or even transient chaos. Fixing $\sigma = 10$, $b = 8/3$, transient chaos can be found in the interval $r \in [13.93, 24.06]$ as described in [29, 30]. For our simulations, we have chosen the value $r = 20.0$. In this regime, as we show in Fig. 4.1, there are transient chaotic orbits that eventually decay towards one of the two point attractors which physically represent a steady rotation of a fluid flow, one clockwise, and the other counterclockwise. The point attractors are located in the following positions,

$$\begin{aligned} C^+ &= (\sqrt{b(r-1)}, \sqrt{b(r-1)}, r-1) \approx (7.12, 7.12, 19) \\ C^- &= (-\sqrt{b(r-1)}, -\sqrt{b(r-1)}, r-1) \approx (-7.12, -7.12, 19). \end{aligned}$$

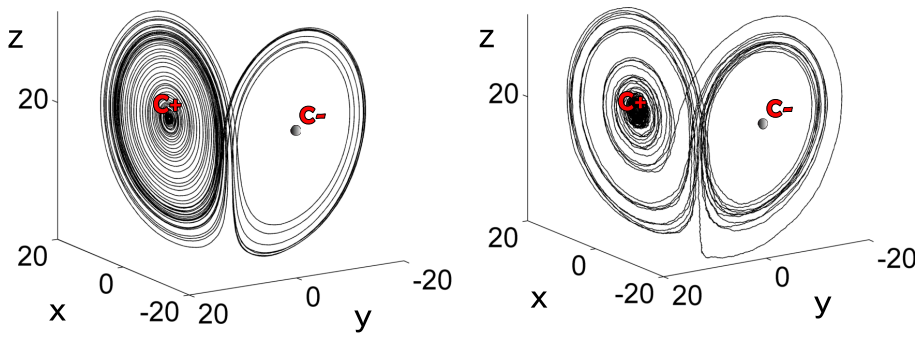

Figure 4.1. Dynamics of the Lorenz system. We select the transient chaotic regime with $\sigma = 10$, $b = 8/3$ and $r = 20$. On the left, the trajectory is deterministic. On the right, the trajectory is affected by some disturbances. The disturbances here, were enlarged in order to help the eye. Almost all trajectories eventually spiral to one of the two attractors (C^+ or C^-). Here both trajectories spiral to C^+.

In this figure, we also represent the case where some noise is present in the trajectory. The noisy trajectory behaves similarly to the deterministic one. The main difference is the time involved to reach the attractors, which can be increased or reduced.

The goal of applying control here is to avoid trajectories falling in one of the attractors. To apply the control method, we need first to built a map, however we have found many interesting possibilities. Here we explore three of them, consisting of a 1D, 2D and 3D maps respectively.

4.1.1 The 1D map

As shown by Lorenz [28], when plotting the pairs of maxima (z_n, z_{n+1}), one gets (approximately) a function f where $z_{n+1} \approx f(z_n)$. We can see this clearly in Fig. 4.2. Knowing a local maximum of z is Z, allows one to estimate $|x|$ and $|y|$ with considerable precision. Transient chaos can be observed in the interval $z_n \in [27.3, 30.7]$, so we have chosen this interval as the set Q_0. We have taken $\xi_0 = 0.080$ and the control bound $u_0 = 0.055$ ($u_0 < \xi_0$). This control value is approximately the minimum value for which a safe set exists. Then, we have obtained the safe set by using the Sculpting Algorithm. In Fig. 4.2, we can see how the algorithm sculpts the initial region Q_0 until it finds Q_4 where it converges, so $Q_4 = Q_\infty$ is the safe set. For this computation we have used a grid of 4000 points in the interval $z_n \in [26.8, 30.8]$, so the grid resolution is 0.001.

In Fig. 4.3 we show a controlled time series of the z variable in contrast with an uncontrolled trajectory. We can see that chaos is sustained by applying small perturbations in the maxima of the variable z. Although the map only contains the variable z, the control in the original phase space must be applied in the three variables. The reason is because each local maximum of z is described by 3 coordinates (x_m, y_m, z_m), and the coordinates x_m and y_m vary from maximum to maximum. Sometimes, if this variation is negligible, it is not necessary to apply control in these

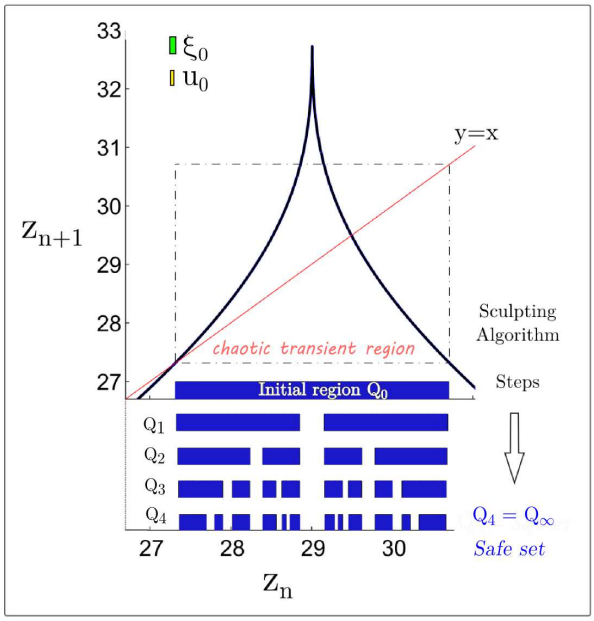

Figure 4.2. The 1D safe set. The black curve is the 1D map built with the successive maxima of z. We take as initial set Q_0 (upper segment in blue) the region where transient chaos occurs. The map is affected by disturbances with an upper bound $\xi_0 = 0.080$, while we choose the upper bound of the control as $u_0 = 0.055$, (the bounds are the width of the bars displayed in the upper left side). The figure shows the successive steps computed by the Sculpting Algorithm, from an initial region Q_0 until it converges to the subset $Q_4 = Q_\infty \subset Q_0$. We use a grid of 4000 points in the interval $z_n \in [26.8, 30.8]$, that corresponds to a resolution of 0.001.

coordinates (x_m and y_m) as in the case of the ecological model treated in the previous chapter where we have applied control to one of the variables (the predators species). The main advantage of this 1D map is that the computation of the safe set is easy and fast. This kind of map is useful when the main component of the disturbance affects the variable we use to built the map.

4.1.2 The 2D map

It is straightforward to build a 2D map taking a Poincaré section that intersects the flow. For our purpose, we have chosen the plane $z = 19$ with the ranges $x \in [-3, 3]$ and $y \in [-3, 3]$, as shown in Fig. 4.4. The trajectories that cross this plane are in the transient chaotic regime, while the attractors $C^+ = (7.12, 7.12, 19)$ and $C^- = (-7.12, -7.12, 19)$ that we want to avoid, are situated outside this plane (see the location in Fig. 4.4). Since we want to keep the trajectories passing through the plane, we have taken as $Q = Q_0$, the square $x \in [-3, 3]$ and $y \in [-3, 3]$ in the plane

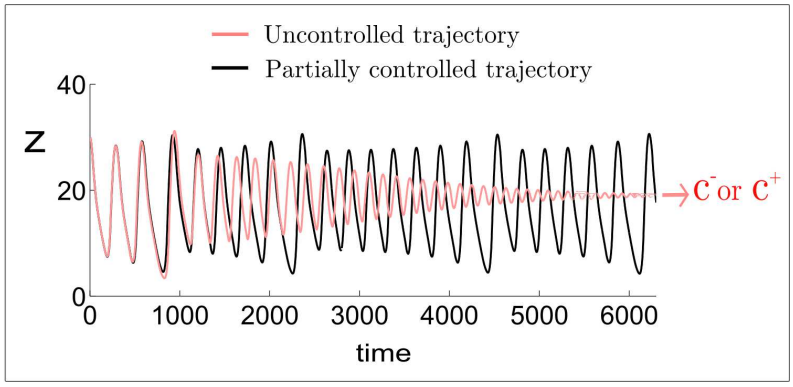

Figure 4.3. Time series of the variable z for the Lorenz system with r = 20. The figure shows a comparison between an uncontrolled trajectory that escapes from chaos (red line) and a partially controlled trajectory (black line). Starting with the same initial condition, the uncontrolled trajectory eventually decays to C^+ or C^-, which physically means a steady rotation of the fluid flow. On the other hand the partially controlled trajectory is maintained in the chaotic transient regime, that is, the rotation of the fluid flow remains chaotic forever.

$z = 19$. Then we have used the Sculpting Algorithm to find the safe set $Q_\infty \subset Q$.

As an example, we have assumed that the map is affected by some disturbances with upper bound $\xi_0 = 0.09$. The minimum control found for which the safe set exists is $u_0 = 0.06$. In Fig. 4.5(a), this safe set is displayed. A partially controlled trajectory is represented in Fig. 4.5(b), where we have also shown the safe set in phase space in order to see how it is used to control the system. Notice that, we are able to avoid the attractors, applying only small perturbations in the plane. A zoom of this region is shown in Fig. 4.5(c). The computation was carried out taking a grid size of 1200×1200 points, (grid resolution is 0.005 in both variables x and y).

The main advantage of the 2D map is that allows to partially control systems where all the variables are affected by disturbances since the image $x_{n+1} = f(x_n) + \xi_n$ in the Poincaré surface is a certain ellipse, and both dimensions of the surface are controlled. In addition, as opposed to the 1D map, where we have to act on the x, y and z variables to control the system, the control in the 2D map is only applied in the variables x and y, since z is constant. This can be an advantage in systems where it is difficult or expensive to apply the control in each variable.

4.1.3 The 3D map

The 1D approach as well as the 2D approach, have the disadvantage of having to track the trajectory to know when it passes through the control region (a maximum or the Poincaré section), where we apply the control corrections. Another strategy is to use a time discretization of the Lorenz system, by taking a suitable time interval Δt between the current state of the system and the future state, that is,

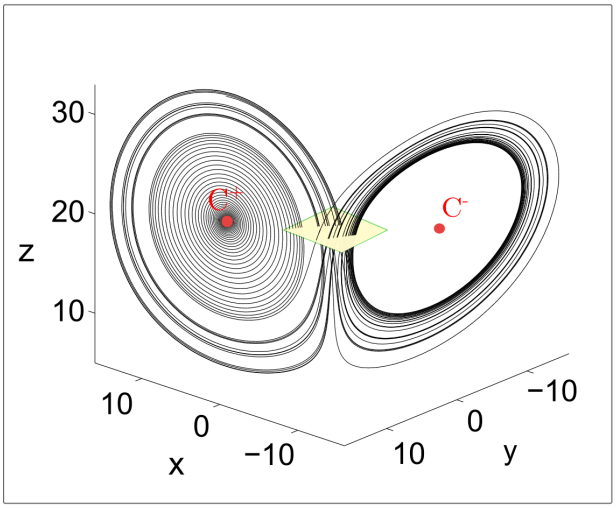

Figure 4.4. The Lorenz system with r = 20 (transient chaos). The figure shows an uncontrolled trajectory in phase space crossing the square with $x \in [-3, 3]$ and $y \in [-3, 3]$ in the plane $z = 19$. To built the map, we use a grid of initial conditions in the plane, and evaluate the images of the trajectories when they cross again the plane. The goal of the control will be to keep the trajectories in this plane, avoiding the escape to one of the attractors C^+ or C^-, placed outside.

$x(t_0), y(t_0), z(t_0) \to x(t_0 + \Delta t), y(t_0 + \Delta t), z(t_0 + \Delta t)$. By computing the time-$\Delta t$ image of each point of a 3D grid that covers the phase space, we can obtain the 3D map. We discuss the advantages of this map below.

To built this kind of map, a suitable choice of Δt is important. For too small values, safe sets (with $u_0 < \xi_0$) does not exist. The topological explanation for this, is that the flow is acting like a pastry transformation which takes some time to be completed. Once this time is reached, the safe set appears. For our Lorenz system, there are safe sets for values of $\Delta t \geq 1.2$.

For the computation of the safe sets, we consider the domain with $x \in [-20, 20]$, $y \in [-20, 20]$, $z \in [0, 40]$, with a grid size of $400 \times 400 \times 400$, so the grid resolution is 0.1 for each variable. In this region the transient chaotic trajectories eventually decay to the attractors $C^+ = (7.12, 7.12, 19)$ and $C^- = (-7.12, -7.12, 19)$. In order to avoid C^+ and C^-, balls centered in these attractors are removed. See the region Q and a transient chaotic trajectory in Fig. 4.6. To obtain the map, we have computed the image of each point of Q with $\Delta t = 1.2$. Then, as an example, we have taken the value $\xi_0 = 1.5$ and $u_0 = 1.0$ (note $u_0 < \xi_0$). After applying the Sculpting Algorithm, the safe set shown in Fig. 4.7(a) is obtained.

To describe the controlled dynamics in the 3D map we write q_n for the controlled trajectory at time $n\Delta t$. To obtain a particular trajectory, we start with a given state q_n and then we compute the image $q_{n+1} = f(q_n) + \xi_n + u_n$, where ξ_n is chosen at random with $|\xi_n| \leq \xi_0$, and u_n is the convenient control that put the image in the

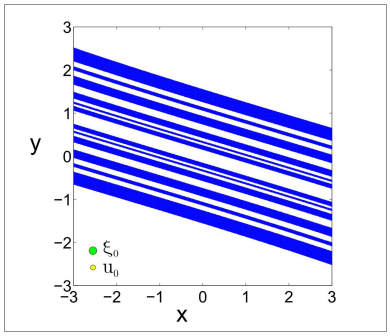

(a) Safe set

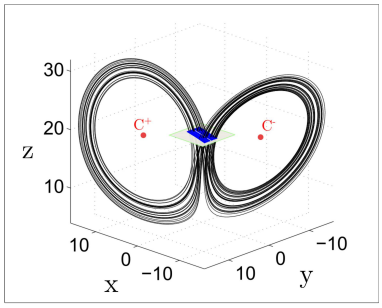

(b) Safe set and controlled trajectory

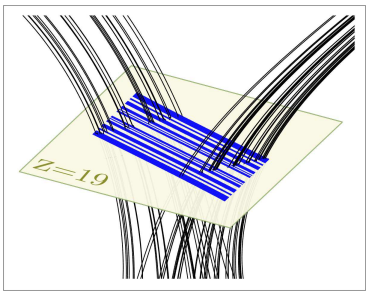

(c) Zoom of the controlled trajectory

Figure 4.5. The 2D safe set and how it is used to control the trajectory. (a) The safe set obtained using the map built with the plane displayed in Fig. 4.4. We show in blue the computed safe set Q_∞ for $\xi_0 = 0.09$ and $u_0 = 0.06$ ($u_0 < \xi_0$). The grid size used is 1201×1201 points. The radius of the balls in the lower left side indicates the bounds of the disturbance, $\xi_0 = 0.09$ (green) and the control $u_0 = 0.06$ (yellow). (b) A partially controlled trajectory in phase space. Each time that the trajectory crosses the safe set plane (placed in $z = 19$), the control is applied pushing the trajectory onto the set avoiding the escape from chaos. (c) Zoom of how the control is applied in the safe set.

safe set. In each case, ξ_n represents the disturbance accumulated by the trajectory in the time interval $\Delta t = 1.2$, while the control is always applied at a discrete time. In this case, we apply the minimum control, however other criterion is possible as long as the constraint $|u_n| \leq u_0$ is respected.

In Figs. 4.7(b) the asymptotic safe set (where the controlled trajectories converge) was drawn alone and in Fig 4.7(c) a half section of it to visualize the partially controlled trajectory inside. Notice that the trajectory does not leave the asymptotic safe set once it is reached, (unless the control is turned off). Once the dynamics converges, it is sufficient to use the asymptotic safe set to control the trajectories.

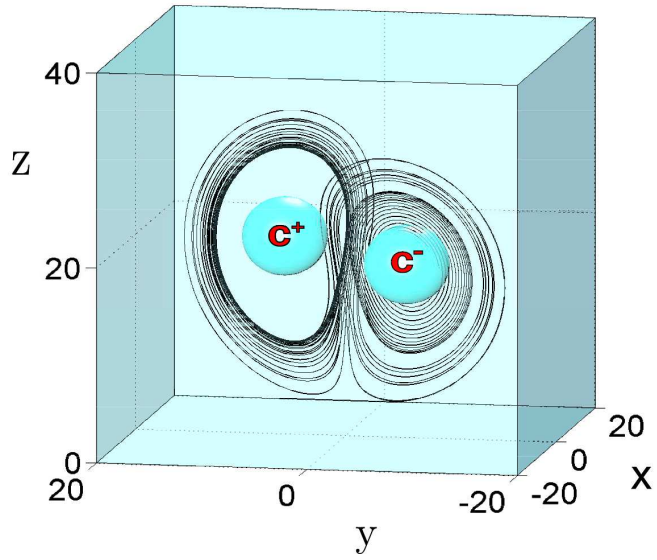

Figure 4.6. A choice of 3D set Q. The 3D set Q is the cube $x \in [-20, 20]$, $y \in [-20, 20]$, $z \in [0, 40]$ except the balls of radius 4, centered in $C^+ = (7.12, 7.12, 19)$ and $C^- = (-7.12, -7.12, 19)$ that are removed from Q. We want trajectories to stay in Q and not fall to these attractors. A trajectory is plotted to show the chaotic transient behavior in this region.

The controls, represented as yellow segments distributed along the trajectory, are applied every $\Delta t = 1.2$. We show this fact with a zoom in Fig. 4.7(d). As a result, the trajectories never fall into the attractors C^+ or C^-, keeping the dynamics in the chaotic region forever.

As we have mentioned, the safe set appears for values of $\Delta t \geq 1.2$, so it is possible to adapt the control frequency to our specific requirements, taking longer Δt values. To show that, we compute in Figure 4.8(a) the asymptotic safe set for $\Delta t = 1.8$, and with ξ_0 and u_0 unchanged. With this set we could control the system applying a control every $\Delta t = 1.8$ (see Fig. 4.8(b)) instead of $\Delta t = 1.2$ as in the previous case. However taking a longer Δt has a downside since in most scenarios that the cumulative effect of disturbances grows exponentially with time due to chaos, and therefore it is expected that the bound of control u_0 needed increases as well.

The use of a fixed Δt time to discretize the dynamics can be advantageous since in some situations the application of control in periodic time intervals can be easier and more convenient. In addition, the frequency of these controls can be adapted making it very flexible. For example, in the context of medicine, a medical treatment based on the partial control method, could be applied a fixed day of the week, which may suppose an easy and convenient control relationship between the physician and the patient. To highlight this feature, we compare in Fig. 4.9, three controlled trajectories obtained with the respective map (3D, 2D and 1D).

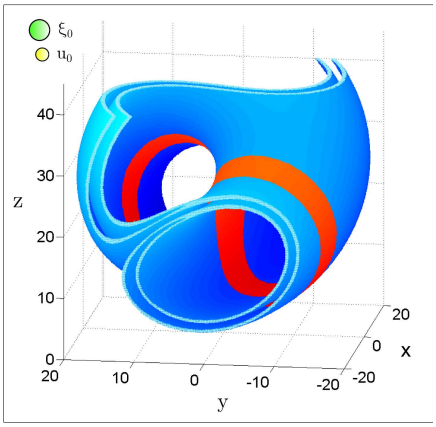

(a) Safe set with $\Delta t = 1.2$

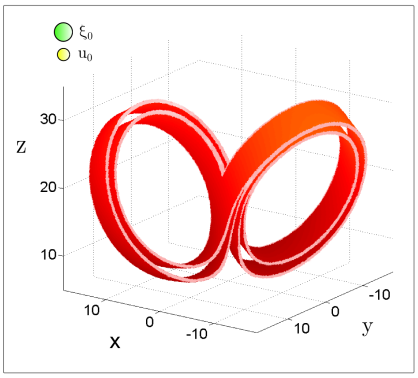

(b) Asymptotic safe set

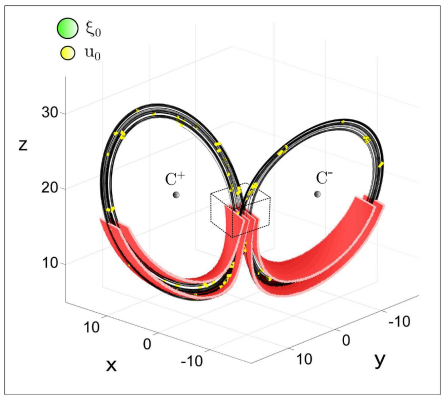

(c) Controlled trajectory

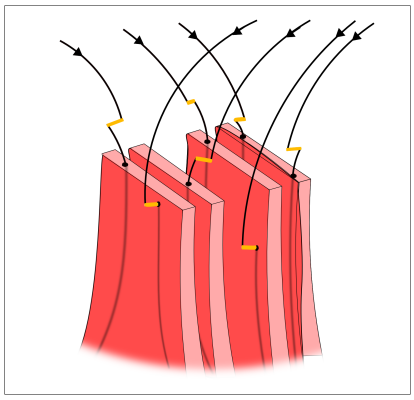

(d) Zoom of the controlled trajectory

Figure 4.7. The 3D safe set and how it is used to control the trajectory. (a) In blue the 3D *safe set* Q_∞ for Fig. 4.6, obtained after applying the Sculpting Algorithm. We set $\Delta t = 1.2$, $\xi_0 = 1.5$ (ξ_0 = radius of the green ball) and $u_0 = 1.0$ (u_0 = yellow ball's radius). In red the asymptotic safe set which is a subset of the safe set. This is the region in which the controlled trajectories eventually lie. (b) The asymptotic safe set alone. Partially controlled trajectories converge rapidly to this region. (c) A cut-away section of the asymptotic safe set in order to see a partially controlled trajectory (with $\Delta t = 1.2$) displayed in black. The controls (yellow segments inserted in the trajectory) are applied every $\Delta t = 1.2$. As a result, the trajectory is kept in the chaotic region and the attractors C^+ and C^- are avoided. (d) Zoom in the small cube displayed in Fig. 4.7(c). Only few trajectories are displayed for a better visualization. The controls (yellow segments) are applied to move the trajectories (in black) into the asymptotic safe set (in red).

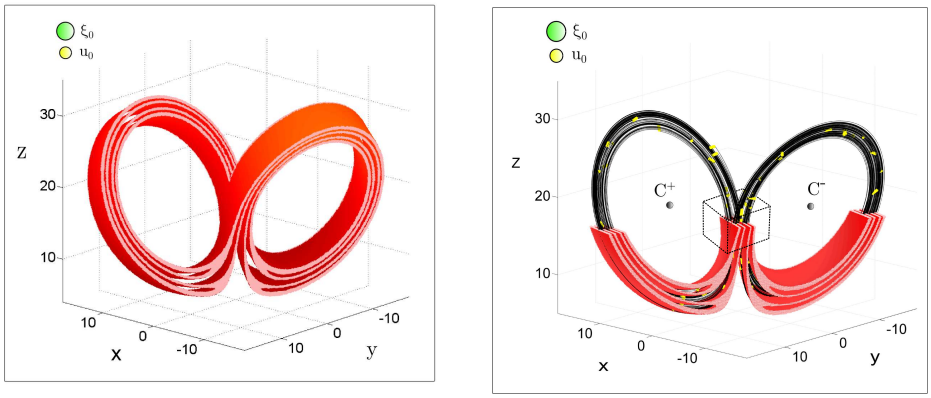

(a) Safe set with $\Delta t = 1.8$ (b) Asymptotic safe set

Figure 4.8. Different safe set for different values of Δ time. (a) The asymptotic safe set computed for $\Delta t = 1.8$. To compute this set we have taken $\xi_0 = 1.5$ (green ball) and $u_0 = 1.0$ (yellow ball).(b) A half section of the asymptotic safe set (red) and a partially controlled trajectory (in black). In this case the controls (yellow segments inserted in the trajectory) are applied every $\Delta t = 1.8$.

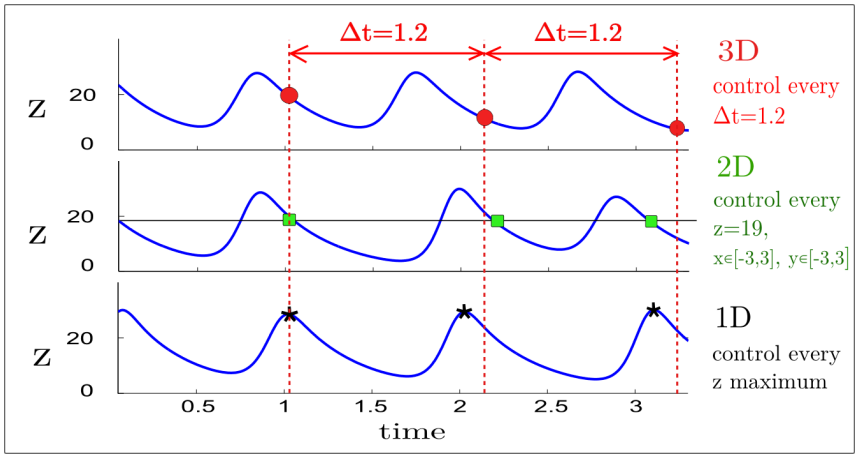

Figure 4.9. Comparison of the three controlled trajectories of the z variable obtained with the 3D, 2D and 1D map respectively. The marks indicate the moment where the control is applied. Only in the 3D case are the controls time periodic.

4.2 Conclusions

We have applied the partial control method to the Lorenz system in the presence of disturbances, for a particular choice of parameters where it shows transient chaos. Typical uncontrolled trajectories in this system follow a transient chaotic motion until they escape to one of its two stable non-chaotic attractors. With the goal of avoiding these escapes, we have applied the partial control method in three different

ways. We have built 1D, 2D and 3D maps, and obtained the respective safe sets with the Sculpting Algorithm.

Using the respective safe sets in each case, we have shown that is possible to control the trajectories, using a small amount of control in comparison with the disturbances affecting the system. Another remarkable feature is that the partially controlled trajectories keep the chaotic behavior of the original system.

The possibility of using different kinds of maps to control the dynamics allows us flexibility. However, in some situations it can be convenient to apply the control in periodic time intervals. This strategy is shown in the 3D case with a fixed time discretization Δt. This novel approach, allows us to focus the attention only in the time instead of the control region. In addition, the frequency of these controls can be adapted depending on the specific experimental requirements, which can suppose an easy and flexible way to control the system.

Chapter 5
A different application of partial control

There are certain situations in noisy nonlinear dynamical systems, where it is required a fast transition between a chaotic and a periodic state. Here, we present a novel procedure to achieve this goal in the context of the partial control method of chaotic systems. We will show that, by only using the safe sets it is possible to handle the stabilization and destabilization of the chaotic dynamics of the partially controlled system.

5.1 Safe set to avoid the escape or force it

In contrast with the previous chapters where the partial control method was used to keep trajectories close to the chaotic saddle and to avoid an undesirable escape [31, 32, 33, 34], the goal here is to maintain the chaotic transient as much as we desire, before forcing an immediate escape. To do that, we use the same safe sets defined in the partial control method in a completely different way.

It is reasonable to think that, in the case of a transient chaotic dynamics, the simplest strategy to force the escape of the trajectories is just to stop applying the control and wait until the trajectory naturally escapes. However, in many cases the average time between the moment in which the application of the control is stopped and the moment in which the trajectory reaches the escape may be very long. It is here where we found that the safe set can be used in a different way to speed up the escape time of the trajectory and therefore to get a higher control in the behaviour of the system. We show here that a practical way to achieve this goal is simply to apply the control to drive the trajectories outside the safe set. This strategy is supported by the fact that non-safe points usually have longer escape times than the safe points. In addition points far from the safe set typically have longer escape times.

The strategy to accelerate the escape of the trajectory, consist on applying a control $|u_n| \leq u_0$ each iteration to the most far away point of the safe set. As we

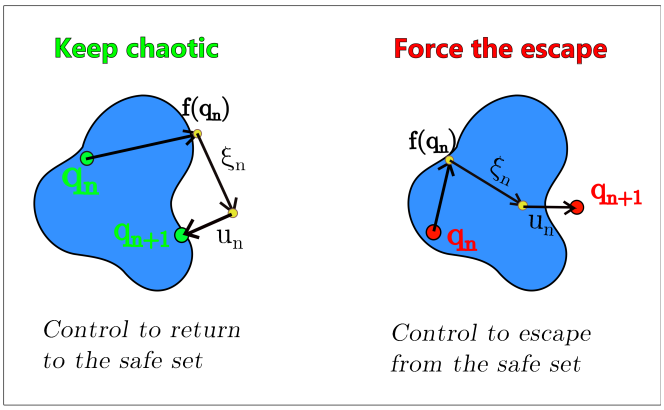

Figure 5.1. The two ways to apply the control in the safe set. In this picture we represent a scheme of the safe set and how the control is applied. We assume that some disturbance ξ_n is affecting the dynamics, so that $q_{n+1} = f(q_n) + \xi_n + u_n$. In the figure on the left the goal of the control u_n is to go back to the safe set to keep the chaotic transient behaviour. In the figure on the right the control is applied to push aside the orbit from the safe set and therefore produce the escape.

will show in the examples, this action reduces significantly the average escape time, in comparison with the natural average escape time if no control is applied.

In Fig. 5.1 we represent how the safe set can be used in a dual way. In an attractive mode when the trajectories are kept chaotic, and in a repulsive mode to speed up the escape of the trajectories. To show this procedure, two examples are drawn in the next section.

5.1.1 The logistic map

In the first example we take the logistic map defined as follows,

$$x_{n+1} = r x_n (1 - x_n), \tag{5.1}$$

where $x \in [0, 1]$ and $r \in [0, 4]$. The goal here is to keep orbits in the interval $[0, 1]$. Transient chaos appears for parameter values $r > 4$. In order to compute an example, we have fixed $r = 4.1$. For this value the orbits starting in the interval $[0, 1]$ typically abandon the interval after a long transient. We have also considered that these orbits are affected by disturbances with a bound ξ_0. The effect of this disturbance can be both, to accelerate or to slow down the escape time depending on the particular contribution of the random disturbances in each iteration of the map. To keep the chaotic trajectories in the interval $x = [0, 1]$, we consider to apply the control u_n bounded by u_0. In this way, the dynamics of the partially controlled map is given by

$$\begin{aligned} &x_{n+1} = r x_n (1 - x_n) + \xi_n + u_n \\ &|\xi_n| \leq \xi_0, \qquad |u_n| \leq u_0. \end{aligned} \tag{5.2}$$

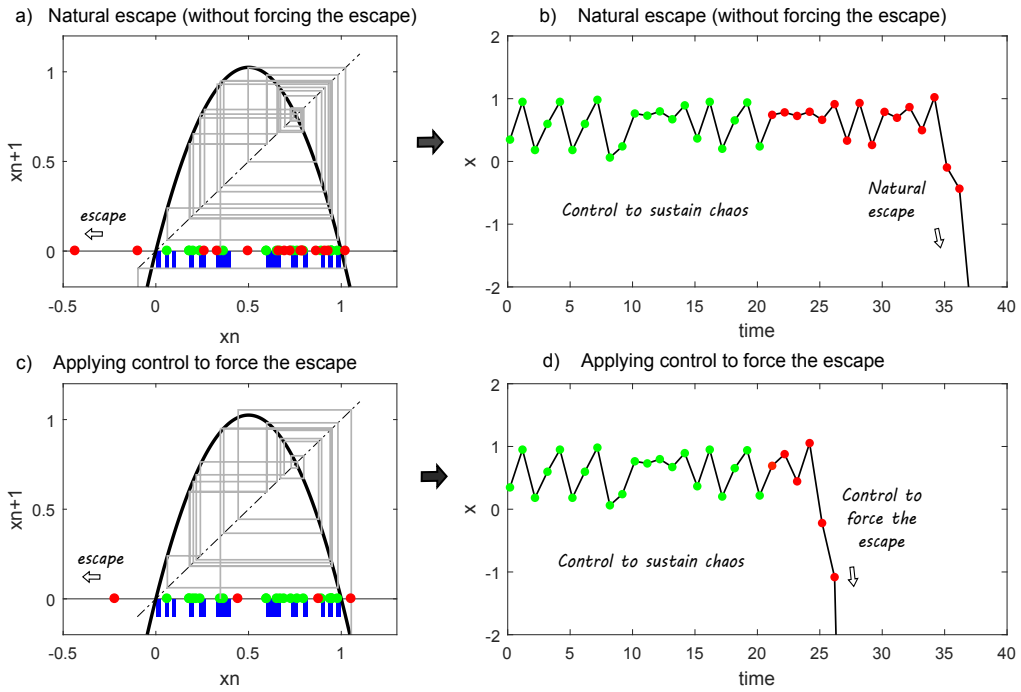

Figure 5.2. Controlled dynamics in the logistic map. The black line in figures (a) and (c), represents the logistic map for the parameter $r = 4.1$. For this value, transient chaos appears and orbits starting in the interval $[0, 1]$ eventually escape to $-\infty$. In order to apply the control, the safe set was computed for the value of disturbance $\xi_0 = 0.03$ and control value $u_0 = 0.02$. The safe set is showed with thick blue bars to improve the visualization. In the first 20 iterations (green points) the control is applied to return the orbit to the safe set. After that, in figure (a) the orbit is free to escape (no control is applied). However in figure (c) the orbit is forced to escape (red points). In figures (b) and (d) the corresponding time series are displayed. Notice that, by inducing the escape, the time to abandon the interval $[0, 1]$ is greatly reduced.

As an example we have chosen the values $\xi_0 = 0.03$ and $u_0 = 0.02$ to compute the safe set showed in Fig. 5.2.

Imagine now an experiment that requires to keep the trajectory in the interval $[0, 1]$ during 20 iterations and then induce the escape as fast as possible. In order to compare the effect of the control, we have considered two scenarios, one in which the escape is not accelerated, and the other in which it is accelerated by applying a control. In Fig. 5.2(a) and 5.2(b) we show the evolution of the variable x, when the control is applied in the first 20 iterations to return orbits to the safe set. After that, we stop applying the control and the trajectory eventually escapes after a long time. In Fig. 5.2(c) and 5.2(d) we represent the same situation with the difference that, after the first 20 iterations, the control is still applied with the goal of forcing its escape. As we can see in Fig. 5.3, the average escape time is much smaller when the control is applied. In addition, the standard deviation of the escape time associated

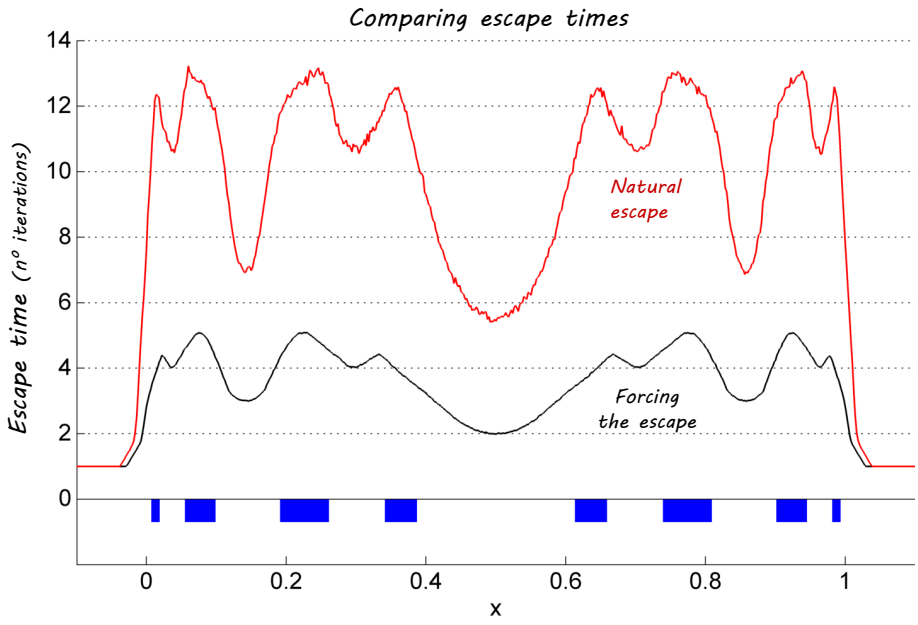

Figure 5.3. Average escape times. In figure represents the interval $[0, 1]$ and the safe set (in blue) for the same conditions as the previous figure. The upper red line shows the average escape time when the orbit abandons the interval $[0, 1]$ without the application of any perturbation. The lower black line shows the average escape time when the orbits are forced to escape by applying small controls. In this way, the trajectory escapes about 2.5 times faster than without control.

to the forced orbits is much smaller, which ensures that most orbits will escape very soon.

5.1.2 The Hénon Map

The second example is the Hénon map which is defined as follows,

$$\begin{aligned} x_{n+1} &= a - by_n - x_n^2 \\ y_{n+1} &= x_n. \end{aligned} \tag{5.3}$$

Transient chaos appears in this system for a wide range of parameters a and b. To show how the control method works in this system, we have taken $a = 2.13$ and $b = 0.3$. In addition, we consider that a bounded disturbance ξ is affecting the variables x and y. For this map, the trajectories starting in the square $x \in [-4, 4]$ and $y \in [-4, 4]$ have a chaotic transient characterized by a long escape time. After that, the trajectories escape out of this region toward infinity and never get back.

In order to keep trajectories in the square $x \in [-4, 4]$ and $y \in [-4, 4]$, we have applied a bounded control u in the variables. The partially controlled dynamics can

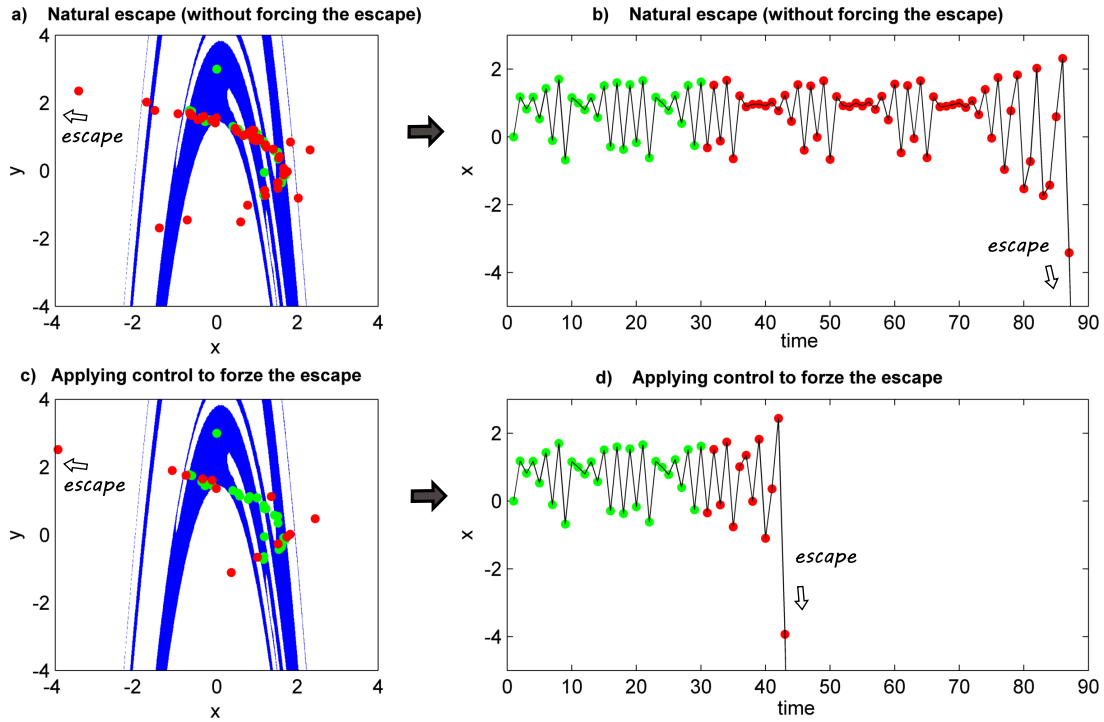

Figure 5.4. Controlled dynamics in the Hénon map. Figures (a) and (c), represent in blue the safe set computed for the Hénon map with the parameters $a = 2.13$ and $b = 0.3$, and for the value of disturbance $\xi_0 = 0.09$ and control $u_0 = 0.06$. The control is applied in two different ways represented by green and red points. In the first 30 iterations (green points), the control drives the orbits to return to the safe set. In figure (a), after these first 30 iterations the control is stopped, and the orbits are free to escape (red points). However, in figure (c) the control is applied to induce the escape and as a result the time escape is significantly reduced. In figures (b) and (d) the corresponding time series of the variable x is showed.

be rewritten as

$$\begin{aligned} x_{n+1} &= a - by_n - x_n^2 + \xi_{in} + u_{in} \\ y_{n+1} &= x_n + \xi_{jn} + u_{jn} \\ \sqrt{(\xi_{in})^2 + (\xi_{jn})^2} &\leq \xi_0, \qquad \sqrt{(u_{in})^2 + (u_{jn})^2} \leq u_0. \end{aligned} \tag{5.4}$$

In this case, we choose as an example the values $\xi_0 = 0.09$ and $u_0 = 0.06$ for the disturbances and control respectively. Next, we compute the safe set showed in Fig. 5.4. In this case we choose to keep 30 iterations the trajectory in the safe set, and after that, induce the escape. In Fig. 5.4a we represent a trajectory in which the escape is not forced, while in Fig. 5.4c the trajectory is forced to escape by the application of control. As a result the trajectory escapes in a lot less iterations (see the corresponding time series in Figs Fig. 5.4b and 5.4d). To show a fair compar-

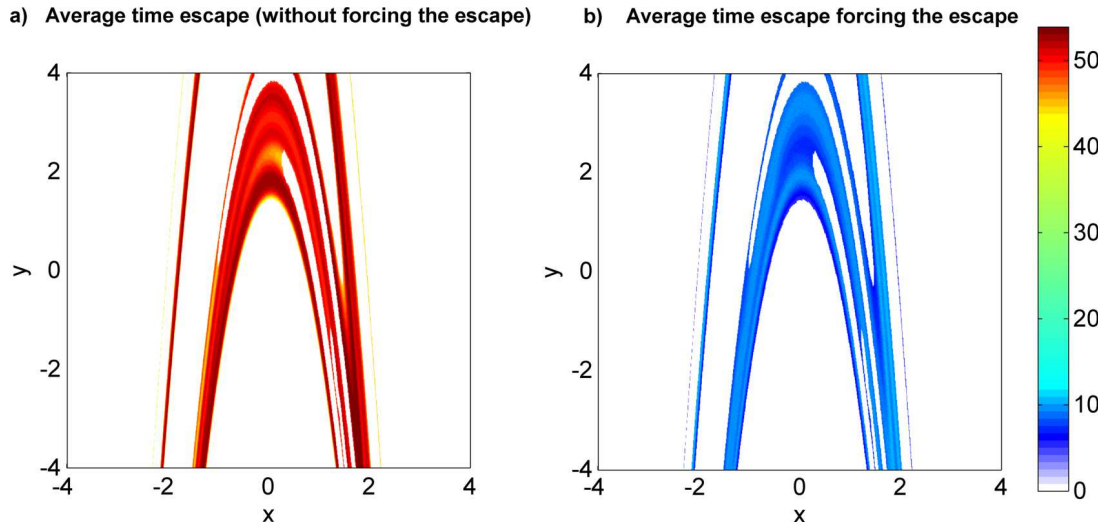

Figure 5.5. Average time escapes. The figures (a) and (b) represent the square $x \in [-4, 4]$ and $y \in [-4, 4]$ in which we have computed the safe set. The figure (a) shows the average escape time of trajectories when no perturbation to escape is applied. In figure (b) the trajectories are induced to escape applying small controls to go far away from the safe set. With this strategy the average time escape is reduced about a factor of 5.

ison of the time escape, we represent in Fig. 5.5 the average time escape for both strategies, free escape and forced escape. The second strategy is about 5 times faster which supposes a big improvement.

5.2 Conclusions

We have proposed a new approach based on the partial control method, to handle transient chaotic dynamics affected by external disturbances. The goal of control is to keep trajectories chaotic during a desired time, and after that, to force the escape in the shortest possible time. To do that, we only have to compute the corresponding safe set which can be used in a dual way. In the attractive way, the perturbations are applied to put back the orbits in the safe set. In the repulsive way, the control led the trajectory far away from the safe set to produce the escape. The control method was tested in the paradigmatic models, the 1D logistic map and the 2D Hénon map for a choice of parameters where the transient chaotic dynamics appears. In both cases we show how to compute the safe set and how to use it to control the trajectories.

Chapter 6
When the disturbance affects a parameter

Discrete dynamical systems where one or several of their parameters vary randomly every iteration are usually referred to as random maps in the literature. However very few methodologies have been proposed to control these kind of systems when chaos is present. Here, we propose an extension of the partial control method, that we call *parametric partial control*, and can be applied to random maps [35, 36, 37] We show that using this control method it is possible to avoid escapes from a region of the phase space with a transient chaotic behavior. The main fingerprint of this method is the ability to control the system even if the corrections applied to the parameter are smaller than the disturbances affecting it. To illustrate how the method works, we have applied it to three paradigmatic models in nonlinear dynamics, the logistic map, the Hénon map and the Duffing oscillator.

6.1 Partial control applied on parameters

In the classical partial control method, the disturbances ξ_n and the control u_n were applied directly on the phase space variables of the system, that is, $q_{n+1} = f(q_n, p) + \xi_n + u_n$. In this last equation p represents the parameters of the system (which are supposed to be constant over time). Here, we study a completely new control problem where the disturbances and the control terms are affecting directly some parameter of the system (instead of the phase space variables), that is, $q_{n+1} = f(q_n, p + \xi_n + u_n)$. For that reason, we call it *parametric partial control*. This study is motivated by the fact that the parameters usually fluctuate from one iteration to another in most real physical systems. These kind of maps are called random maps in the literature. In the context of transient chaos, random maps are widely used to model systems where two different time scales dynamics coexist, one slow and predictable, and another with a small and fast fluctuating component. For example, this is the case in advective fluid dynamics [38], where the velocity field can be written as an average periodic field, plus a fluctuating component, or in some scattering processes [39, 40, 41] where the force field varies in time in a complex manner. As far as we know, the control scheme that we introduce here (parametric partial control) is the first that is able to sustain a transient chaotic dynamics in random maps.

This approach is based on the idea of the partial control method [17] with the difference that the disturbances are introduced in a parameter of the map instead of the variables. Following this scheme, the controlled dynamics in the region Q_0

where we want to keep the trajectories will be:

$$q_{n+1} = f(q_n, p + \xi_n + u_n), \tag{6.1}$$

where f is a function with a chaotic transient in Q_0, q is a point of Q_0, p is the central value of the parameter, ξ_n is a bounded disturbance $|\xi_n| \leq \xi_0$ and u_n is a bounded control, so that, $|u_n| \leq u_0 < \xi_0$. Note that in this chapter, we use the notation Q_0 instead of Q for convenience.

We have developed an algorithm to compute the parametric safe set on an arbitrary set Q of the phase space that has the following steps:

1. Select the region in phase space in which f has a chaotic transient. We call the set of points of this region as the initial set Q_0. Then, we estimate the upper bound of the disturbance ξ_0, and we choose the upper bound of the control $u_0 < \xi_0$. Note that if the chosen u_0 is too small, the parametric safe set may be the empty set, and a bigger value of u_0 must be chosen.

2. For every point $q \in Q_i$ ($i = 0$ for the initial set), we need to check whether it is safe and can be part of an admissible trajectory or not. To do that, we compute $q_{n+1} = f(q_n, p + \xi_n + u_n)$ where the control u_n is applied with the knowledge of $p+\xi_n$, to place the trajectories back in Q_i, if it escapes, otherwise $u_n = 0$. For every point q_n, we have to check all possible disturbances ξ_n. If for all of them, the absolute value of the applied control $|u_n|$ is smaller than u_0, then the point q is safe, otherwise, it is removed from Q_i.

3. After having removed all the points that do not satisfy the control condition, a new set $Q_{n+1} \subset Q_n$ is obtained. Then, we repeat again the step 2 with the new set Q_{n+1}. The process is repeated until it converges, in which case $Q_{n+1} = Q_n$, and this will be the *parametric safe set*. See Fig. 6.1.

Some practical considerations have to be done. In order to compute the parametric safe set, a finite grid covering Q_0 has to be used, since is not possible to compute the infinite number of points in Q_0. For an analogous reason, only a finite sample of disturbances ξ_n can be checked for every point q. We will refer to the grid resolution as the distance between two adjacent points q, and the parameter resolution as the distance between two adjacent values of the parameter affected by different disturbances. Higher resolutions give a more accurate parametric safe set. In this sense, we have found that beyond a critical resolution of the grid over Q and ξ, the safe set remains unchanged. For that reason and from a practical point of view, we recommend to compute the safe set with the algorithm proposed with increasing resolutions until finding the critical value for which the shape of the safe set found remains unchanged.

In order to show how the parametric partial control approach works, we have considered three well known models, the 1D logistic map, the 2D Hénon map and the Duffing oscillator, all of them for a choice of parameters where transient chaos is present. In all cases we consider that the parameter is affected by a disturbance with

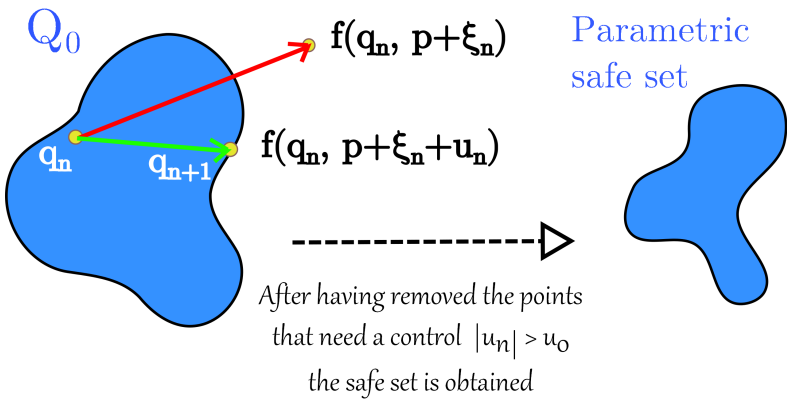

Figure 6.1. Scheme of the parametric partial control. The red arrow shows the mapping of a point q, under the application of a random map in which a parameter p is affected by a bounded disturbance $|\xi_n| < \xi_0$. The green arrow shows the mapping of a point q, once the control u_n was applied to the parameter to keep the point in the blue region. Given the upper values of the disturbance ξ_0 and the control $u_0 < \xi_0$, the partial control method removes the points of the blue region that need a control $|u_n| > u_0$ for some possible $|\xi_n| < \xi_0$. For every point we have to evaluate all possible disturbances $|\xi_n| < \xi_0$. Once the "bad" points are removed, a new region $Q_1 \subset Q_0$ is obtained. Iterating this process until it converges, we get a final region $Q_k \subset ... \subset Q_1 \subset Q_0$. We call this region, the *parametric safe set*.

a uniform probability distribution $|\xi_n| \leq \xi_0$. But any other distribution is possible, provided that it is bounded.

6.1.1 The logistic map

The logistic map is a 1D map and is defined as follows:

$$x_{n+1} = r x_n (1 - x_n). \tag{6.2}$$

For a parameter value $r \in [0, 4]$ the interval $x \in [0, 1]$ maps to itself. However for $r > 4$, the orbits starting in this interval, escape towards infinity after a chaotic motion (see Fig. 6.2(a)). With the aim of keeping the trajectories in $Q_0 = [0, 1]$ and assuming that the parameter is affected by some disturbances $|\xi_n| \leq \xi_0$, the parametric partially controlled dynamics for this map can be written as

$$x_{n+1} = (r + \xi_n + u_n) x_n (1 - x_n), \tag{6.3}$$

where $|u_n| \leq u_0 < \xi_0$ is the control applied. To show an example of control we have taken the values $r = 5$, $\xi_0 = 0.6$ and $u_0 = 0.5$. After the computation of the algorithm described in the previous section, we have obtained the parametric safe set shown in Fig. 6.2(b). The blue wide segments represent the safe points of x. In this figure, it has also been displayed a partially controlled trajectory (in red), which as can be seen, remains chaotic and within Q_0 indefinitely.

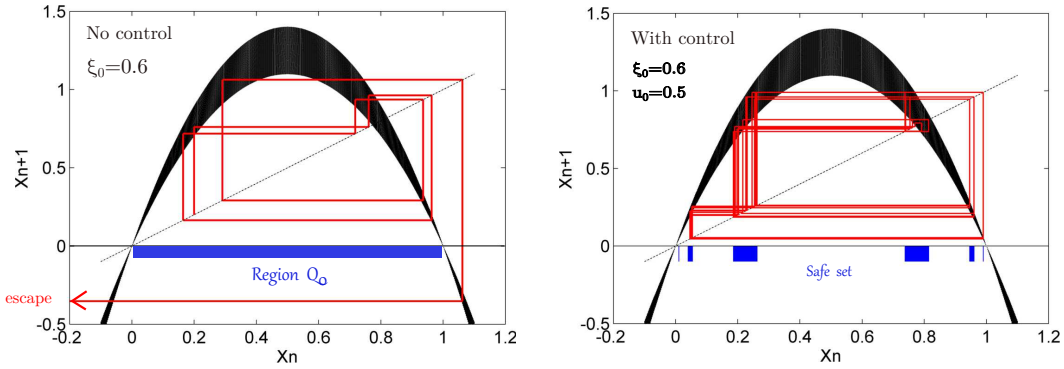

(a) Uncontrolled trajectory (b) Controlled trajectory

Figure 6.2. Logistic map where the parameter r is affected by disturbances. (a) Logistic map $x_{n+1} = rx_n(1-x_n)$ where the parameter $r = 5$ is affected by disturbances with upper bound $\xi_0 = 0.6$. The black wide curve is obtained for all possible values of the parameter, $r \in [5 - \xi_0, 5 + \xi_0]$, of the logistic map. In red, we show an example of an uncontrolled trajectory that after a chaotic motion in Q_0, escapes to minus infinity. (b) We apply the partial control method to the logistic map, with $\xi_0 = 0.6$ and $u_0 = 0.5$ and a grid resolution of 0.001, to obtain the parametric safe set which is shown with the wide blue segments to help the visualization. The orbits starting in this set, remain there after applying a control $u_n \leq 0.5$ every iteration. In red, we show an example of a partially controlled trajectory. We are plotting only 50 iterations.

6.1.2 The Hénon map

The Hénon map is a 2D map defined by

$$\begin{aligned} x_{n+1} &= a - by_n - x_n^2 \\ y_{n+1} &= x_n. \end{aligned} \tag{6.4}$$

This map shows transient chaos for a wide range of the parameters a and b. We have chosen here the parameter values $a = 2.16$ and $b = 0.3$. For these values, the trajectories with initial conditions in the square $[-4, 4] \times [-4, 4]$ have a very short chaotic transient, before finally escaping from this region toward infinity. An example of this behavior is shown Fig. 6.3(a) for a given initial condition. We consider now, a situation where the parameter b is affected by some disturbance $|\xi_n| \leq \xi_0$. To keep the orbits in $Q_0 = [-4, 4] \times [-4, 4]$ we apply a control $|u_n| \leq u_0 < \xi_0$, so that the controlled dynamics can be described as:

$$\begin{aligned} x_{n+1} &= a - (b + \xi_n + u_n)y_n - x_n^2 \\ y_{n+1} &= x_n. \end{aligned} \tag{6.5}$$

As an example we have computed two different safe sets corresponding to the values $\xi_0 = 0.20$, $u_0 = 0.15$ and $\xi_0 = 0.050$, $u_0 = 0.036$ respectively. The safe sets obtained are shown in Fig. 6.3(b) and Fig. 6.3(c), where it was also drawn a partially controlled orbit (red points), which remains chaotic in the square forever.

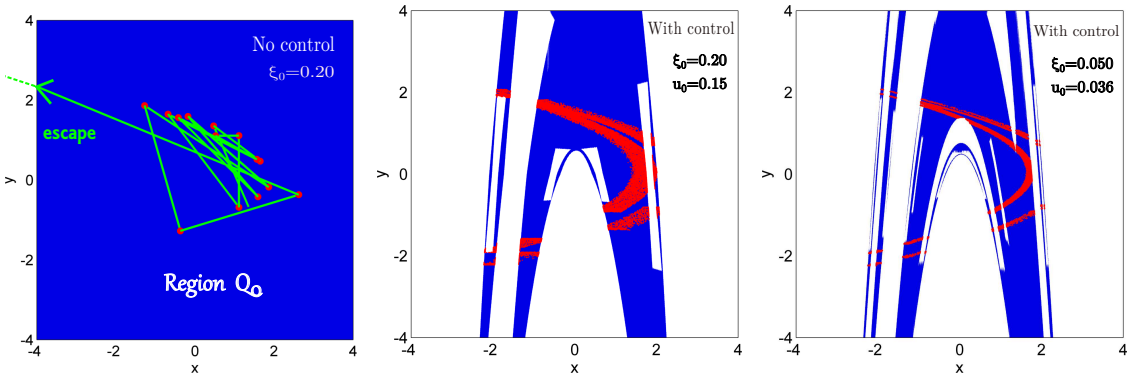

(a) Uncontrolled trajectory (b) Safe set and controlled trajectory (c) Safe set and controlled trajectory

Figure 6.3. The Hénon map where the parameter b is affected by disturbances. (a) An uncontrolled trajectory in the Hénon random map with $a = 2.16$ and $b = 0.3$. The parameter b is affected by disturbances with upper bound $\xi_0 = 0.20$. The blue square $[-4, 4] \times [-4, 4]$ is the region Q_0. In absence of an external control, the trajectories in Q_0 escape outside the square after a very short chaotic transient. An example of an uncontrolled trajectory is displayed with the red points connected by the green lines. (b) The partial control method has been applied to keep trajectories in Q_0 forever. The upper bound of control is $u_0 = 0.15$. The grid resolution taken is 0.01 and the parameter resolution is 0.005. As a result, the parametric safe set (in blue) is obtained. All the orbits of the map starting in the blue set, remain there after the application of controls smaller than $u_0 = 0.15$. The red points display a partially controlled trajectory, where 20000 iterations of the trajectory have been plotted. (c) For this case the upper value of control is $u_0 = 0.036$, the grid resolution used is 0.001 and the parameter resolution 0.0005. In we compare it with the previous figure, we see that the appearance of the parametric safe set is more complex, due to fact that the disturbance value is smaller.

As revealed by the panels 6.3(b) and 6.3(c), as the disturbance decreases, the parametric safe set becomes more and more complex due to the fractal structure of the chaotic saddle underlying the dynamics. For this reason, a higher resolution is necessary to solve this kind of safe sets. We also should take into account that the finite resolution of the computation is by itself a source of disturbance, so this uncertainty can never be zero.

6.1.3 The Duffing oscillator

In previous chapters, the partial control method was applied to the Duffing oscillator system, where disturbances and control affected the variables of the system. In this case we have studied the same model, with the difference that disturbances and control are now acting in some parameter of the system. In contrast with the logistic and Hénon map, the Duffing oscillator model is a flow, so a previous discretization

of the dynamics is required to apply the control method.

We consider here the following Duffing oscillator equation:

$$\ddot{x} + 0.15\dot{x} - x + x^3 = 0.245 \sin t. \tag{6.6}$$

For this choice of parameters, it is possible to find in the phase space a transient chaotic behaviour of the trajectories. Due to the periodic forcing, it is suitable to build a time-2π map f, where the flow is cut every $\Delta t = 2\pi$. The transient chaotic dynamics is captured in the square $[-2, 2]\times[-2, 2]$. Without external control, almost all initial conditions in this region, after a chaotic transient behaviour, fall in one of the three attractors present in the phase space. The system has two period-1 attractors and one period-3 attractor, as shown in Fig. 6.4.

With the aim of keeping the trajectories far from these attractors, we have applied the partial control method considering that the forcing amplitude is affected by some bounded disturbance $|\xi_n| \leq \xi_0$. Applying the control $|u_n| \leq u_0$ in the same parameter as well, the amplitude of the forcing varies according to $x_{n+1} = f(x, 0.245 + \xi_n + u_n)$ every iteration.

As an example, we have computed the safe set for the values $\xi_0 = 0.020$ and $u_0 = 0.014$. We have used a grid of 1000×1000 in the square $[-2, 2] \times [-2, 2]$, where the balls centered in each attractor have been removed to prevent the periodic behaviour. The safe set obtained is shown in Fig. 6.4, where a controlled trajectory (30000 iterations in red) also appears. Notice that the partially controlled trajectory never falls into the attractors.

6.1.4 Controlling more parameters

Although we have dealt with examples where the control is applied on a certain parameter, situations where more than one parameter need control are possible. The scheme of the method is easily expandable, for example, in the case of m parameters $p^1, p^2, ..., p^m$, the partially controlled dynamics would be described as

$$q_{n+1} = f(q_n, (p^1 + \xi_n^1 + u_n^1), ..., (p^m + \xi_n^m + u_n^m)), \tag{6.7}$$

with the conditions

$$\begin{aligned} &\sqrt{(\xi_n^1)^2 + ... + (\xi_n^m)^2} \leq \xi_0 \\ &\sqrt{(u_n^1)^2 + ... + (u_n^m)^2} \leq u_0 < \xi_0. \end{aligned} \tag{6.8}$$

The main drawback of considering the extra parameters is the considerable increase of computational time to obtain a parametric safe set due to the curse of dimensionality. However it is possible to accelerate this computation parallelizing some parts of the Sculpting Algorithm code or also by using GPU computing techniques.

6.2 Conclusions

In this chapter we have presented a new control method that we call parametric partial control of chaotic systems, which is an extension of the partial control method.

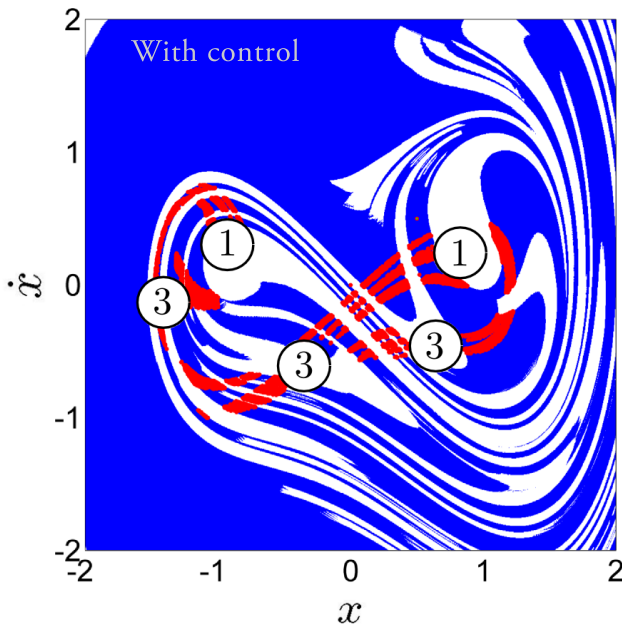

Figure 6.4. Controlled trajectory in the Duffing oscillator with $\xi_0 = 0.020$ and $u_0 = 0.014$. Numbers indicates the three attractors of the system, two period-1 and one period-3. The aim of applying control is to avoid trajectories falling in these attractors. After removing the holes, corresponding to the attractors, the safe set (in blue) was computed with a grid of 1000×1000, (grid resolution 0.004, parameter resolution 0.0002). The red dots represent a controlled trajectory made up of 30000 iterations in the stroboscopic map.

This scheme is applied on maps where some parameter is affected by a bounded disturbance ξ_0. The goal of the method is to keep the transient chaotic motion forever in Q_0, by the application of a bounded control u_0 in the parameter. Parametric safe sets were obtained for values $u_0 < \xi_0$, which is the most relevant result.

The parametric partial control was applied to the 1D logistic random map, the 2D Hénon random map, and the Duffing oscillator with some disturbance affecting the forcing amplitude. In all the systems considered, we have taken a choice of parameters where transient chaos is present. We have computed the parametric safe sets for different values of the disturbance, showing how the parametric safe set changes with it.

Chapter 7
Controlling time-delay coordinate maps

Delay-coordinate maps have been widely used recently to study nonlinear dynamical systems, where there is only access to the time series of one of their variables [42, 43, 44] Here, we show how the partial control method can be applied in this kind of framework in order to prevent undesirable situations for the system or even to reduce the variability of the observable time series associated with it [34]. To illustrate how it works, we have applied it to three well-known models in the field of nonlinear dynamics with different delays such as the two-dimensional cubic map, the standard map and the three-dimensional hyperchaotic Hénon map. We show for the first time here how hyperchaotic systems can be partially controlled.

7.1 The partial control applied to time-delay coordinates maps

In this chapter we consider a time-delay coordinate map under external additive disturbances of the form $f(x_n, x_{n-1}, ...) + \xi_n$, where the control is also applied in an additive way $f(x_n, x_{n-1}, ..) + \xi_n + u_n$. This kind of framework is the one that is usually found after having used the delay reconstruction method to study the phase space dynamics of a chaotic system [45, 46, 47, 48]. These maps are usually expressed in the following way:

$$x_n = f(x_{n-1}, x_{n-2} \dots x_{n-m}). \tag{7.1}$$

We examine here the problem of controlling this kind of maps possessing a chaotic behaviour (see the scheme of Fig. 7.1). The main difference with the classical partial control scheme is that the control can only be applied in the present state x_n, since it is not physically possible to control the past states $(x_{n-1}, x_{n-2} \dots))$. Therefore we need to introduce a modified approach.

Following the idea of the partial control method we assume that the system can be modelled as:

$$x_n = f(x_{n-1}, x_{n-2} \dots x_{n-m}) + \xi_n + u_n, \tag{7.2}$$

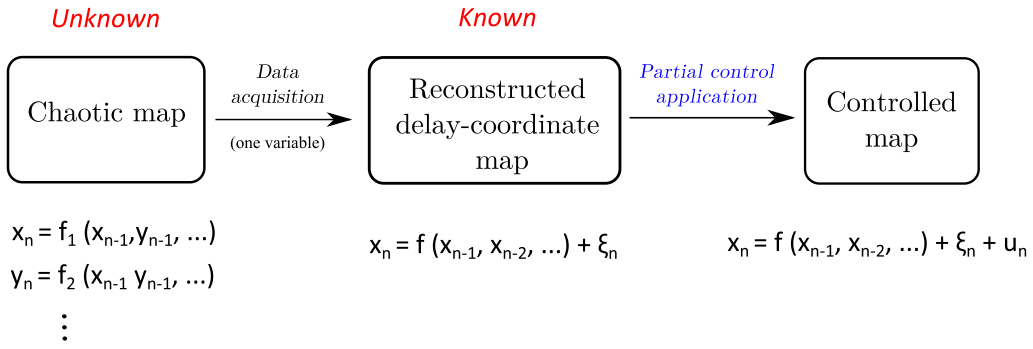

Figure 7.1. Conceptual framework. From left to right. Step 1: data acquisition from a chaotic system. We assume here that only one variable is observable. Step 2: using embedding and parametric reconstruction techniques, construct a delay-coordinate map. The term ξ_n represents a disturbance term that encloses all possible deviations from the real dynamics. Step 3: apply the partial control method introducing and additive control term u_n acting on the observable variable. In this work we assume that we already possess the knowledge of the delay-coordinate map.

where ξ_n is the disturbance affecting the state x_n, and u_n is the respective control applied, both limited by the conditions

$$|\xi_n| \leq \xi_0, \qquad |u_n| \leq u_0.$$

Once we know the form of the time-delay coordinate map, all we have to do to apply the partial control method is to define the region Q_0 in the phase space $(x_{n-1}, x_{n-2} \ldots)$ where we want to keep the trajectories, and determine the upper value of the disturbance ξ_0, and the upper value of the control u_0 used.

To compute the safe set, we have developed a modified version of the *Sculpting Algorithm* [16], which evaluates the points from Q_0 and remove them if they do not satisfy the safety condition. The *ith* step of this algorithm can be summarized as follows:

1. Morphological dilation of the set Q_i by u_0 along the x_{n-1} direction, obtaining the set denoted by $Q_i + u_0$.

2. Morphological erosion of set $Q_i + u_0$ by ξ_0 along the x_{n-1} direction, obtaining the set denoted by $Q_i + u_0 - \xi_0$.

3. Let Q_{i+1} be the points $(x_{n-1}, x_{n-2} \ldots)$ of Q_i, so that $f(x_{n-1}, x_{n-2} \ldots)$ maps inside the set $Q_i + u_0 - \xi_0$.

4. Return to step 1, unless $Q_{i+1} = Q_i$, in which case we set $Q_\infty = Q_i$. We call this final region, the *safe set*. Note that if the chosen u_0 is too small, then Q_∞ may be the empty set, so that a bigger value of u_0 must be chosen.

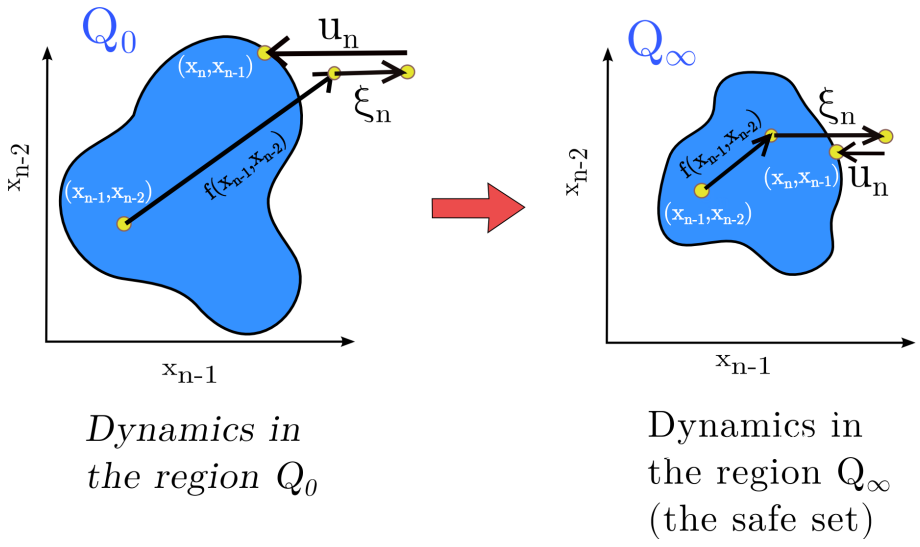

Figure 7.2. Dynamics in $\mathbf{Q_0}$ and $\mathbf{Q_\infty}$. The left side shows an example of a $2D$ region Q_0 (in blue) in which we want to keep the dynamics described by $x_n = f(x_{n-1}, x_{n-2}) + \xi_n + u_n$. We say that $|\xi_n| \leq \xi_0$ is a bounded disturbance affecting the map, and u_n is the control chosen so that q_{n+1} is again in Q_0. Notice that disturbance and control arrows are drawn parallel to current state of the variable since only the present state is affected by them. To apply the control, the controller only needs to measure the state of the disturbed system, that is $[f(x_{n-1}, x_{n-2}) + \xi_n]$. The knowledge of $f(x_{n-1}, x_{n-2})$ or ξ_n individually is not required. The right side of the figure, shows the region $Q_\infty \subset Q_0$ (in blue), called the *safe set*, where each $(x_{n-1}, x_{n-2}) \in Q_\infty$ has $(x_n, x_{n-1}) \in Q_\infty$ for some control $|u_n| \leq u_0$, which is chosen depending on ξ_n. Notice that the removed region does not satisfy $|u_n| \leq u_0$.

This final set is formed by the points $(x_{n-1}, x_{n-2} \ldots)$ belonging to the region Q_0, where the image $x_n = f(x_{n-1}, x_{n-2} \ldots) + \xi_n + u_n$ can be re-injected again on the safe set by using a control $|u_n| \leq u_0$. In Fig. 7.2 we illustrate the controlled dynamics in the region Q_0 and the safe set Q_∞. Notice that, due to the fact that the control and disturbance affects the present state of the variable, then they are drawn in the current axis direction.

In order to show that the method can be applied on different chaotic maps, we have chosen three examples of well-known chaotic maps to illustrate it. We do not reproduce here the embedding and reconstruction model step, since is not the goal of this work. Instead of that, we have deduced by simple calculation, the expression of the delay-coordinate maps. Next, we apply the control scheme with the aim of keeping the orbits in a desirable region of phase space.

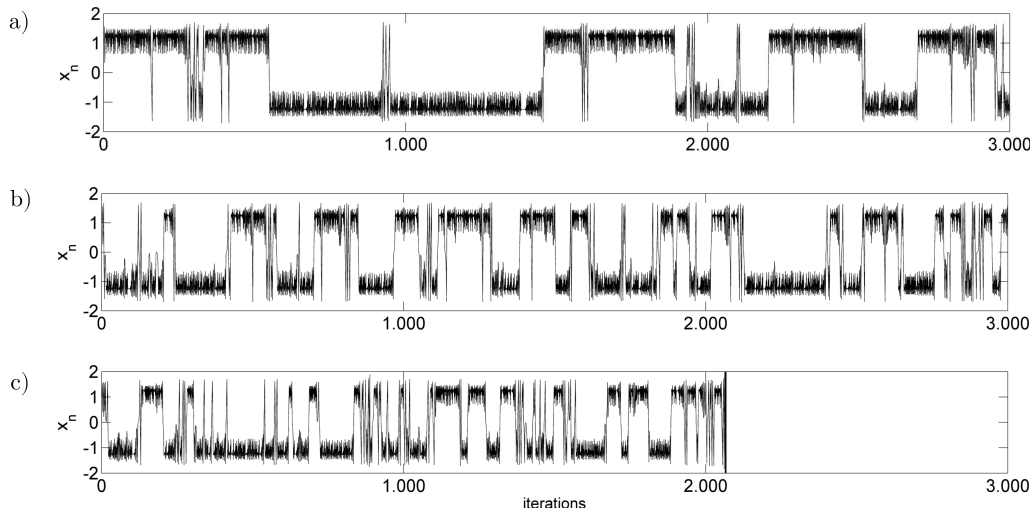

Figure 7.3. Time series of the two-dimensional cubic map for different disturbances. (a) Time series of variable x_n with no disturbance affecting it. (b) Time series with $|\xi_n| \leq \xi_0 = 0.02$ affecting the map. (c) Time series with $|\xi_n| \leq \xi_0 = 0.20$ affecting the map. After some iterations the trajectory escapes towards $-\infty$.

7.1.1 The two-dimensional cubic map

We consider here the system given by:

$$\begin{aligned} x_n &= y_{n-1} \\ y_n &= -bx_{n-1} + ay_{n-1} - y_{n-1}^3, \end{aligned} \tag{7.3}$$

which represents the two-dimensional cubic map [49].

This two-dimensional cubic map depends on two parameters and exhibits chaos for different values of them. We have selected here the values $a = 2.75$ and $b = 0.2$. For this choice of parameters it is represented in Fig. 7.3(a) an example of the time series of the variable x_n without the influence of noise. Here, the trajectories oscillate between two well differentiated regions (top and bottom), where the transitions between them occurs after some typical time. However, when we introduce additive disturbances, the frequency of the transitions increases (Fig. 7.3(b)). And for large disturbances the trajectory eventually escapes toward an external attractor due to the extra energy applied (Fig. 7.3(c)).

As an example, we assume now that due to experimental limitations we only have access to the variable x_n. With that information, we are interested in preventing the big oscillations, that is, to keep the x_n values small, such that $-2 < x_n < 0$ forever, even in presence of large disturbances.

The form of the reconstructed delay-coordinate map can be deduced by substituting $y_{n-1} = -bx_{n-2} + ay_{n-2} - y_{n-2}^3$ into Eq. 7.3 and taking into account that $x_{n-1} = y_{n-2}$, it follows that,

$$x_n = ax_{n-1} - bx_{n-2} - x_{n-1}^3. \tag{7.4}$$

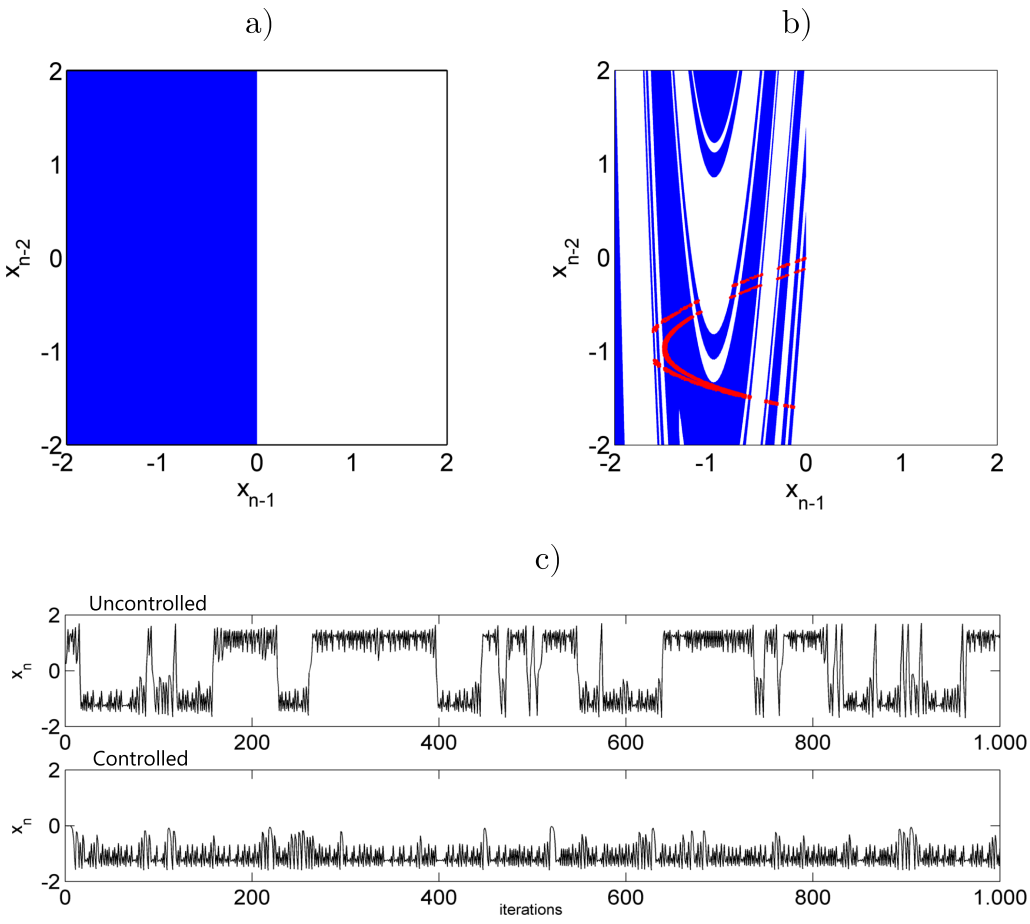

Figure 7.4. Safe set and controlled dynamics in the two-dimensional delayed cubic map ($\mathbf{x_n = ax_{n-1} - bx_{n-2} - x^3_{n-1}}$). (a) In blue the initial region Q_0 where we want to keep the trajectories. (b) The safe set obtained with the values of disturbance $\xi_0 = 0.020$ and control $u_0 = 0.015$. A grid of 1000×1000 points has been used. The red dots represent 1000 iterations of a partially controlled trajectory. (c) In the top it is represented an uncontrolled time series affected with $\xi_n \leq \xi_0 = 0.020$. In the bottom the controlled time series corresponding to the red dots shown in case b.

We call this map the *two-dimensional delayed cubic map*. In addition, we add to the model a disturbance term ξ_n in order to consider the potential noise present in the data acquisition or also mismatches in the reconstruction model technique.

Taking into account the disturbance and the control term u_n in the system, the controlled time-delay coordinate map is given by:

$$x_n = ax_{n-1} - bx_{n-2} - x^3_{n-1} + \xi_n + u_n, \tag{7.5}$$

with $|\xi_n| \leq \xi_0$ and $|u_n| \leq u_0$.

In order to avoid the oscillation of the trajectories, we have defined the initial region Q_0 (Fig. 7.4(a)) as the interval $(-2 < x_{n-1} < 0)$. Notice that, in this way all successive x_n values remain in this interval. The safe set (Fig. 7.4(b)) was computed

with the values $\xi_0 = 0.020$ and $u_0 = 0.015$. The safe set obtained is used to keep the trajectories in the interval $(-2 < x_n < 0)$, avoiding the oscillation present in absence of control. In Fig. 7.4(b) the safe set and a partially controlled trajectory (red dots) are drawn. In Fig. 7.4(c) it is represented the corresponding controlled time series, where we also show an uncontrolled trajectory in order to compare.

7.1.2 The standard map

The standard map represents the discrete dynamics corresponding to the Poincaré section of the kicked rotator system. The system is given by:

$$\begin{aligned} y_n &= y_{n-1} + K \sin x_{n-1} \\ x_n &= x_{n-1} + y_n, \end{aligned} \tag{7.6}$$

where x_n and y_n are taken *modulo* 2π. The standard map shows hamiltonian chaos for different values of the parameter $K > 0$. Depending on the initial conditions, it is possible to observe the coexistence of periodic orbits, quasiperiodic orbits, and chaotic orbits.

We contemplate here the case $K = 4.8176$. In absence of any disturbance ($\xi_0 = 0$), this map exhibits chaotic regions and quasiperiodic orbits depending on the initial conditions (Fig. 7.5a), however when some amount of disturbance is present ($\xi_0 = 0.002$), some quasiperiodic orbits vanish, and chaotic behaviour arises (Fig. 7.5b). For a large enough disturbance ($\xi_0 = 0.15$), no periodic or quasiperiodic orbits exist and chaotic behaviour is the only behaviour present in the system (Fig. 7.5c).

Assume now that we want to avoid the KAM islands region (red circles in Fig. 7.5), in order to avoid the potential quasiperiodic behaviour of the trajectories. To do that we have applied the partial control method. In this case, the dynamics of the variable x_n can be reconstructed after some arrangements, obtaining the following time delay map:

$$x_n = 2x_{n-1} - x_{n-2} + K \sin x_{n-1}, \tag{7.7}$$

where x_n is taken *modulo* 2π. We call this map the *delayed standard map*. Considering again the disturbance and control terms, the resulting dynamics is as follows:

$$x_n = 2x_{n-1} - x_{n-2} + K \sin x_{n-1} + \xi_n + u_n, \tag{7.8}$$

with $|\xi_n| \leq \xi_0$ and $|u_n| \leq u_0$.

In this case we consider the largest value of the disturbance ($\xi_0 = 0.15$). The next step is to define the region Q_0 where we will keep the trajectories. This region is shown in Fig. 7.6a where the two holes correspond to the KAM islands present in the deterministic case. Then, we apply the modified Sculpting Algorithm to obtain the safe set shown in Fig. 7.6b. For this value of the disturbance, it was possible to control the system with controls smaller than $u_0 = 0.08$. We also represent in Fig. 7.6c a partially controlled trajectory (red dots). Due to the non dissipative dynamics of the standard map, the controlled trajectory covers all the safe set.

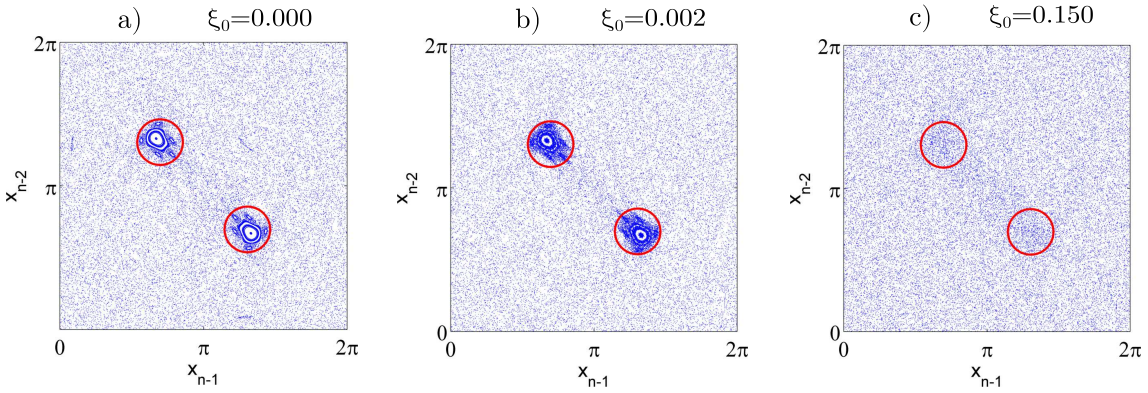

Figure 7.5. Delayed standard map ($\mathbf{x_n = 2x_{n-1} - x_{n-2} + K \sin x_{n-1}}$) affected by different disturbances ξ_0. The points represent different trajectories in the standard map. Several initial conditions were taken to show the different dynamical behaviours (chaotic, periodic and quasiperiodic orbits). The figures represent three different cases where the trajectories are affected by random disturbances with upper bound $\xi_0 = 0.000$, $\xi_0 = 0.002$ and $\xi_0 = 0.150$ respectively.

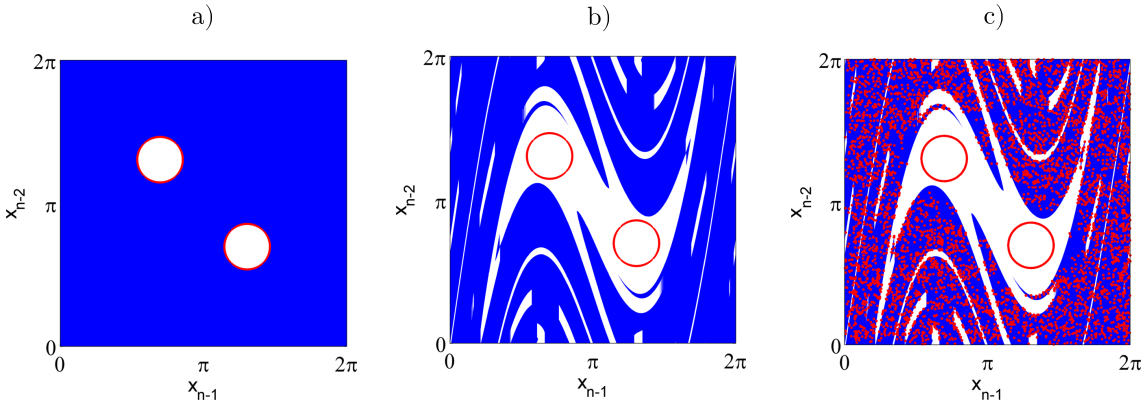

Figure 7.6. Safe set and controlled trajectory in the delayed standard map ($\mathbf{x_n = 2x_{n-1} - x_{n-2} + K \sin x_{n-1}}$) a) In blue the initial region Q_0 that we select to keep the trajectory. b) The safe set computed with the values $\xi_0 = 0.15$ and $u_0 = 0.08$. The grid used here is 1000×1000 points. c) Partially trajectory with 5000 iterations on the safe set.

7.1.3 The 3-dimensional hyperchaotic Hénon map

In this example we explore the possibility of controlling an hyperchaotic system which involves two or more positive Lyapunov exponents. To do that we have taken the three-dimensional Hénon map [50].

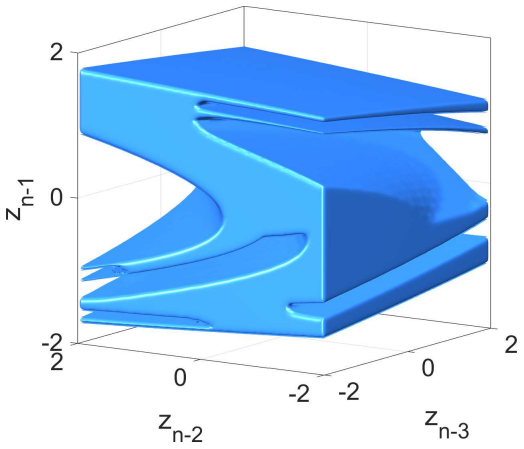

(a) Safe set

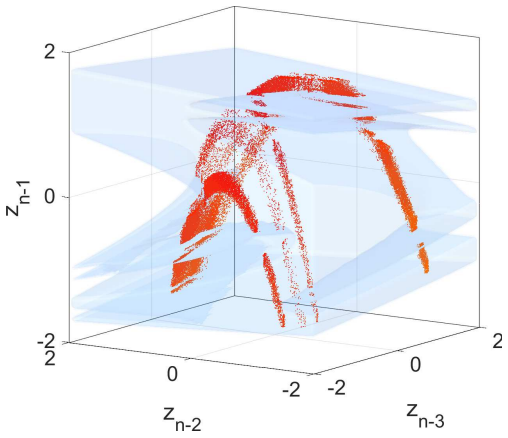

(b) Controlled trajectory by using the safe set

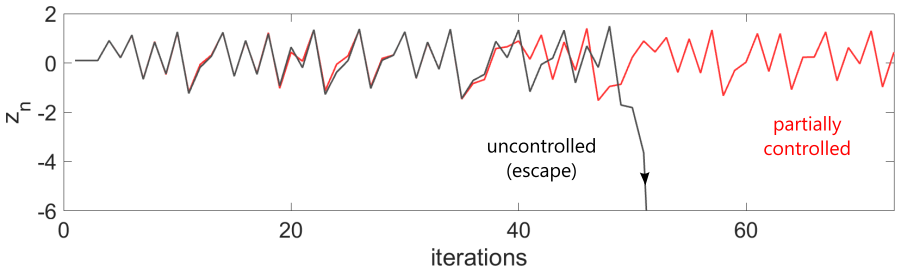

(c) Time series of the controlled trajectory

Figure 7.7. Safe set and controlled dynamics for the 3D delayed Hénon map ($\mathbf{z_n = 1 - az_{n-1}^2 + bz_{n-2} - cbz_{n-3}}$). (a) The safe set computed for the parameter values $a = 1.1$, $b = 0.3$, $c = 1$. A grid of $1000 \times 1000 \times 1000$ was taken in the box $[-2, 2] \times [-2, 2] \times [-2, 2]$ that represents the initial region Q_0. Taking the upper bound of the disturbance $\xi_0 = 0.12$ and the control $u_0 = 0.08$, the safe set converges after 15 iterations. (b) The safe set is represented in transparent blue to see the controlled trajectory inside (red dots). The variable z_n is affected by a random disturbance with upper bound $\xi_0 = 0.12$ and control $u_0 = 0.08$. (c) Comparison between an uncontrolled trajectory and a controlled one in the 3D delayed Hénon. In black, the uncontrolled trajectory which after some iterations escapes to $-\infty$. In red, the controlled trajectory. For a fair comparison, both trajectories start with the same initial condition and are affected by the same sequence of random disturbances.

This system is given by:

$$\begin{aligned} x_n &= bz_{n-1} \\ y_n &= cx_{n-1} + bz_{n-1} \\ z_n &= 1 + y_{n-1} - az_{n-1}^2. \end{aligned} \tag{7.9}$$

This map shows transient chaos for a wide range of the parameters a, b and c.

To compute an example, we have chosen the parameter values $a = 1.1$, $b = 0.3$ and $c = 1$. For these values, the trajectories with initial conditions in the box $(x_n, y_n, z_n) \in [-0.5, 0.5] \times [-1, 1] \times [-2, 2]$ have a chaotic transient, before eventually escaping from this region towards infinity. In this case, the effect of the disturbances in the dynamics does not change dramatically the behaviour of the trajectories. It just increases or reduces the escape time in comparison with the deterministic trajectory.

Suppose now that we have collected data from the variable z_n so that we were able to reconstruct a delay-coordinate map. In this case, taking three delays is sufficient to describe correctly the dynamics of the system, that is, $z_n = f(z_{n-1}, z_{n-2}, z_{n-3})$.

The form of this delay-coordinate map can be obtained by simple calculation:

$$z_n = 1 - az_{n-1}^2 + bz_{n-2} - cbz_{n-3}. \tag{7.10}$$

We will call this map the *three-dimensional delayed Hénon map*.

In these coordinates, values of $|z_n| > 2$ involve the escape to $-\infty$ of the trajectories. In order to avoid the escape, the goal is to apply control in the variable z_n to keep it in the box $(z_{n-1}, z_{n-2}, z_{n-3}) \in [-2, 2] \times [-2, 2] \times [-2, 2]$.

Introducing the disturbance term ξ_n and the control term u_n, the partial control scheme is,

$$z_n = 1 - az_{n-1}^2 + bz_{n-2} - cbz_{n-3} + \xi_n + u_n, \tag{7.11}$$

with $|\xi_n| \leq \xi_0$ and $|u_n| \leq u_0$. In order to show the appearance of the safe set depending on the disturbance value, we have computed the safe set taking $\xi_0 = 0.12$ and $u_0 = 0.08$. We have used a grid of $1000 \times 1000 \times 1000$ points covering Q_0, and then applied the modified Sculpting Algorithm to the safe set shown in Fig. 7.7(a). We have also represented in Fig. 7.7(b), 10000 iterations of a partially controlled trajectory (red dots). Notice that the trajectory remains in the box $[-2, 2] \times [-2, 2] \times [-2, 2]$ forever. In absence of control, the trajectory abandons this box after some iterations as it is illustrated in the time series represented in Fig. 7.7(c).

Although the variable z_n was taken here as an example, in the case that the reconstructed delayed map was built with other variable x_n or y_n, the methodology would be the same as the one presented here. The only difference would be the shape of the safe set obtained and possibly the minimum ratio u_0/ξ_0 achieved, since this depends on the embedded variable.

7.2 Conclusions

Delay-coordinate maps can be obtained from the delay reconstruction method to study the phase space dynamics of a chaotic time series. In this chapter, we have shown how to apply the partial control method to different delay-coordinate nonlinear maps with chaotic behaviour and affected by random disturbances. The aim of the control scheme presented here was to keep the chaotic trajectories in a desirable region of the phase space, applying small corrections in the observables of the sys-

tem. The novelty introduced here is that, it is possible to apply the partial control method with the only knowledge and control of one variable.

The three examples presented here, the two-dimensional cubic map, the standard map and the three-dimensional hyperchaotic Hénon map, were considered in the chaotic regime and with some disturbances affecting them. By applying a smaller control $u_0 < \xi_0$, we have shown that it is possible to keep the trajectories within a desirable region of the phase space. In this sense we want to recall that the desirable regions selected here to maintain the trajectories were only examples, and many other choices are possible depending on our control convenience. We have also applied for the first time the partial control method to a hyperchaotic map. Another interesting result of this work is the dynamics of a partially controlled Hamiltonian system. As we have shown it covers the whole safe set. This is a fundamental difference with the dissipative case.

Finally, although we consider here mathematical models to express the maps, we believe that the method can be applied in the same way to delay-coordinate maps built from experimental time series. That would be the next step in the development of this control method.

Chapter 8
A new approach: the safety functions

8.1 Introduction

The partial control method is based on finding certain sets in the phase space, allowing us to sustain a transient chaotic trajectory in certain region forever. As a consequence, the possible escapes from a given phase space region are avoided. However some limitations arise when the control method is applied in more general systems or experimental data. With the aim of overcoming these difficulties, we have developed a new partial control approach.

8.2 Extending the partial control method

In previous chapters, when the partial control method was applied, it was assumed that the disturbance term affected either the variable [33] or a parameter [51] of the system, but not both at the same time. It was also assumed that the bound of the disturbance was homogeneous in all the phase space, however is not uncommon to find systems where the magnitude of the disturbance can vary across different regions of the phase space.

In addition, we have found that partial control works well when the system behaves exactly as the model predicts (including some amount of disturbance). However if some unexpected event interferes with the system, leading the trajectory to an unknown state, it would be useful to know how safe is that state or the surrounded region, in order to apply an efficient control. This information could highly improve the robustness and efficiency of the control strategy. With this aim, we introduce a new tool in the context of the partial control method.

This new approach is applied on the more general maps described in the following form:

$$q_{n+1} = f(q_n, \xi_n) + u_n, \tag{8.1}$$

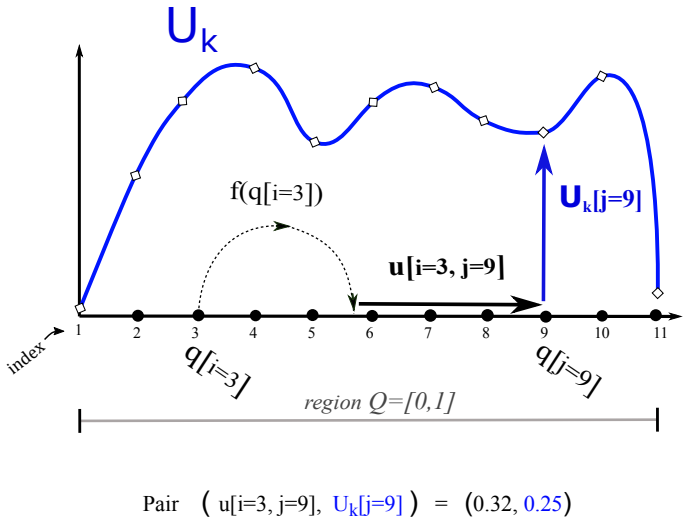

Figure 8.1. The safety function approach. In this figure a region Q and a safety function U_k are represented. We assumed that the dynamics in this region have escapes and the control is applied to avoid these escapes. In order to reduce the computational complexity, a grid covering the region Q (in this case N=11 points). The controlled dynamics is given by $q_{n+1} = f(q_n) + u_n$. We identify the starting and arrival point as $q[i] = q_n$ and $q[j] = q_{n+1}$ respectively. The control corresponding to a point $q[i]$ to go to the point $q[j]$, is denoted as $u[i, j]$. The value $U_k[j]$ represents an upper bound of control for the point $q[j]$. This means that, each individual control u_n of a controlled trajectory starting in the point $q[j]$, will not exceed the value $U_k[j]$. The idea here is to obtain the value $U_{k+1}[i]$. To do that, it is necessary to evaluate all the possible pairs of values $\big(u[i, j], U_k[j]\big)$, (note that each pair represents a choice of control). Among all of them, we select the pair with the minimum upper bound of control. This value will be the new $U_{k+1}[i]$. Proceeding similarly with all the points $q[i]$, the function $U_{k+1}[i]$, $\forall i$ can be obtained.

where ξ_n is a disturbance term (random perturbation), belonging to a bounded distribution that can be space-dependent, and can actuate over the variables or parameters of the map. The u_n term is the control applied on the variables of the system with the aim of keeping the trajectory in the desirable region Q.

This method is based on the existence of a special function that we call the safety function $U_\infty(q)$ that represents the minimum upper bound of control needed for each point q to remain in Q forever (infinite iterations). Once the safety function is computed, it is only necessary to pick a bound $u_0 \geq \min(U_\infty)$. Controlled trajectories are possible by applying a suitable control $|u_n| \leq u_0$ every iteration.

The safety function can be computed through a recursive algorithm. To do that, we introduce first the notion of the function U_k. This function is defined in the region Q where we want to keep the trajectory. Given a point $q \in Q$, the value $U_k(q)$ represents the minimum upper bound of control for the next k iterations, that is, the controlled trajectory starting in the point q can be sustained in Q during k iterations

by using a control $|u_n| \leq U_k(q)$ in each iteration. This means that the sequence of k controls applied to the trajectory satisfy that $\max(|u_1|, |u_2|, .., |u_k|) \leq U_k(q)$. This bound is minimal, so no other controlled trajectory exists with a smaller bound of control.

The computation of the U_k function is not trivial due to the chaotic dynamics present in the region Q. However, it is possible to obtain the function U_k, following a backwards recursive algorithm. We will show that U_k can be computed with the knowledge of U_{k-1} and this, in turn, from U_{k-2}, and so on. To explain the algorithm, we consider first the case where no disturbances are present in the controlled dynamics, and then we extend the reasoning to the case where the disturbances appear in the map.

8.2.1 Computing the function U_k in absence of disturbances.

In this case we consider a map of the form $q_{n+1} = f(q_n) + u_n$ and the goal is to obtain the function $U_k(q)$, $\forall q \in Q$. Now, we introduce some notation. As the region Q contains infinite points, an initial grid on Q must be taken to perform some computations. If the grid consists of N points, we use the index $i = 1 : N$, to identify the starting point $q[i] \equiv q_n$. Alternatively, we use the index $j = 1 : N$ to denote the arrival point $q[j] \equiv q_{n+1}$. A simple representation is shown in Fig. 8.1.

In this figure the region Q is the interval $[0, 1]$ and a grid of $N = 11$ points was taken. We show an iteration of the map, where the point $q[i = 3]$ maps (control included) to the point $q[j = 9]$. The particular control used is represented as $u[i = 3, j = 9]$. In the same figure, we also display a hypothetical function U_k and its value in the arrival point $U_k[j = 9]$. The pair of values $(\, u\,[i, j], U_k[j]\,)$ can be read as *(current control corresponding with the point i to reach the point j, control bound corresponding with the point j to remain in Q the next k iterations)*. This representation will be useful to explain the operation of the algorithm.

To describe the procedure that we use, the slope-three tent map shown in Fig. 8.2 will be used as an example. The region Q selected is the interval $[0, 1]$. Note that the central points escape after one iteration. The idea is to compute recursively the functions $U_0 \to U_1 \to U_2 \to ...U_k$. Taking into account that $U_0[i]$ represents the bound of control needed by $q[i]$ to keep its trajectory in Q during 0 iterations, it follows that $U_0[i] = 0$, $\forall i$. This function is displayed in blue in Fig. 8.2(a). For visual convenience, both the tent map and the U_0 function are represented using the same $y - axis$ since the x_{n+1} scale and the control scale coincide. In the following, we will use this joint representation when both $y - axis$ labels overlap.

To explain how to compute $U_1[i]$, we take for instance, the point $q[i = 3]$ shown in the figure. This point maps into $f(q[i = 3])$ and then a control $u[i = 3, j]$ is applied. All possible choices of control are indicated in the figure with the horizontal arrows at the bottom. For each control, it corresponds a value $U_0[j]$. All the possible pairs $(\, u[i = 3, j], U_0[j]\,)$ are indicated. By simple observation, it can be found that the pair that minimizes the control bound is $(\, u[i = 3, j = 6], U_0[j = 6]\,) = (0.02, 0.0)$ (marked in red). This value represents the minimum upper bound for 1 iteration

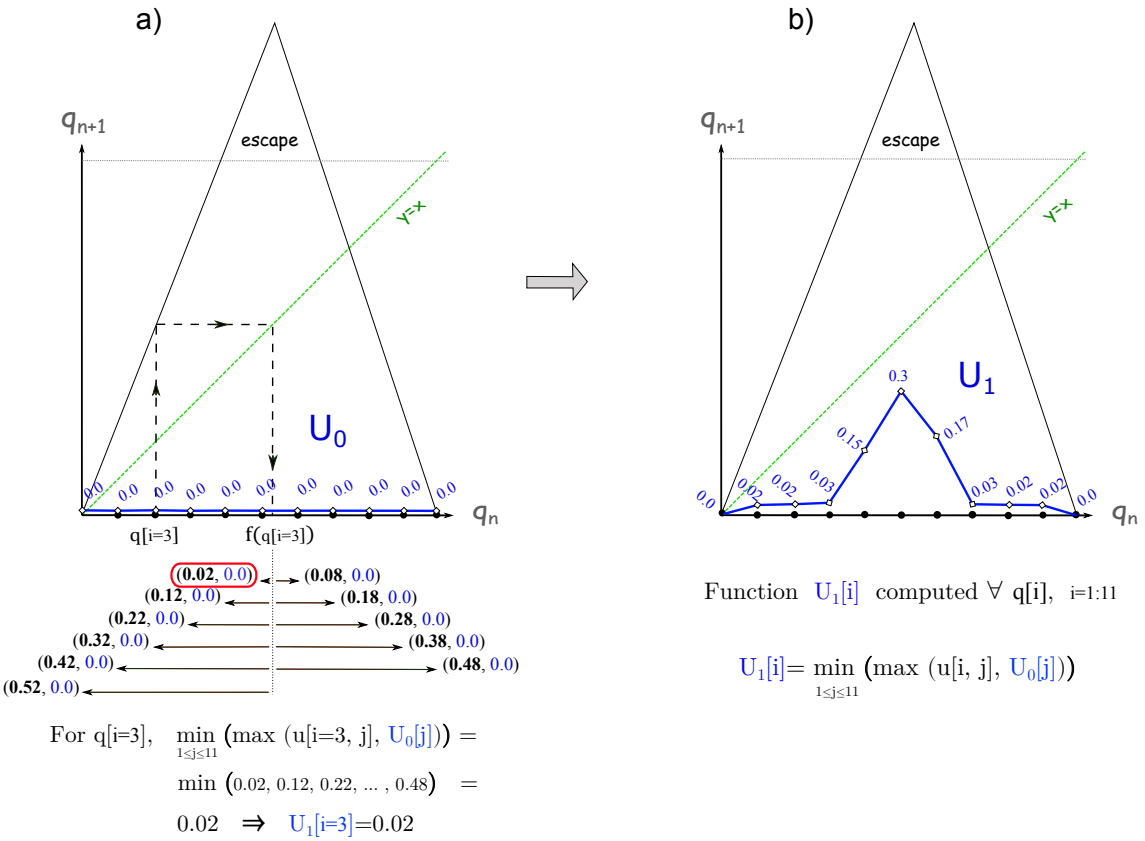

Figure 8.2. Computing the function $U_0 \to U_1$ in the slope-three tent map. The region Q selected is the interval $[0, 1]$. The initial function $U_0[i] = 0$, $\forall i$, is indicated in blue. Every new value $U_1[i]$ can be computed individually. In the left panel we represent the computation of $U_1[i = 3]$. To do that, it is necessary to know the image $f(\,q[i = 3]\,)$ and then, compute all possible controls $u[i = 3, j]$. Then the corresponding pairs $(\,u[i = 3, j],\, U_0[j]\,)$ are built. The upper bound (or maximum) of each pair is indicated in bold. To minimize the new bound of control $U_1[i = 3]$, the pair with a minimum upper bound has to be selected, that is $U_1[i = 3] = \min\limits_{1 \le j \le N} \big(\max(\,u[i = 3, j],\, U_0[j]\,)\big) = 0.02$. On the right panel, the final function $U_1[i]$, $\forall i$ is drawn, that was computed similarly (the values indicated are approximate).

and therefore $U_1[i = 3] = 0.02$. This value can be also computed as $U_1[i = 3] = \min\big(\max(\,u[i = 3, j], U_0[j]\,)\big) = 0.02$.

Proceeding similarly with the rest of the points $q[i]$ it is possible to obtain the function $U_1[i]$ $\forall i$. The result is shown in Fig. 8.2(b). Notice that the points in the extremes of Q, after the action of the map $f(q)$ do not escape, and therefore a zero control would be expected. However, due to the finite grid considered, a tiny control is needed to reach a point of the grid. In contrast, the central points of Q escape directly, and therefore they need a big control to remain in Q after one iteration. This fact is reflected in the central peak of the function U_1.

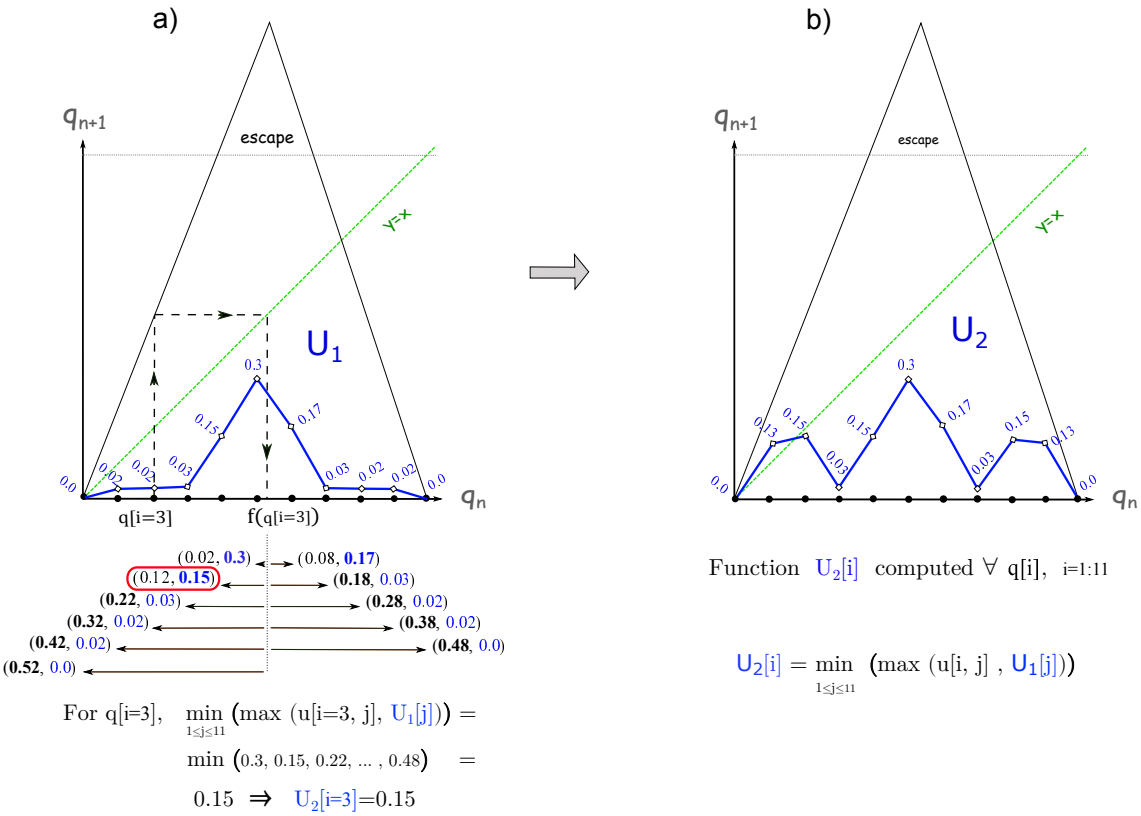

Figure 8.3. Computing the function $U_1 \to U_2$ in the slope-three tent map. The previous function $U_1[i] = 0$ (computed in Fig. 8.2), $\forall i$, is indicated in blue. Every new value $U_2[i]$ can be computed individually. In the left panel we represent the computation of $U_2[i = 3]$. To do that, it is necessary to know the image $f(\,q[i]\,)$ and then, compute all possible controls $u[i = 3, j]$. Then all the pairs $(\,u[i = 3, j],\, U_1[j]\,)$ are built. The upper bound (or maximum) of each pair is indicated in bold. To minimize the new control bound $U_2[i = 3]$, the pair with a minimum upper bound has to be selected, that is $U_2[i = 3] = \min\limits_{1\le j\le N} \big(\max\,(\,u[i = 3, j],\, U_1[j]\,)\,\big)$. On the right panel, the final function $U_2[i]$, $\forall i$, that was computed similarly (the values indicated are approximate) is drawn. To compute the functions U_3, U_4... etc, the computation is equivalent.

Once we have U_1, the function U_2 can be computed following the same process (see Fig. 8.3). Taking again the initial point $q[i = 3]$, the action of the tent map $f(\,q[i = 3]\,)$ is shown in the figure. Then a control $u[i = 3, j]$ is applied. All possible pairs $(u[i = 3, j], U_1[j])$ are indicated. In this case, the pair $(u\,[i = 3, j = 6],\, U_1\,[j = 6]) = (0.12, 0.15)$ marked in red has the minimum bound (0.15). This value represents the minimum upper bound of control for 2 iterations. Therefore $U_2[i = 3] = 0.15$. This value can be also obtained as $U_2[i = 3] = \min\big(\,\max\,(\,u[i = 3, j], U_1[j]\,)\,\big)$.

Notice that now, the strategy that minimizes the bound of control is to apply first a control $u[i = 3, j = 6] = 0.012$, to then apply a control of 0.15. If the smallest

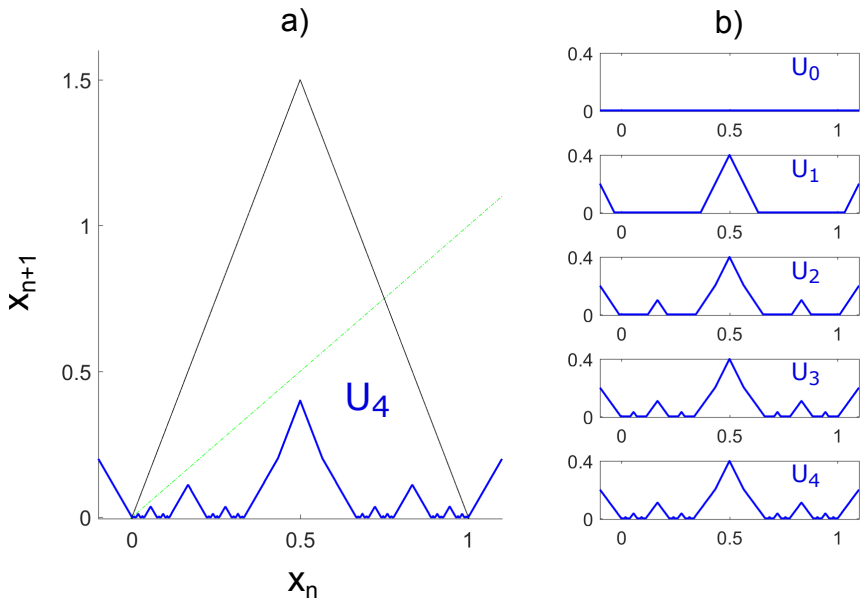

Figure 8.4. Safety functions $U_0 \to U_1 \to U_2 \to U_3 \to U_4$ in the slope-three tent map. In this case, the region Q is the interval $[-0.1, 1.1]$, and a uniform grid of 1000 points was taken. On the left panel, the slope-3 tent map and the safety function U_4 is shown. On the right panel , the successive functions U_k (starting with U_0) to obtain U_4.

control (0.02) is applied first, then the control needed to remain in Q would be 0.3, doubling the control bound of the controlled trajectory. In Fig. 8.3(b) the function U_2 is shown, where the values $U_2[i]$ were obtained following a similar procedure.

The computation of U_3, U_4.. etc. is equivalent. In general, in absence of any disturbance, we have the following recursive formula to compute the safety functions:

$$U_{k+1}[i] = \min_{1 \le j \le N} \big(\max \left(u[i,j],\, U_k[j] \right) \big) \tag{8.2}$$

In this formula, the values of $u[i,j]$ remain unchanged for every iteration of the algorithm, so they only need to be calculated once. In Fig. 8.4 we display the process for the slope-3 tent map. The region Q was selected to be the interval $[-0.1, 1.1]$. In this interval a uniform grid of 1000 points was taken. On the right side of the figure, the successive functions $U_0 \to U_1 \to U_2 \to U_3 \to U_4$ are shown.

8.2.2 Computing the function U_k in presence of disturbances

The extension of the recursive algorithm in the case of systems affected by disturbances is rather straightforward. Now the dynamics is given by $q_{n+1} = f(q_n, \xi_n) + u_n$, where ξ_n is the disturbance term belonging to a bounded distribution. In Fig. 8.5, we illustrate a map affected by a disturbance distribution (bounded). Notice that just the boundaries of the distribution are relevant to compute upper control bounds.

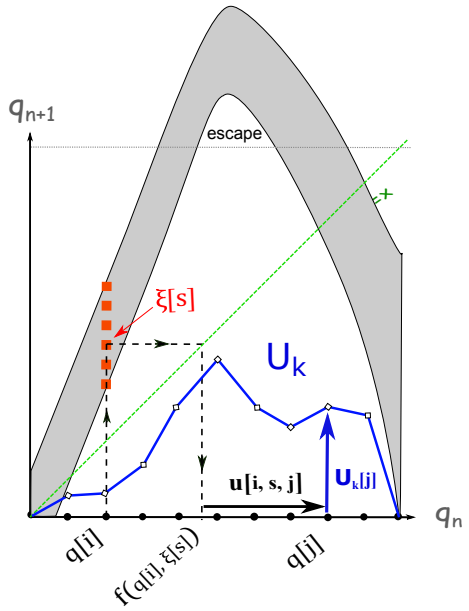

Figure 8.5. Scheme of a map affected by some disturbance distribution (bounded). The extension of the algorithm in the case of maps affected by a bounded disturbance distribution, is rather straightforward. In this case, given a point $q[i]$, to compute the upper bound of control $U_{k+1}[i]$, we have to consider all disturbed images $f(q[i], \xi[s])$. Then compute all the corresponding control bounds (as in the case of no disturbance), and finally extract the maximum among them all.

Due to the disturbance, the same point has multiple images. This number can be infinite in case of a continuous disturbance and therefore, a discretization must be taken, as shown in Fig. 8.5. Given a point $q[i]$, we denote the grid of possible images as $f(q[i], \xi[s])$, where $s = 1 : M_i$ is the index of every individual disturbance. The number M_i can take different values depending on the particular point $q[i]$. The control corresponding to the point $q[i]$ and affected by the disturbance $\xi[s]$, to reach the point $q[j]$, is denoted as $u[i, s, j]$.

To compute the functions U_k in presence of disturbances, the multiple images of every point $q[i]$ must be taken into account. First, we have to compute the individual upper control bound corresponding to each possible image $f(\,[q[i], \xi[s]\,)$, as in the case of no disturbance. Then, the maximum control value among all of them, will be the overall upper control bound corresponding to $q[i]$. The recursive formula in presence of disturbances is given by:

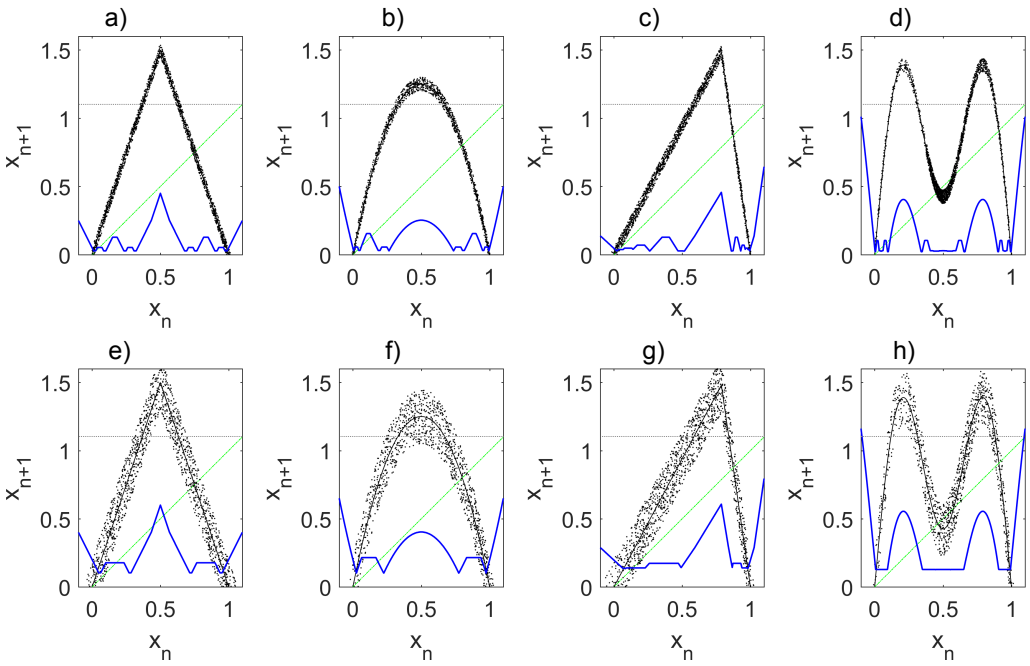

Figure 8.6. Safety function U_∞ for different maps affected by a disturbance. This figure shows how the safety function changes depending on the map and the disturbance affecting it. The maps represented are the following: (a,e) Tent map. (b,f) Logistic map. (c,g) Asymmetric tent map. (d,h) Map with two symmetric hills. The figures on the top (a,b,c,d) are affected by a uniform disturbance distribution bounded by $\xi_0 = 0.05$. In contrast, for the maps at the bottom (e,f,g,h), the disturbance bound is $\xi_0 = 0.2$. The horizontal line at "y-axis=1.1" indicates the escape. Points q that map above this line, escape directly from region $Q = [-0.1, 1.1]$. The safety functions U_∞ (in blue) have been computed for each map. By simple observation, it can be seen that safety functions for the bottom maps, take larger values than the respective maps on the top. This is because the maps at the bottom are affected by bigger disturbances and therefore bigger bounds of control are needed to control it.

$$U_{k+1}[i] = \max_{1\le s\le M_i} \left(\min_{1\le j\le N} \left(\max\left(u[i,s,j],\, U_k[j] \right) \right) \right)$$

$i \equiv$ index of the starting point $q[i],\ i = 1:N.$
where $N =$ total number of grid points.

$s \equiv$ index of the disturbance $\xi[s],\ s = 1:M_i.$
where $M_i =$ number of disturbed images corresponding with $q[i]$.

$j \equiv$ index of the arrival point $q[j],\ j = 1:N.$

(8.3)

Notice that the $u[i, s, j]$ values remain unchanged every iteration of the algorithm. Thus, they only need to be calculated once.

8.3 The safety function U_∞ and the safe sets.

If the aim of the controller is to keep the trajectory in the region Q forever with the smallest control bound, it is necessary to find U_∞ and therefore iterate infinite times the algorithm. However, when we use a finite grid to compute the safety function we have found that the algorithm converges in a finite amount of steps k. In that case we have that $U_{k+1} = U_k$ and therefore it follows that $U_\infty = U_k$. We do not intend here to explore the mathematical conditions necessary to achieve the convergence. Our finding is that for the transient chaotic maps analysed, the algorithm converges in a few iterations (in the next sections some examples supporting this point will be provided).

If the computation of the function U_k converges, the safety function U_∞ can be computed in a finite number of steps using a finite grid.

In Fig. 8.6 the safety function U_∞ was computed for different maps. The maps at the top (a,b,c,d) are affected by the same disturbance bound $\xi_0 = 0.05$. The maps at the bottom (e,f,g,h) are the same respectively, but affected by a bigger disturbance bound ($\xi_0 = 0.2$). Note that the safety function U_∞ has larger values in this case, since a larger control bound is needed to sustain trajectories affected by larger disturbances. The safety function U_∞ (in blue) was computed for each map. In all cases, the convergence was achieved with 15 iterations or less of the algorithm.

Once the safety function is computed, we need to specify the level of control u_0. This value guarantees that the trajectory can be sustained in Q by applying every iteration a control $|u_n| \leq u_0$. The u_0 value must be chosen so that $u_0 \geq \min(U_\infty)$. Above this minimum, any value u_0 is allowed. The specific choice will depend on the preferences and limitations of the controller. In general, more control will allow the trajectory to explore more points of the region Q.

Once the u_0 level is selected, the points q for which $U_\infty(q) \leq u_0$ conform what we call the *safe set*. Note that the larger the value u_0, the larger the safe set. Only this set of points can be controlled. To do that, we only need to apply every iteration, the suitable control $|u_n| \leq u_0$ to force the trajectory to pass through the safe set. Very often, the choice of the control u_n is not unique and therefore multiple controlled trajectories are possible. This makes the method very flexible.

In Figs. 8.7 (a-b-c) the safety functions corresponding to the maps of the Fig. 8.6(a) are shown. Different control levels u_0 were taken and at the bottom the respective safe sets were drawn. For each value u_0, a particular controlled trajectory is shown in Figs. 8.7 (d-e-f). Every trajectory consists of 100 iterations of the map. The control applied in every iteration of these trajectories is represented at the bottom of Figs. 8.7 (g-h-i) respectively.

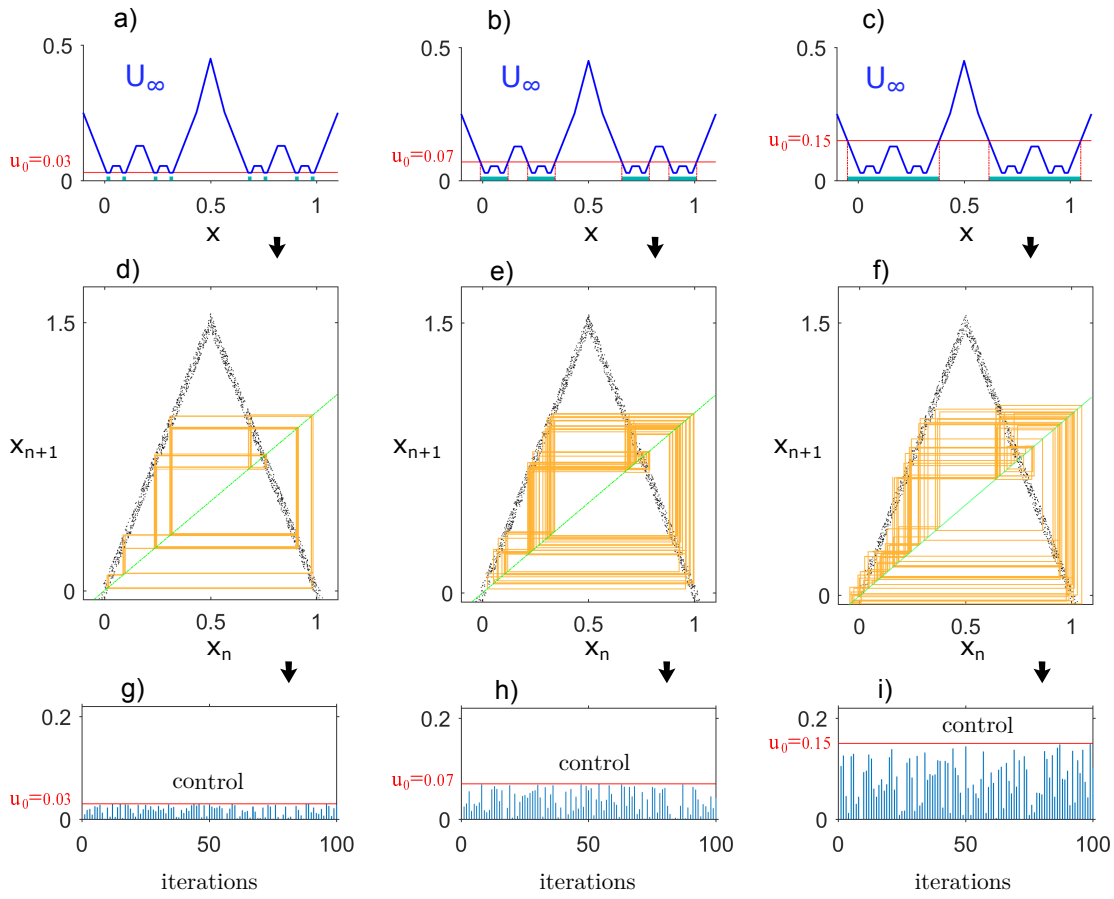

Figure 8.7. Extracting the safe sets from the safety function. Once the safety function U_∞ is computed a control level $u_0 \geq \min(U_\infty)$ has to be chosen. This control specify the upper bound of control that we want to apply. The safe set is the set of points q that satisfy $U_\infty(q) \leq u_0$. In panel (a) we draw the safety function corresponding to the map of Fig. 8.6(a). The safe set corresponding to $u_0 = 0.03$ is shown at the bottom (green bars). To control the trajectory we only need to choose a control that forces the trajectory to pass through the safe set. In panel (d) it is represented the corresponding controlled trajectory using a control bound $u_0 = 0.03$ (100 iterations were drawn). The controls $|u_n|$ applied in the 100 iterations of the map are shown in panel (g). Notice that all controls satisfy $|u_n| \leq u_0 = 0.03$. Panels (b,e,h) are equivalent but taking instead a bound of control $u_0 = 0.07$. In panels (c,f,i) the control bound is $u_0 = 0.15$. Note that the larger the u_0 value, the bigger the safe set, and therefore the trajectory is allowed to explore more points of the $Q = [-0.1, 1.1]$ region.

8.3.1 Application to the tent map affected by asymmetric disturbances

In the previous examples, we have considered maps where the disturbance ξ_n affecting the trajectories were uniformly bounded so that $|\xi_n| \leq \xi_0 \; \forall x \in Q$. However there

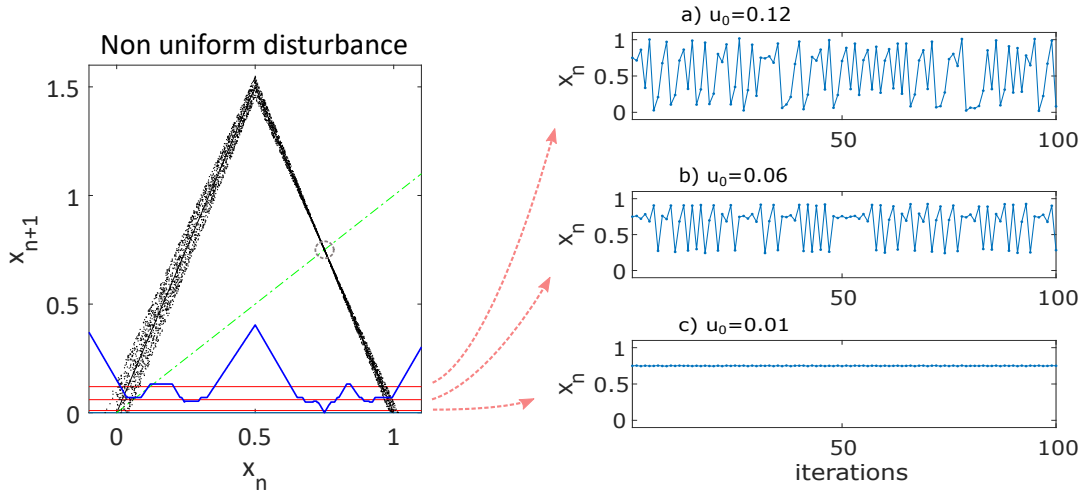

Figure 8.8. Asymmetric disturbance affecting the map. On the left panel we show the slope-three tent map affected by an asymmetric disturbance. In particular the disturbance was set to have a zero value in the fixed point $x^* = 0.75$ highlighted with a circle. This choice was made on purpose to show that the safety function U_∞ has a minimum in this point, since no control is needed to keep the trajectory in the fixed point due to the zero disturbance affecting it. Three different bounds of control u_0 have been tested. On the right panel we represent the corresponding controlled trajectories. Depending on the control level the qualitative behaviour changes drastically. A small control keeps the trajectory around the fixed point, while bigger u_0 values let the trajectory explore other points of the region [-0.1,1.1].

is no impediment to apply the algorithm in case of non-uniform disturbance bounds. To show an example, we consider the slope-3 tent map affected by a non-uniform disturbance. The system is given by:

$$x_{n+1} = \begin{cases} 3x_n + \xi_n(4x_n - 3) + u_n & \text{for } x_n \leq \frac{1}{2} \\ 3(1 - x_n) + \xi_n(4x_n - 3) + u_n & \text{for } x_n > \frac{1}{2}. \end{cases} \tag{8.4}$$

The map affected by the asymmetric disturbance is shown in Fig. 8.8. This particular choice of disturbance was made on purpose. In particular, the unstable fixed point of this map $x^* = 0.75$ is affected by zero disturbance, and therefore it needs zero control since $f(x^*) = x^*$. For this reason, we expect that the safety function evaluated in the fixed point should be $U_\infty(x^*) = 0$.

Having chosen the region $Q = [-0.1, 1.1]$ and a uniform grid of 1000 points, the U_∞ function drawn in the figure, was obtained (it takes 14 iterations to converge). We can observe that this function has a minimum in the fixed point $x = 0.75$. This minimum control is virtually zero, as we expected. For increasing control values u_0, different controlled trajectories are possible as shown in Figs. 8.8(a,b,c). Note that with the control bounds $u_0 = 0.12$ and $u_0 = 0.06$ the trajectory behaves chaotically (affected by the disturbances), while in the case of $u_0 = 0.01$, the trajectory remains

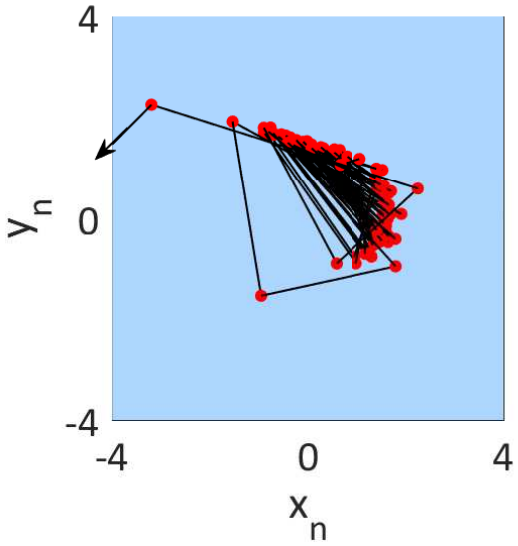

Figure 8.9. Uncontrolled trajectory in the Hénon map. The Hénon map for the parameter values $a = 2.16$ and $b = 0.3$ exhibits transient chaos. The red dots represent an uncontrolled trajectory that eventually escapes from the square $Q_0 = [-4, 4] \times [-4, 4]$. The trajectory is affected by a uniform disturbance bound with $\xi_0 = 0.1$. Black lines are displayed only to indicate the path of the trajectory.

in the fixed point. This interesting result could be used by the controller to change the qualitative behaviour of the trajectory, just varying the control value u_0.

8.3.2 Application to the Hénon map

The Hénon map is a 2D map defined as follows:

$$\begin{aligned} x_{n+1} &= a - by_n - x_n^2 \\ y_{n+1} &= x_n. \end{aligned} \tag{8.5}$$

This map shows transient chaos for a wide range of the parameters a and b. We have chosen here the parameter values $a = 2.16$ and $b = 0.3$. For these values, the trajectories with initial conditions in the square $[-4, 4] \times [-4, 4]$ have a very short chaotic transient, before finally escaping this region towards infinity. An example of this behaviour is shown in Fig. 8.9 for a given initial condition. We consider now, a situation where the variables (x, y) are affected by some uniform and bounded disturbance (ξ_n^x, ξ_n^y) so that $\parallel \xi_n^x, \xi_n^y \parallel = \sqrt{(\xi_n^x)^2 + (\xi_n^y)^2} \leq \xi_0$. To keep the orbits in $Q = [-4, 4] \times [-4, 4]$ we apply a control (u_n^x, u_n^y) also bounded $\parallel u_n^x, u_n^y \parallel \leq u_0$. The controlled dynamics of the system is then given by:

$$\begin{aligned} x_{n+1} &= a - by_n - x_n^2 + \xi_n^x + u_n^x \\ y_{n+1} &= x_n + \xi_n^y + u_n^y. \end{aligned} \tag{8.6}$$

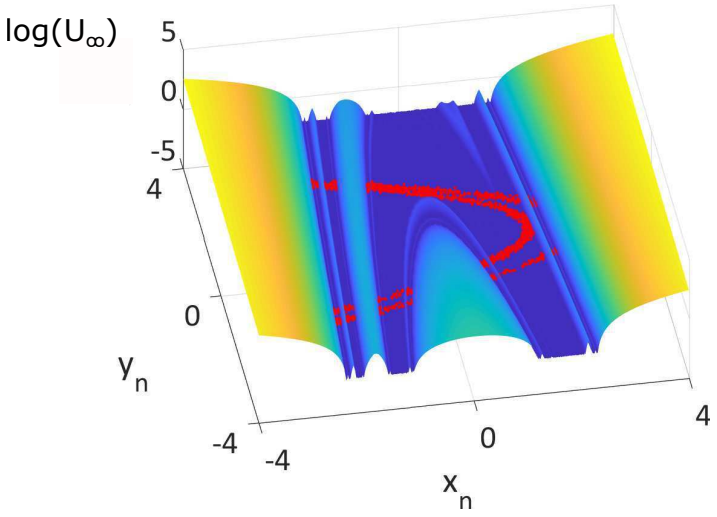

Figure 8.10. The 2D safety function for the Hénon map. Taking a uniform disturbance bounded by $\xi_0 = 0.1$ and with the goal of keeping the trajectory in the square $Q_0 = [-4, 4] \times [-4, 4]$, the safety function U_∞ was computed. This function has a minimum value of 0.08. The logarithm of U_∞ is shown here to enhance the visualization. Taking the control bound $u_0 = 0.08$, a controlled trajectory is represented (red dots). This trajectory never abandons the square $Q_0 = [-4, 4] \times [-4, 4]$.

Taking a grid of 2000×2000 points in the square $[-4, 4] \times [-4, 4]$, we have applied the extended partial control algorithm with a bound of disturbance $\xi_0 = 0.10$, obtaining after 13 iterations the safety function U_∞. The $2D$ safety function is shown in Fig. 8.10 where the logarithm of U_∞ has been plotted for a better visualization. The minimum of U_∞ is found at $u_0 = 0.07$ and with this upper bound of control, a trajectory was controlled. The red dots in the Fig. 8.10 represent the controlled orbit which remains chaotic forever in the square $[-4, 4]$.

8.3.3 Application to a time series from an ecological system.

In this example, we use the ecological model described in Chapter 3. However, here we applied the new partial control approach. This model, describes the interaction between 3 species: resources R, consumers C and predators P. The interest of this model lies in the fact that, for some choices of parameters, transient chaos appears involving the extinction of one of the species. Without no control, the system evolves from a situation where the three species coexist towards a state where just two species survive, while predators get extinct.

The resulting model is given by the following set of nonlinear differential equa-

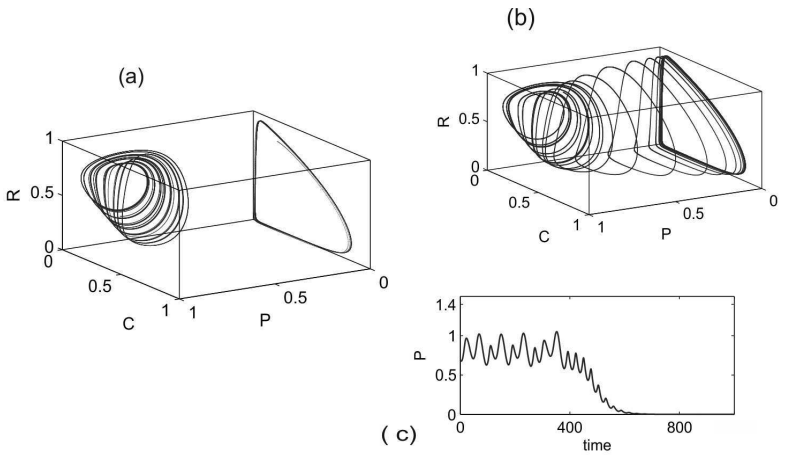

Figure 8.11. Dynamics of the extended McCann-Yodzis (Eqs. 8.7). Depending on the values of the parameters different dynamics are possible. (a) Before the boundary crisis ($K = 0.99$, $\sigma = 0$), there are two possible attractors depending on the initial conditions: one chaotic attractor where the three species coexist, and one limit cycle where only the resources and consumers coexist. (b) The case treated here, for values ($K = 0.99$, $\sigma = 0.07$), a chaotic crisis appears and the limit cycle is the only asymptotic attractor. (c) Time series of the predators population corresponding to the case (b). The predators eventually get extinct.

tions:

$$\begin{aligned}
\frac{dR}{dt} &= R\left(1-\frac{R}{K}\right) - \frac{x_c y_c C R}{R+R_0} \\
\frac{dC}{dt} &= x_c C\left(\frac{y_c R}{R+R_0} - 1\right) - \psi(P)\frac{y_p C}{C+C_0} \\
\frac{dP}{dt} &= \psi(P)\frac{y_p C}{C+C_0} - x_p P.
\end{aligned} \tag{8.7}$$

Depending on the parameters values, different dynamical behaviours can be found (see Fig. 8.11). Following [27] we have fixed the model parameters : $x_c = 0.4$, $y_c = 2.009$, $x_p = 0.08$, $y_p = 2.876$, $R_0 = 0.16129$, $C_0 = 0.5$, $K = 0.99$ and $\sigma = 0.07$. For these values transient chaos appears, and the predators eventually get extinct as shown in Figs. 8.11(b) and 8.11(c).

With the aim of avoiding the extinction, we have applied the new approach of partial control method. To do that, first we have discretized the dynamics to obtain a map. It is straightforward to build a map taking a Poincaré section that intersects the flow. In this case, we have chosen the plane $C = 0.24$ as shown in Fig. 8.12(a). For this Poincaré section the intersection of the plane and the flow, gives us a set of points (R_n, C_n, P_n) that is approximately one-dimensional. Note that C_n has a constant value equal to 0.24, and the variable R_n is practically constant. Therefore it is possible to construct a return map of the form (P_n, P_{n+1}) and control the system

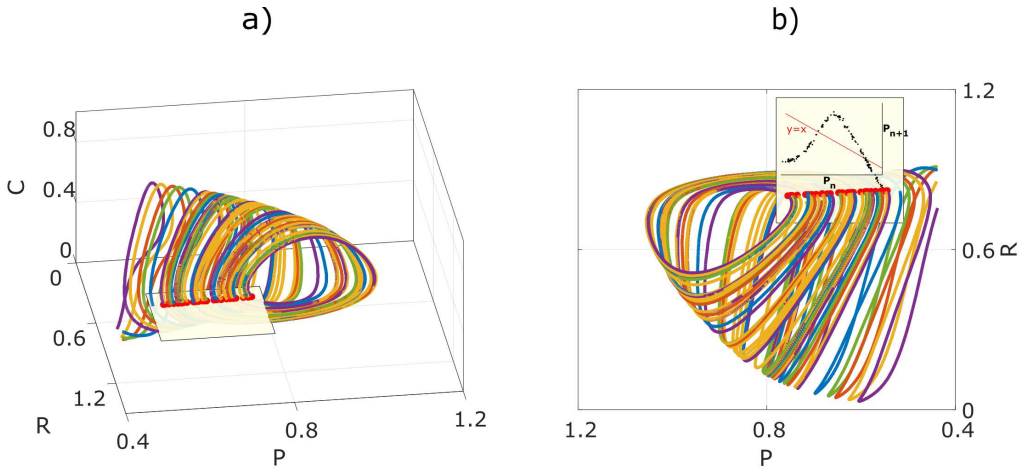

Figure 8.12. Building the map from several trajectories. It is possible to discretize the dynamics of the ecological model by taking a Poincaré section. In this case, we have chosen the section with $C = 0.24$ as shown on the left panel. With the set of points (R_n, C_n, P_n) intersecting the plane, it is possible to build a return map of the form $P_{n+1} = f(P_n)$ as represented on the right panel. Note that the values R_n and C_n in the Poincaré section remain practically constant.

just perturbing the variable P_n. Due to the finite escape time of transient chaotic trajectories, several trajectories were simulated (displayed with different colors in Fig. 8.12) to obtain a representative return map.

We consider here two different cases. First, a situation where the trajectories are affected by continuous noise in the variables. Second, the case where a continuous noise is affecting the parameter K of the system. Do not confuse here the disturbance and noise meanings. The disturbance term only appears in the map and represents the amount of uncertainty measured in this map. In this sense, the disturbance is the product of the accumulated noise affecting the continuous trajectory during one iteration of the map. The controlled scheme is given by:

$$P_{n+1} = f(P_n, \xi_n) + u_n, \tag{8.8}$$

where ξ_n is some particular disturbance whose bound ξ_0 may be space-dependent.

In the first scenario, the trajectories were obtained by using a RK4 integrator with a Gaussian noise affecting the variables (R, C, P). In Fig. 8.13(a) the return map obtained via 3000 intersections of the trajectories with the Poincaré section is shown. With these points it is possible to reconstruct the map including the disturbance. Note that in this sense, noise removal techniques are useless here since we want to include the disturbances. To do that, different statistical techniques can be used. One very powerful is the bootstrapping technique that allows the estimation of the sampling distribution of almost any statistic using random sampling methods. Here for simplicity, a quantile regression technique has been used to estimate the

upper and lower bounds of the map. Taking the quantile values 0.01 (lower bound) and 0.99 (upper bound) the two red curves shown in Fig. 8.13(a) were obtained. The gap between the two curves contains the disturbed points corresponding to each P_n value. We can see that the disturbance gap is rather uniform in this case.

The Q region where we want to keep the trajectory is the interval $[0.58, 0.76]$, where a grid of 2000 points were taken for the computations. To compute the safety function U_∞ we have applied the algorithm, which has converged in only 10 iterations. The resulting safety function U_∞ is shown in Fig. 8.13(b). The minimum of this function corresponds to the value 0.010. Taking a control level $u_0 = 0.011$ a trajectory was controlled using the corresponding safe set. In Fig. 8.13(c) 500 iterations of the controlled trajectory are displayed. Every time the Poincaré section is crossed, a suitable control $|u_n| \leq 0.11$ is applied. As a result, the extinction of the predators is avoided and the 3 species coexist in a stable chaotic regime. Here, it is important to point out that what we are doing in the phase space is to apply control only in the variable P_n to move the point (R_n, C_n, P_n) to the point $(R_n, C_n, P_n + u_n)$, since C_n is constant and R_n remains practically unchanged. In this sense a suitable Poincaré section choice can simplify the control requirements greatly.

In the second situation, we consider a small Gaussian noise affecting the parameter K of the system. This noise affects continuously K and it was included in the integrator. Proceeding in a similar way to the previous case, we obtain the return map shown in Fig. 8.14(a). It can be appreciated that, in comparison with the first scenario, the disturbance interval (gap between red lines) is smaller and less uniform and therefore the U_∞ function obtained will be quite different. After 15 iterations of the algorithm, the U_∞ is obtained. The final function is shown in Fig. 8.14(b) with a minimum value of 0.005. Taking the control bound $u_0 = 0.006$, the controlled trajectory drawn in Fig. 8.14(c) was obtained. The trajectory displayed passes through the Poincaré section 500 times and the controls $|u_n|$ made never exceeded the value 0.006.

The important result of this section is the potential application of this method to experimental time series without the need of knowing the mathematical equations of the map. We have shown that this map can be reconstructed and used to obtain the safety function U_∞. This function allows us to control the trajectories successfully.

Specially in the case where the maps is built from experimental data, it is reasonable to expect that unusual events not covered by the map can happen. In this sense, the estimation of the disturbance bounds by means of some statistical technique can be settled with a certain degree of confidence. For example, in the case of a normal disturbance distribution, if we take the three-sigma interval, the safety function U_∞ obtained and the upper bound u_0 selected, will be valid the 99.7% of the times. The rest of iterations, an extra control will minimize the risk of having to do a big control in the following iterations.

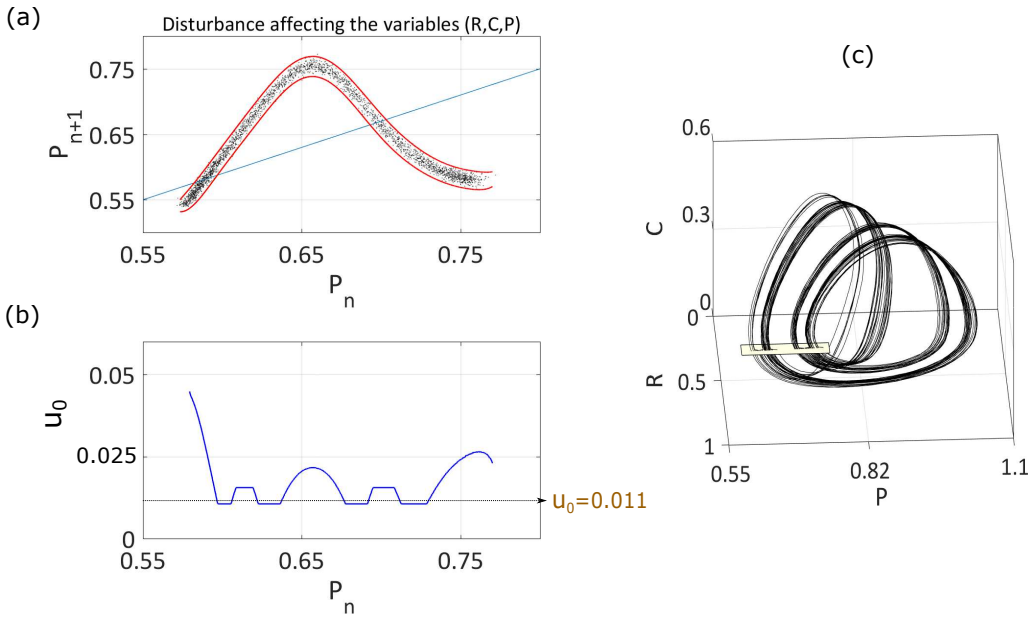

Figure 8.13. Continuous noise affecting the variables. (a) Return map obtained by means of 3000 intersections of the trajectories with the Poincaré section. A continuous noise is affecting the variables (R, C, P) and it arises in the return map as a stripe. Red lines represent the quantile regression calculated for quantiles 0.01 and 0.99. The gap between the red lines represent the disturbance bound. In this case the gap is rather uniform in all the map. (b) Taking the region Q as the interval $[0.58, 0.76]$, the safety function U_∞ was computed obtaining a minimum value of 0.010. (c) A controlled trajectory was computed with a control bound of $u_0 = 0.011$. Every time the trajectory crosses the section, a control $|u_n| \leq 0.11$ is applied to put the orbit again in the nearest point P_n where $U_\infty(P_n) \leq 0.011$.

8.4 Conclusions

We have presented here a new algorithm in the context of the partial control method. This method is applied to maps of the form $q_{n+1} = f(q_n, \xi_n) + u_n$, where ξ_n is the disturbance and u_n the control. Given a region Q where the dynamics presents an escape, the method calculates directly the minimum upper control bound needed for each point $q \in Q$ to remain in Q forever. To do that, we have introduced the safety function $U_\infty(q)$ that can be computed through the recursive algorithm. Once the safety function is computed, we only need to pick a bound $u_0 \geq \min(U_\infty)$. Controlled trajectories are possible by applying a suitable control $|u_n| \leq u_0$ every iteration.

In comparison with the classical partial control method, this extended approach can be applied to more general maps where the disturbance may appear in different ways. In addition, there is no need to indicate in advance a bound of control u_0. The safety function U_∞ automatically gives us all the information, including the minimum possible control bound for the system. The use of the safety function U_∞

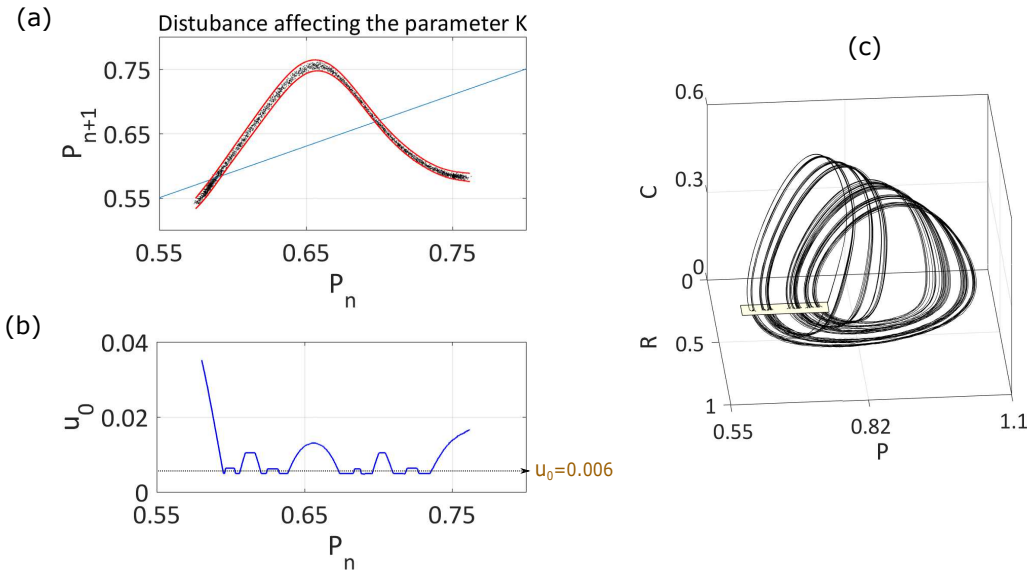

Figure 8.14. Continuous noise affecting the parameter K. (a) Return map obtained by means of 3000 intersections of the trajectories with the Poincaré section. A continuous noise is affecting the parameter K and it arises as a stripe in the return map. Red lines represent the quantile regression calculated for quantiles 0.01 and 0.99. The gap between the red lines represent the bound of the disturbance. The gap in this case is not uniform, since some points P_n are affected by bigger disturbances than others. (b) Taking the region Q as the interval $[0.58, 0.76]$, the safety function U_∞ was computed obtaining a minimum value of 0.005. (c) A controlled trajectory was computed with a control bound of $u_0 = 0.006$. Every time the trajectory crosses the section, a control $|u_n| \leq 0.006$ is applied to put the orbit again in the nearest point P_n, where $U_\infty(P_n) \leq 0.006$.

instead of only the safe set, makes the method very robust and specially useful in case of experimental time series.

The new partial control algorithm has been proven in the one-dimensional tent map and the two-dimensional Hénon map, under a non-uniform and a uniform disturbance bound respectively. We have also applied the control method to a continuous ecological system where one of the species eventually gets extinct via a chaotic crisis. In order to avoid the extinction the partial control technique was applied. Two different scenarios were studied, a continuous noise affecting the variables, and a continuous noise affecting one parameter of the system. In both cases a one-dimensional return map was built and the disturbance bound distribution estimated via a quantile regression technique. Then, the safety function U_∞ was obtained and after picking the desirable u_0 bound value, the system was controlled avoiding the extinction.

Finally, we want to highlight the potential of this approach to keep bounded and low the effort necessary for controlling the system. In this work, the method was applied to avoid escapes in systems with a transient chaotic behaviour. However, we believe that under small modifications of the algorithm described here, the

same method can be applied in other scenarios. For example, the reverse problem of forcing the trajectories to escape in a certain amount of iterations, the stabilization of periodic orbits or the suppression of the bursting dynamics in chaotic systems affected by disturbances. All these cases can also be studied under this new approach.

Chapter 9
Discussion

The presence of a nonattractive chaotic set, also called chaotic saddle, in phase space implies the appearance of a finite-time kind of chaos known as transient chaos. For a given dynamical system in a certain region of phase space with transient chaos, trajectories eventually abandon the chaotic region and escape to an external attractor. In some situations, this attractor may involve an undesirable behavior, so the application of a control in the system is necessary to avoid it.

The nonattractive nature of transient chaos and eventually the presence of noise may hinder this task. In this thesis, the recently developed partial control method was applied to several nonlinear dynamical systems affected by different disturbances. By computing certain special sets in the phase space (called the safe sets), it is possible to sustain the transient chaotic behavior, avoiding the escape of the trajectories. One of the main results of this method is that, the safe sets exist even for control values smaller than the disturbance magnitude affecting the system, becoming this method very efficient in terms of control effort.

Before the work developed here, the method had been applied to paradigmatic systems in Nonlinear Dynamics like the one-dimensional tent map, the two-dimensional Hénon map or the flow of the Duffing oscillator. All of them have been studied for a choice of parameters where transient chaos appears, and it was assumed that a bounded disturbance and a bounded control affects the variables of the system.

In this thesis, one of the first studies it was to prove this control method in a very interesting system found in the field of Ecology field. This model exhibits transient chaos involving the undesirable extinction of one species. In order to simulate a more realistic system we also introduce in the dynamics of this model a certain amount of disturbance. After having applied the partial control method, we have shown that this technique is able to avoid the extinction by using a small amount of control. Furthermore, a comparison with another well-know control method was presented, demonstrating the high performance of the partial control technique.

It is not always possible to have access to the variables of the system, and for that reason we explore in later works, the possibility of applying control to some available parameter of the system. After studying different control scenarios, we conclude that the safe sets (with the control smaller than the disturbance) can exist

in the situation where the disturbance affects a parameter (known as random maps), and the control is applied on the same parameter. In this scheme we assume that the parameter p has a nominal value p_0 and small variations $p_0 + \Delta p$ are allowed. Different safe sets for different random maps were successfully computed.

In order to apply the control method to different dynamical scenarios, we consider the interesting case of the time-delay coordinate maps. This maps are specially relevant since they usually arise from the reconstruction of experimental time series. The main obstacle that we have found in these systems is that only one variable can be controlled. This restriction affects severely the performance of the computed safe set. We have shown that the safe sets exist for these maps. However, the ratio control/disturbance was bigger than in the case where all variables are controllable.

To overcome the difficulties found when we tried to implement the partial control to time series, we have developed a more general approach of this technique. The underlying idea is to characterize every point of the region where we want to keep the trajectory controlled. By knowing how safe is every point of that region, we can design a more efficient and robust approach of the partial control method. In this sense we introduced the concept of safety function, and the algorithm to compute it. This new tool is able to deal with additive and multiplicative disturbances affecting variables or parameters of the system, and allows to improve the efficiency of the control applied, specially in cases of large deviations of the real trajectory from the model predictions.

9.0.1 Considerations about the method

In general, we observe that in most systems analysed, the safe sets or the safety functions approximately resemble the stable manifold of the chaotic saddle. If the available variables and/or parameters can be perturbed such that the deviation in the trajectory is locally perpendicular to the stable manifold, then the best ratio control/disturbance is achieved. However, due to the complex shape of the manifolds (in case of chaotic dynamics), analytical results to study the performance of the control method are quite complicated.

For the same reason, mathematical proofs about convergence and existence of the safe sets or the safety functions are not trivial, due to the complex shape of the chaotic saddle and the dependence with respect to the values of the disturbance ξ_0 affecting the system. However, from a computational point of view, the algorithm to compute the safe sets converges because we work with a finite grid resolution, that is, a finite amount of points on which the safe condition is evaluated. In the case of the safety functions, computations with increasing resolutions had been made in all the systems presented here, to ensure that the shape of the functions do not change significantly.

In this work we also obtain for the first time a 3-dimensional safe set. No theoretical restrictions have been found to apply the control method to higher dimensions. However all the algorithms developed here lack of the curse of dimensionality problem, that is, higher dimensions demands an exponential increase of computations.

In this sense, a possible option to reduce this effect is to parallelize the algorithm, since both the algorithm to compute the safe sets and the algorithm to compute the safety functions possess parts that can be split and computed at the same time.

9.0.2 Future work

In the last chapter of this thesis, it was proposed a new approach of the partial control method that allows to extend the method to more general scenarios. With this technique, the minimum possible control arises directly from the computation of the safety functions and a general picture of how safe is each region of the phase space is obtained.

This new approach was applied with the aim of avoiding the escape of transient chaotic trajectories. However we think that other dynamical goals can be achieved under minimum variations of the algorithm. For example, a scenario where it is necessary to force a noisy trajectory trapped in a chaotic attractor, to escape to an external attractor. Or also a situation where the goal is to conduct a chaotic orbit, from a given starting state to a final desired state, in no more than a certain number of iterations.

The other scenario that we think it deserves some exploration, is the possibility to create a partial control version to apply it directly in continuous systems without having to build a map. With that approach it is reasonable to think that the efficiency of the control can be improved, since the restriction to apply the control only at specific times or in an specific Poincaré plane is eliminated. In this sense, many interesting questions appear. For example, for this version of the method, the amount of continuous control would be smaller than the amount of continuous disturbance, like in the case of maps?, how the safe sets or safety functions arise?. Based on the idea that this method is based on the formation of the horseshoe in the phase space, and this process takes some minimum time, it may be possible that the discrete control plan was the best possible strategy?. This and other challenging questions still remain open to explore in future works.

Chapter 10
Conclusions

The main conclusions of this thesis are described below:

- We have applied the partial control method to an ecological model of 3 species. This system presents transient chaos involving the extinction of one species. By applying small controls just on the predator population, the method is able to avoid the extinction. In addition, a comparison with another well-known method was carried out. Taking different intensities of noise, it was shown that the amount of control needed by the partial control, is smaller than the control strategy proposed by Dhamala and Lai (1999), specially for small disturbances.

- We have studied the Lorenz system in the presence of disturbances for a particular choice of parameters where it shows transient chaos. Typical uncontrolled trajectories in this system follow a transient chaotic motion until they escape to one of the two stable non-chaotic attractors. To avoid these escapes, we have applied the partial control technique in three different ways, obtaining for the first time a 3D safe set.

- A new use of the safe sets have been proposed. The goal of control here is to keep trajectories with a chaotic behaviour during a desired time, and after that, to force the escape in the shortest possible time. With the only information given by the safe set, we have shown that the escape times can be accelerated several times respect to the average escape time if no control is applied. This ability to sustain the trajectories, and then accelerate their escape endow the method a great flexibility.

- We have introduced the parametric partial control method. In this scheme, the control is applied on some parameter affected by a bounded disturbance. Parametric safe sets were obtained for different random maps, showing that the partial control approach can be also applied to parameters of the chaotic system to avoid escapes.

- The control method was also applied to different delay-coordinate nonlinear maps with chaotic behaviour and affected by random disturbances. By applying small corrections in the observables of the system we show that it is possible to control the orbits with the only observation and control of one variable.

- Finally, a new approach with the same philosophy of partial control has been developed. By computing a new tool called the safety function, it is possible to treat more general maps and increase the efficiency of the control. One of the main advantages of this approach is that the minimum possible control bound is obtained automatically, rather than guessing it in advance. The use of the safety function instead of only the safe set, makes the method more robust and specially useful in case of experimental time series.

Bibliography

References

[1] T. Tél and M. Gruiz. *Chaotic Dynamics.* (Cambridge University Press, UK 2006).

[2] E. Ott, C. Grebogi and J.A. Yorke. Controlling chaos. *Phys. Rev. Lett.* **64**, 1196-1199, (1990).

[3] K. Pyragas. Continuous control of chaos by self-controlling feedback. *Phys. Lett. A* **170**, 421-428, (1992).

[4] I.B. Schwartz and I. Triandaf. The slow invariant manifold of a conservative pendulum-oscillator system. *Int. J. Bifurcation Chaos* **6**, 673-692, (1996).

[5] V. In, M.L. Spano, J.D. Neff, W.L. Ditto, C.S. Daw, K.D. Edwards and K. Nguyen. Maintenance of chaos in a computational model of thermal pulse combustor. *Chaos* **7**, 605-613, (1997).

[6] M. Perc and M. Marhl. Chaos in temporarily destabilized regular systems with the slow passage effect. *Chaos Soliton Fract.* **27**, 395-403, (2006).

[7] W. Yang, M. Ding, A.J. Mandell and E. Ott. Preserving chaos: Control strategies to preserve complex dynamics with potential relevance to biological disorders. *Phys. Rev. E* **51**, 102-110, (1995).

[8] I.B. Schwartz and I. Triandaf. Sustaining Chaos by Using Basin Boundary Saddles. *Phys. Rev. Lett.* **77**, 4740-4743, (1996).

[9] M. Dhamala and Y.C Lai. Controlling transient chaos in deterministic flows with applications to electrical power systems and ecology. *Phys. Rev. E* **59**, 1646-1655, (1999).

[10] D.P. Bertsekas. Infinite-time reachability of state-space regions by using feedback control. *IEEE Trans. Autom. Control* **17**, 604-613, (1972).

[11] D.P. Bertsekas and I.B. Rhodes. On the minimax reachability of target set and target tubes. *Automatica* **7**, 233-247, (1971).

[12] J. Aguirre, F. d'Ovidio and M.A.F. Sanjuán. Controlling chaotic transients: Yorke's game of survival. *Phys. Rev. E* **69**, 016203, (2004).

[13] S. Zambrano, M.A.F. Sanjuán and J.A. Yorke. Partial control of chaotic systems. *Phys. Rev. E* **77**, 055201(R), (2008).

[14] S. Zambrano and M.A.F. Sanjuán. Exploring partial control of chaotic systems. *Phys. Rev. E* **79**, 026217, (2009).

[15] J. Sabuco, S. Zambrano and M.A.F. Sanjuán. Partial control of chaotic transients using escape times. *New J. Phys.* **12**, 113038, (2010).

[16] J. Sabuco, S. Zambrano, M.A.F. Sanjuán and J.A. Yorke. Finding safety in partially controllable chaotic systems. *Commun. Nonlinear Sci. Numer. Simul.* **17**, 4274-4280, (2012).

[17] J. Sabuco, S. Zambrano, M.A.F. Sanjuán and J.A. Yorke. Dynamics of partial control. *Chaos* **22**, 047507, (2012).

[18] K. McCann and P. Yodzis. Bifurcation structure of a three-species food chain model. *Theor. Popul. Biol.* **48**, 93-125, (1995).

[19] V. Hutson and K. Schmitt. Permanence and the dynamics of biological systems. *Math. Biosci.* **111**, 1-71, (1992).

[20] I.V. Kolmanovski and E.G. Gilbert. Multimode regulators for systems with state & control constraints and disturbance inputs, in *Control Using Logic-Based Switching*, edited by Stephen Morse (Lecture Notes in Control and Information Sciences, vol 222. Springer, Berlin, 1997).

[21] F. Blanchini. Set invariance in control. *Automatica* **35**, 1747-1767, (1999).

[22] R. Genesio, M. Tartaglia and A. Vicino. On the estimate of asymptotic stability regions: State of art and new proposal. *IEEE Trans. Autom. Control* **30**, 747-755, (1985).

[23] M. Nagumo. Über die Lage der Integralkurven gewöhnlicher Differentialgleichungen. *Proc. Phys. Math. Soc. Japan* **24**, 551-559, (1942).

[24] A.S. Shiriaev and A.L. Fradkov. Stabilization of invariant sets for nonlinear systems with applications to control of oscillations. *Int. J. Robust Nonlin.* **11**, 215-240, (2001).

[25] P.O. Gutman and M. Cwikel. Admisible sets and feedback control for discrete-time linear systems with bounded control and states. *IEEE Trans. Autom. Control* **31**, 373-376, (1986).

[26] See supplementary material at http://www.fisica.urjc.es/physics/partialcontrol for the software for partial control.

[27] J. Duarte, C. Januário, N. Martins and J. Sardanyés. Chaos and crises in a model for cooperative hunting: a symbolic dynamics approach. *Chaos* **58**, 863-883, (2009).

[28] E. Lorenz. Deterministic nonperiodic flow. *J. Atmos. Sci.* **20**, 130-141, (1963).

[29] J.L Kaplan and J.A. Yorke. Preturbulence: A regime observed in a fluid flow model of Lorenz. *Commun. Math. Phys.* **67**, 93-108, (1979).

[30] J.A. Yorke and E.D. Yorke. Metastable chaos: the transition to sustained chaotic behavior in the Lorenz model. *J. Stat. Phys.* **21**, 263-277, (1979).

[31] R. Capeáns, J. Sabuco and M.A.F. Sanjuán. When less is more: Partial control to avoid extinction of predators in an ecological model. *Ecol. Complex.* **19**, 1-8, (2014).

[32] A.G. Lopéz, J. Sabuco, J.M. Seoane, J. Duarte, C. Januário and M.A.F. Sanjuán. Avoiding healthy cells extinction in a cancer model. *J. Theor. Biol.* **349**, 74-81, (2014).

[33] R. Capeáns, J. Sabuco, M.A.F. Sanjuán and J.A. Yorke. Partially controlling transient chaos in the Lorenz equations. *Phil. Trans. R. Soc. A* **375**, 2088, (2017).

[34] S. Das and J.A. Yorke. Avoiding extremes using partial control. *J. Differ. Equations Appl.***22**, 217-234, (2015).

[35] W.L Ditto, S.N. Rauseo and M.L. Spano. Experimental control of chaos. *Phys. Rev. Lett.* **65**, 3211-3215, (1990).

[36] F. Romeiras, C. Grebogi and E. Ott. Multifractal properties of snapshot attractors of random maps. *Phys. Rev. A* **41**, 784-799, (1990).

[37] L. Arnold. *Random dynamical systems.* (Springer-Verlag, Berlin, 1998).

[38] J. Jacobs, E. Ott, T. Antonsen and J.A. Yorke. Modeling fractal entrainment sets of tracers advected by chaotic temporally irregular fluid flows using random maps. *Physica D* **110**, 1-17, (1997).

[39] Z. Neufeld and T. Tél. Advection in chaotically time-dependent open flows. *Phys. Rev. E* **57**, 2832-2842, (1995).

[40] M.A.F Sanjuán, J. Kennedy, C. Grebogi and J.A. Yorke. Indecomposable Continua in Dynamical Systems with Noise: Fluid Flow past an Array of Cylinders. *Chaos* **7**, 125-138, (1997).

[41] M.A.F Sanjuán, J. Kennedy, E. Ott and J.A. Yorke. Indecomposable Continua and the characterization of strange sets in Nonlinear Dynamics. *Phys. Rev. Lett.* **78**, 1892-1895, (1997).

[42] T. Kuang. *Delay differential equations: with applications in population dynamics.* (Academic Press, 1993).

[43] N.H. Packard, J.P. Crutchfield, J.D. Farmer and R.S. Shaw. Geometry from a time series. *Phys. Rev. Lett.* **64**, 712-716, (1980).

[44] F. Takens. Detecting strange attractors in turbulence, in *Dynamical Systems and Turbulence*, edited by D. Rand, L.S. Young (Lecture Notes in Mathematics, vol 898. Springer, Berlin, 1981) pp. 366-381.

[45] T. Sauer, J.A. Yorke and M. Casdagli. Embedology. *J. Stat. Phys.* **65**, 579-616, (1991).

[46] A. Eftekhari, H.L. Yap, M.B. Waking and C.J. Roxell. Stabilizing Embedology: Geometry-Preserving Delay-Coordinate Maps. *Phys. Rev. E.* **97**, 022222, (2018).

[47] J.D. Farmer and J.J. Sidorowich. Predicting chaotic time series. *Phys. Rev. Lett.* **59**, 845-848, (1987).

[48] H. Ye, R.J. Beamish, S.M. Glaser, S.C.H. Grant, C. Hsieh, L.J. Richards, J.T. Schnute and G. Sugihara. Equation-free mechanistic ecosystem forecasting using empirical dynamic modeling. *Proc. Natl. Acad. Sci.* **112**, E1569-E1576, (2015).

[49] P. Holmes. A Nonlinear Oscillator with a Strange Attractor. *Phil. Trans. R. Soc. Soc. Lond. Ser. A* **292**, 419, (1979).

[50] Shao-Fu Wang, Xiao-Cong Li, Fei Xia and Zhan-Shan Xie. The novel control method of three dimensional discrete hyperchaotic Hénon map. *Appl. Math. Comput.* **247**, 487-493, (2014).

[51] R. Capeáns, J. Sabuco and M.A.F. Sanjuán. Parametric partial control of chaotic systems. *Nonlinear Dyn.* **2**, 869-876, (2016).

Resumen de la tesis en castellano

Introducción

Antecedentes del control parcial

A diferencia de los primeros métodos de control aplicados a sistemas caóticos donde se buscaba suprimir el caos, el método de control parcial busca todo lo contrario: mantener el comportamiento caótico en sistemas que presentan caos transitorio.

En algunos sistemas, el comportamiento caótico puede resultar una propiedad deseable. Sin embargo, existen situaciones dinámicas donde este comportamiento caótico no es permanente y desaparece con el tiempo. Con el objetivo de convertir este caos transitorio en permanente, se han propuesto diferentes métodos de control. En este sentido, métodos como el de Dhamala y Lai [9] propuesto en 1999, ya mostraron el enorme potencial de este tipo de control en importantes aplicaciones de ciencia e ingeniería. Este método, junto con otros similares se basan en la identificación de ciertas regiones de escape en el espacio de fases a través de las cuales las trayectorias abandonan la zona caótica para migrar hacia otro atractor del sistema.

En 2004 surge una novedosa idea con el trabajo de Aguirre et al. 2004 [12], en el estudio de mapas unidimensionales con caos transitorio. En él se identifican por primera vez una serie de regiones en el espacio de fases, posteriormente llamadas conjuntos seguros, a través de los cuales se puede evitar el escape de las trayectorias, forzándolas a pasar a través de estos conjuntos mediante la aplicación de pequenãs perturbaciones.

Este método destaca sobre los anteriores por la excelente capacidad de estos conjuntos seguros para lidiar con dinámicas afectados por ruido, el cual en mayor o menor medida, aparece en todo sistema real. En este sentido, para cada amplitud de ruido existen unos conjuntos seguros apropiados. En particular, dada una cota máxima de ruido, existe un conjunto seguro tal que es capaz de controlar la trayectoria aplicando una cantidad de control menor que la cantidad de ruido que afecta la trayectoria.

Esta idea fue generalizada por Zambrano et al. 2008 [13], a aquellos sistemas que presentan una herradura de Smale, donde la acción de la dinámica estira y dobla una región del espacio de fases. Posteriormente Sabuco et al. 2010 [15], exploró la posibilidad de modificar los conjuntos de tiempos de escape como conjuntos seguros. Estos conjuntos permiten incrementar la región de control y así hacer más eficiente el método. Finalmente, Sabuco et al. 2012 [16], presenta un algoritmo que es capaz

de automatizar la búsqueda de conjuntos seguros. La única información que se requiere es el mapa, la región Q donde se quiere mantener la trayectoria, la cota de ruido y control. Esta automatización permitió encontrar conjuntos seguros de mayor complejidad.

Avances en el método de control parcial

Esta tesis constituye un estudio y desarrollo del método de control parcial. En los primeros capítulos se exploran diferentes aplicaciones del método a sistemas donde se asume que las variables que están afectadas por cierta cantidad de ruido. Bajo este esquema, en el capítulo 3 se estudia la aplicación del método a un sistema ecológico modelado por 3 ecuaciones diferenciales acopladas. Este modelo puede presentar caos transitorio, conduciendo al sistema a un estado indeseado. Mediante la construcción de un mapa unidimensional se consigue determinar un conjunto seguro apropiado que permite hallar el control necesario para mantener la dinámica caótica para siempre. En la misma línea, en el capítulo 4 se explora la aplicación del método al sistema de Lorenz, obteniendo por primera vez conjuntos seguros tridimensionales a partir de un mapa estroboscópico. En este tipo de mapas se puso de manifiesto la importancia de la elección del intervalo de tiempo entre un punto y su imagen. Para intervalos de tiempo demasiado pequeños, la herradura de Smale subyacente no se desarrolla completamente y por tanto no existen conjuntos seguros (con control menor que ruido). Solo por encima de cierto valor de tiempo, los conjuntos seguros existen.

Aunque el objetivo del control parcial es el de mantener las trayectorias en cierta región, nos hemos dado cuenta de que los conjuntos seguros obtenidos se pueden aprovechar también para el objetivo opuesto, el de acelerar el escape de las trayectorias hacia el atractor externo. De esta forma, en el capítulo 5 se muestra que, simplemente dirigiendo las trayectorias lejos del conjunto seguro, los tiempos de escape de estas trayectorias se reducen considerablemente respecto del tiempo de escape esperado en ausencia control. Por tanto, este trabajo abre la posibilidad de usar los conjuntos seguros de forma dual, tanto para mantener la trayectoria el tiempo deseado como para forzar su salida rápida cuando sea necesario, dando una gran flexibilidad de uso al método de control.

Después de estos trabajos, se explora la posibilidad de extender el método de control a sistemas donde sean los parámetros y no las variables, los afectadas por el ruido. En el capítulo 6 se muestra que es posible encontrar conjuntos seguros también bajo estas condiciones, siempre y cuando el ruido y el control afecten al mismo parámetro. De esta forma se consigue mantener el control menor que el ruido. Sin embargo, debido a la necesidad de conocer cómo la trayectoria cambia con la perturbación del parámetro a controlar, el coste computacional de calcular conjuntos seguros se incrementa considerablemente. En este sentido queda abierto el desarrollo de posibles optimizaciones del algoritmo.

Otro de los objetivos de esta tesis era el de aplicar el control parcial a series temporales por su importancia experimental. Para ello un primer paso fue el estudio de mapas con retardo en el capítulo 7. Estos mapas pueden aparecer como fruto de la reconstrucción del espacio de fases de una serie temporal. La dificultad de estos mapas reside en que solo tiene sentido controlar la variable en su estado presente, y no sus estados pasados. Dado que el conjunto seguro se encuentra cerca de la variedad estable de la silla caótica, lo deseable sería que el control pudiese dirigirse hacia esta región. Sin embargo el hecho de poder controlar solo la variable en su estado presente y no en las otras dimensiones limita considerablemente la eficiencia del control. Un objeto de futuro estudio sería el de analizar bajo que condiciones se pueden controlar estos mapas teniendo acceso a una única variable. Por todo ello, en este capítulo asumimos por simplicidad que solo la variable presente posee incertidumbre, obteniendo así conjuntos seguros para los mapas estudiados.

A lo largo de estos trabajos, hemos encontrado algunas dificultades a la hora de implementar el método de control parcial. Por ejemplo, en todos estos capítulos previos se asumió que el ruido que afecta al sistema está acotado. Esto es cierto en la mayoría de los casos ya que uno puede tomar una cota de ruido tan grande como quiera. Sin embargo, en el caso de distribuciones con largas colas es inevitable que aparezcan perturbaciones arbitrariamente grandes, que requieran controles del mismo orden. Además hemos observado en algunos sistemas como flujos afectados por ruido continuo, que tras discretizar la dinámica, es frecuente que el ruido que emerge en el mapa tenga diferentes amplitudes de un punto a otro. Si establecemos la mayor de estas amplitudes como cota superior de ruido, el método de control se hace ineficiente ya que, tal y como está planteado, asume la misma cota de ruido para todos los puntos, comportando ineficiencias en la aplicación del control . Por estos motivos se hace conveniente generalizar el método intentando que tenga las siguientes características:

- Seamos capaces de cuantificar cuan seguro es un punto de la región de control.
- Tenga en cuenta las asimetrías en la cota de ruido que afecta a la dinámica a lo largo de la región de control.
- Sea compatible con la noción de conjunto seguro desarrollada en los trabajos previos.

Con este objetivo se expone en el capítulo 8, el desarrollo de una nueva herramienta, las funciones de seguridad, que son una generalización del concepto de conjunto seguro. Estas funciones pueden calcularse automáticamente mediante un algoritmo iterativo. Para mostrar cómo se comporta, en este capítulo también se muestran algunas aplicaciones sobre mapas conocidos y series temporales, con ruidos de diferente naturaleza.

Este trabajo deja abierta la puerta hacia un futuro desarrollo de este nuevo enfoque para aplicarlo a cualquier tipo de dinámica que presente escapes en una determinada región. Sin la necesidad de que exista caos transitorio en esa región, el

método se puede usar para evitar escapes indeseados de forma poco invasiva. Otra potencial aplicación es que, debido a la gran flexibilidad de este algoritmo y bajo pequeñas modificaciones, creemos posible crear funciones con el objetivo opuesto, el de acelerar o forzar el escape en determinado número de iteraciones del mapa. Esto puede tener importantes aplicaciones en problemas de transporte, donde el objetivo es conducir un cuerpo desde un punto inicial A a un punto objetivo B bajo la acción de un determinado mapa, minimizando la cota de control, lo cual puede ser de gran utilidad en dispositivos donde el uso de control esté limitado.

Metodología

La investigación realizada durante esta tesis es principalmente de carácter teórico-computacional. Si bien se han realizado algunos estudios experimentales relacionados con el oscilador de Duffing, estos estudios están aún en fase de desarrollo. En esta tesis se ha trabajado principalmente con sistemas de ecuaciones diferenciales ordinarias (simulados con métodos Runge-Kutta) y también con mapas. Estos mapas se han construido mediante técnicas de discretización como secciones de Poincaré, mapas estroboscópicos o mínimos/máximos sucesivos. En otros casos se han usado mapas bien conocidos, presentes en la bibliografía. En todos los ejemplos analizados se buscaron sistemas que de antemano se sabía que presentaban caos transitorio. Para el cálculo numérico y representación de figuras se ha usado principalmente el software Matlab, mientras que en los casos que requerían computación más intensiva se hizo uso del lenguaje de programación C++ así como de técnicas de paralelización. Especial mención a la computación de los conjuntos seguros en 3 dimensiones que requirieron del uso de los servidores de alto rendimiento del Grupo de Dinámica No Lineal, Teoría del Caos y Sistemas Complejos de la URJC.

Conclusiones en castellano

En esta sección se resumen esquemáticamente los principales resultados de esta tesis.

- El método de control parcial se ha aplicado a un sistema ecológico consistente en 3 especies que interactúan entre si. Fruto de ello es posible encontrar un escenario de caos transitorio que conlleva la extinción de una de las especies. Con el fin de evitar esa extinción, se aplica el método de control parcial. Además realizamos una comparación de este método con otro propuesto por los autores Dhamala y Lai, que es uno de los más conocidos para control de caos transitorio. A la vista de los resultados, podemos concluir que el control parcial es más eficiente y menos invasivo que el propuesto por dichos autores.

- Uno de los modelos más conocidos en dinámica no lineal es el sistema de Lorenz.

Para cierto valor de sus parámetros, dicho sistema presenta caos transitorio, evolucionando las trayectorias hacia dos posibles puntos fijos. Con el fin de evitar estos atractores y mantener la dinámica caótica, se ha implementado el método de control parcial. En este capítulo se muestran 3 formas diferentes de aplicar el método y se obtiene por primera vez un conjunto seguro en 3 dimensiones.

- Hemos explorado una aplicación alternativa de los conjuntos seguros. Una vez computados, se pueden usar para mantener la trayectoria en la región de interés durante el tiempo que se desee, para luego inducir su escape. Esto se consigue aplicando el control sobre la trayectoria de forma que esta se aleje del conjunto seguro. Con esta simple estrategia es posible disminuir considerablemente los tiempos de escape, confiriendo al método una gran flexibilidad a la hora de mantener o forzar el escape de la trayectoria caótica, según las necesidades del controlador.

- Se ha extendido el método a modelos dinámicos donde es posible controlar algún parámetro del sistema que además está afectado por ruido. Se desarrolla un algoritmo para computar esta nueva clase de conjuntos seguros y se muestra su desempeño con los conocidos mapa logístico y mapa de Hénon.

- El método de control parcial se ha aplicado a mapas con retardo, donde el estado del sistema puede depender de varios estados pasados. El principal inconveniente es que solo tiene sentido físico el control de la variable en su estado presente (no se pueden modificar sus estados pasados), y por tanto son necesarias ciertas modificaciones en el esquema original del control parcial. Se analizan 3 mapas de este tipo y por primera vez, se aplica esta técnica de control a un mapa que presenta caos Hamiltoniano y a un mapa hipercaótico.

- Con el fin de poder tratar mapas afectados por ruido más genéricos, y bajo el contexto del método de control parcial, ha sido desarrollada una nueva herramienta, la función de seguridad que es un concepto más genérico que el de conjunto seguro. Se desarrolla un algoritmo para su computo y se indica la relación directa con los conjuntos seguros. Finalmente se muestra su uso mediante varios ejemplos, poniendo de manifiesto la robustez y flexibilidad de esta nueva aproximación, así como su potencial para futuras aplicaciones.